ESA CONTRACT REPORT

Contract Report to the European Space Agency

Global Validation of ENVISAT Wind, Wave and Water Vapour Products from RA-2, MWR, ASAR and MERIS (2008-2010)

Author: Saleh Abdalla

Final report for ESA contract 21519/08/I-OL

European Centre for Medium-Range Weather Forecasts
Europäisches Zentrum für mittelfristige Wettervorhersage
Centre européen pour les prévisions météorologiques à moyen terme

ECMWF

Series: ECMWF - ESA Contract Report

A full list of ECMWF Publications can be found on our web site under:

http://www.ecmwf.int/publications/

European Centre for Medium Range Weather Forecasts
Shinfield Park, Reading, RG2 9AX, England

Contract Report to the European Space Agency

Global Validation of ENVISAT Wind, Wave and Water Vapour Products from RA-2, MWR, ASAR and MERIS (2008-2010)

Author: Saleh Abdalla

Final report for ESA contract 21519/08/I-OL

European Centre for Medium-Range Weather Forecasts
Shinfield Park, Reading, Berkshire, UK

March 2011

TABLE OF CONTENTS

Abstract

ENVISAT Fast Delivery (FD) surface wind speed and significant wave height (SWH) products from the Radar Altimeter (RA-2) instrument, wet tropospheric correction (WTC) and total column water vapour (TCWV) products from the Microwave Radiometer (MWR) instrument, wave mode spectra (both Level 1b and Level 2) from the Advanced Synthetic Aperture Radar (ASAR) instrument and TCWV product from the Medium Resolution Imaging Spectrometer (MERIS) instrument have been monitored and validated against the corresponding parameters from ECMWF atmospheric and wave models, in-situ buoy and platform instruments and other satellites (specifically: Jason-1 and Jason-2). This report assesses the quality of related ENVISAT products during the last three years (with few references to the earlier years).

In general, the FD RA-2 products are of good quality. The wind speed product is quite good. The issue of capping wind speed ate 21.4 m/s was resolved by the implementation of RA-2 processing chain IPF Version 6.02L04 on 1 February 2010. The Ku-band SWH product used to be about 4% high before the implementation of IPF 6.02L04 which resulted in a bias free product. Other wise, the Ku-band SWH is of high quality in standard deviation sense. The S-band SWH product is not valid anymore due to the failure of the S-band Altimeter in January 2008. Compared to the model, the MWR products are of good quality after filtering out the ice and land contaminated observations.

FD ASAR Wave Mode Level 1b (ASA_WVS_1P) product as inverted using the Max-Planck Institut für Meteorologie (MPIM) scheme agrees well with the wave model counterpart in terms of all integrated parameters used for the comparison. ASAR Wave Mode Level 1b product has been assimilated operationally at ECMWF since 1 February 2006. On the other hand, Wave Mode Level 2 (ASA_WVW_2P) product agrees well with wave model in terms of swell SWH and mean period. Irrespective of a rather recent improvement of the product in October 2008, the agreement is not so good for spectral peakedness factor and the directional spread. There was no noticeable change in the ASAR Wave Mode products during the last year. Work was carried out towards the assimilation of ASAR Wave Mode Level 2 product, but further investigation and/or product improvement are needed.

Significant improvement in the quality of MERIS TCWV product was witnessed after the operational implementation of the MERIS IPF Version 5.02 on 8 May 2006. The product did not change during the last few years. However, there were several incidences of product degradation from time to time. The differences between MERIS and the model are relatively high. However, the product is quite good over land where similar products are lacking. This resulted in the operational assimilation of the product in the ECMWF operational atmospheric model in early September 2009.

The change of ENVISAT orbit in October 2010 did not have any impact on any of the products considered here.

Abbreviations

AN ..... Analysis
ASAR ..... Advanced Synthetic Aperture Radar
BUFR ..... Binary Universal Form for the Representation of meteorological data
CNES..... Centre National d'Etudes Spatiales (French Space Agency)
DCDA..... Delay Cut-off
ECMWF ..... European Centre for Medium-Range Weather Forecasts
ECWAM..... ECMWF wave model
ED ..... Early Delivery
ENVISAT..... Environmental Satellite
ERA-40..... 40-year ECMWF Re-Analysis
ERS..... European Remote Sensing satellite
EUMETSAT..... European Organisation for the Exploitation of Meteorological Satellites
FC ..... Forecast
FD..... Fast Delivery product
FDGDR ..... Fast Delivery Geophysical Data Record
FDMAR..... Fast Delivery Marine Abridged Records Product
FG..... First guess
GTS ..... Global Telecommunication System
IFS ..... Integrated Forecasting System
IPF ..... Instrument Processing Facility
MERIS..... MEdium Resolution Imaging Spectrometer
MWD..... Mean wave direction
MWP ..... Mean wave period
MWR..... MicroWave Radiometer
NH ..... Northern Hemisphere extra-tropics (north of latitude 20□N)
NOAA ..... US National Oceanic and Atmospheric Administration
NRT ..... Near real time
OGDR..... Operational Geophysical Data Record
PF-ASAR ..... ASAR Processing Facility
QWG ..... Quality Working Group
RA ..... ERS Radar Altimeter
RA-2 ..... ENVISAT Radar Altimeter-2
SDD..... Standard Deviation of the Difference
SH..... Southern Hemisphere extra-tropics (south of latitude 20□S)
SI ..... Scatter Index
SWH..... Significant wave height
TCWV ..... Total column water vapour
UTC..... Coordinated Universal Time
WAM..... Wave model
WDS..... Wave directional spread
WM..... Wave Mode
WPF..... Wave spectral peakedness factor of Goda
WTC ..... Wet tropospheric correction

I. RADAR ALTIMETER - 2 (RA-2)

AND

MICROWAVE RADIOMETER (MWR)

I.1 Introduction

RA-2 is a dual-frequency altimeter operating on both Ku- and S-Band. It was derived from the RA of the ERS satellite series, providing improved measurement performance and new capabilities. The main objectives of the RA-2 are the high-precision measurements of the time delay, the power and the shape of the reflected radar pulses for the determination of the satellite height and the Earth surface characteristics. RA-2 transmits radio frequency pulses that propagate at approximately the speed of light. The time elapsed from the transmission of a pulse to the reception of its echo, reflected from the surface of the Earth, is proportional to the altitude of the satellite. The magnitude and shape of the echoes contain information on the characteristics of the surface that caused the reflection. Operating over oceans, these measurements are used to determine the ocean surface topography, thus supporting studies of ocean waves, marine surface winds, circulation, bathymetry, gravity anomalies and marine geoid characteristics. Furthermore, the RA-2 is able to map and monitor sea ice and polar ice sheets. The product to be validated here is the Fast Delivery Marine Abridged Records Product (FDMAR). Specifically, the backscatter coefficient, surface wind speed, Ku-Band significant wave height (SWH) and S-Band SWH are validated.

MWR is a dual-channel nadir-pointing radiometer, operating at frequencies of 23.8 GHz and 36.5 GHz. The main objective of the MWR is the measurement of the integrated atmospheric water vapour column and cloud liquid water content, as correction terms for the radar altimeter signal. In addition, MWR measurement data are useful for the determination of surface emissivity and soil moisture over land, for surface energy budget investigations to support atmospheric studies, and for ice characterization. To measure the strength of the weak water-vapour emission-line at 22 GHz, the frequencies 23.8 GHz and 36.5 GHz are optimally selected in order to eliminate the microwave radiation emitted by the Earth surface. The two products to be verified are the total column water vapour (TCWV) and the wet tropospheric correction (WTC) available in FDMAR product.

The European Centre for Medium-Range Weather Forecasts (ECMWF) monitors routinely the quality of the wind and wave products from RA-2 since an early stage of commissioning phase data dissemination on 18 July 2002. The monitoring is based on the data processed in near real time (NRT) provided by ESA. Radar backscatter coefficient (σ°), surface wind speed and Ku- and S-Band SWH products from the RA-2 instrument and WTC and TCWV products from the MWR instrument are among the parameters monitored and validated against the ECMWF model products and, for wind and wave products, against the in-situ buoy and platform observations available through the Global Telecommunication System (GTS) as well as the ERS-2 RA products. When possible, a combination of all of the observation sources (multiple-collocation) is also used for validation. It must be stressed that the number of in-situ observing stations is very limited (few-several 10's) and most of them are located in the Northern Hemisphere (NH) around the North American and European coasts. The exceptions are few buoys in the Tropics, mainly around Hawaii, and off the South African coasts in the Southern Hemisphere (SH). Therefore, any validation against in-situ data mainly reflects the quality of the products in the NH.

The aim of the validation is to assess and monitor the quality of those products. The Ku-Band SWH product is of significant importance as it is assimilated in the operational forecasting system at ECMWF. For proper validation, the observations and the model results should be of comparable scales. The model scale is much larger than the scale of the altimeter observations. Therefore, an averaging process is used to form altimeter and MWR super-observations of comparable scales as the model. The super-observations are collocated with the model and the in-situ (if applicable) data. The main results of the validation over the last year or so (although some time series extends back to June 2003) are presented here. The following major changes and events during the last few years have some impact on the interpretation of the results:

- 30 Oct. 2007: The implementation of the processing chain of PF-ASAR 4.05.
- 18 Jan. 2008: The loss of RA-2 S-Band.
- 3 Jun. 2008: The advection numerical scheme of the wave model was changed.
- 30 Sep. 2008: Changes to the physics of the atmospheric model.
- 10 Mar. 2009: The operational assimilation of Jason-2 significant wave height replacing that of Jason-1. A change in the treatment of some atmospheric observations impacted the model water vapour.
- 8 Jun. 2009: The re-introduction of the assimilation of Jason-1 significant wave height.
- 8 Sep. 2009: Wave model change to account for the wave damping in the wind input source term. The operational assimilation of MERIS TCWV (over land only) in the ECMWF atmospheric model.
- 10 Nov. 2009: Revised significant wave height bias correction in the wave model.
- 26 Jan. 2010: The high resolution (T1279) atmospheric model with a resolution of 16 km.
  The increase of number of frequency and direction bins in the wave model.
- 1 Feb. 2010: The implementation of the RA-2 IPF 6.02L04 which has impact on significant wave height, wind speed and water vapour products.
- 22 Mar. 2010: Revised significant wave height bias correction to account for the impact of IPF 6.02L04 on wave height.
- 1 Apr. 2010: Assimilation of Jason-1 significant wave heights was halted.

- 19 Oct. 2010: MWR anomaly caused the rain flag in the RA-2 products to be set. This caused the rejection of most of RA-2 products. The anomaly was sorted out within few days during the period of ENVISAT orbit reconfiguration.
- 22-26 Oct. 2010: ENVISAT orbit was lowered by 17 km. The new orbit has a "repeat cycle" of about 30 days. As a precautionary measure, all ENVISAT products were not allowed to be assimilated since 21 Oct.
- 27 Nov. 2010: The start of the leapfrog experiment of ASAR.
- 2 Dec. 2010: Assimilation of RA-2 significant wave height resumed.

Results of the routinely global monitoring and validation of ENVISAT RA-2 wind and wave products as well as MWR WTC and TCWV products are summarised in form of monthly reports. These reports are available online at: http://earth.esa.int/pcs/envisat/ra2/reports/ecmwf/

I.2 RA-2 and MWR Data Processing

The validation is based on FDMAR (Fast Delivery Marine Abridged Record) which is a subset of the Fast Delivery Geophysical Data Record (FDGDR) product produced in NRT. The data files are retrieved in BUFR (Binary Universal Form for the Representation of meteorological data) format from two ftp sites at Kiruna and ESRIN. The raw data product is collected for 6-hourly time windows centred at synoptic times (00, 06, 12 and 18 UTC). For proper validation, the observations and the model results should be of comparable scales. As the model scale (~ 70 km) is much larger than the scale of an individual 1 Hz altimeter observation (~ 7 km), the latter needs to be averaged. Therefore, the stream of altimeter data is split into short observation sequences each consisting of 11 individual (1-Hz) observations. A quality control procedure is performed on each short sequence. Erratic and suspicious individual observations are removed and the remaining data in each sequence are averaged to form a representative super-observation, providing that the sequence has enough number of "good" individual observations (at least 7). The super-observations are collocated with the model and the in-situ (if applicable) data. The raw data pass the quality control and the collocated data are then investigated to derive the conclusions regarding the data quality. It is important to recall that the Ku-Band SWH product is of significant importance as it is assimilated in the operational forecasting system at ECMWF since 21 October 2003. The details of the method used for data processing is an extension to the method used for ERS-2 RA analysis and described in Abdalla and Hersbach (2004).

I.3 FD RA-2 Data Reception

FD RA-2 data reception during the last year (2010) was quite good. However, there were quite a number of data gaps. Fig. (I.1) represents the data reception during the relaxed cut-off condition of the Delay Cut-off (DCDA) the ECMWF IFS model configuration (8~14-hour delay). The products are considered missing if they are delayed beyond the cut-off limit. Therefore, some of the gaps may just represent this fact. The rather long gap towards the end of October 2010 is due to the unavailability of the data products while ENVISAT was manoeuvred to the new orbit.

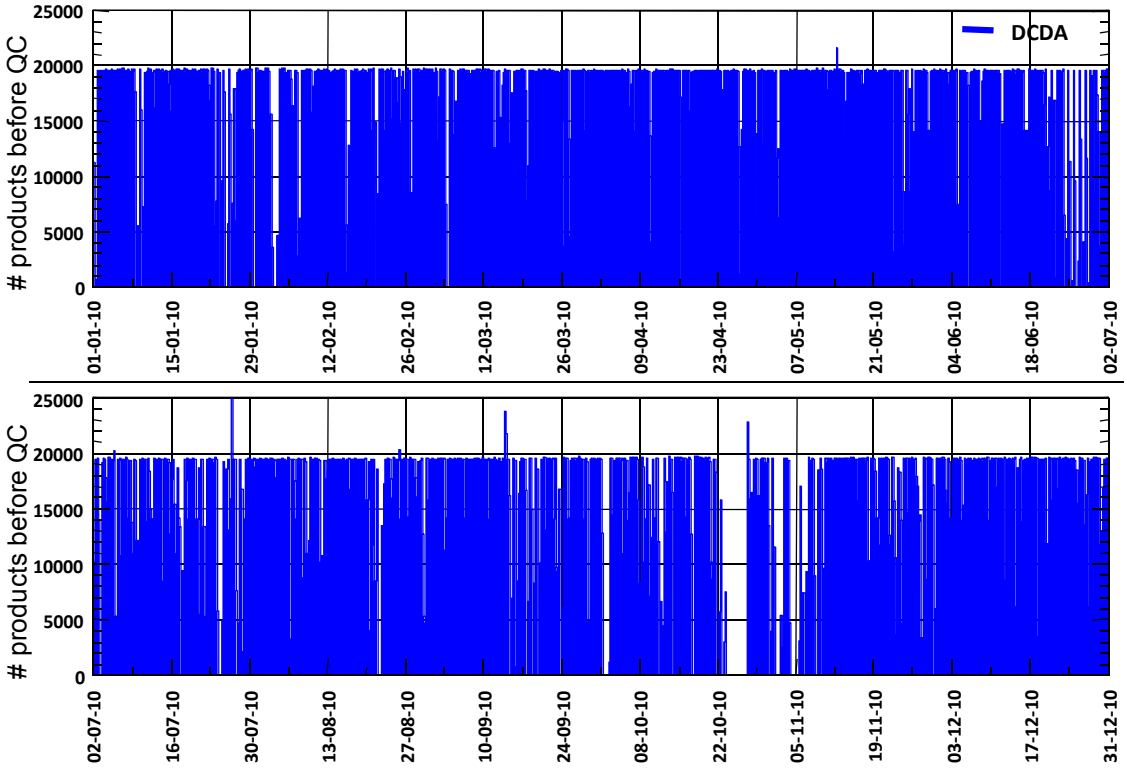

Figure I.1: Total Operational Data Reception of RA-2 Data in 2010.

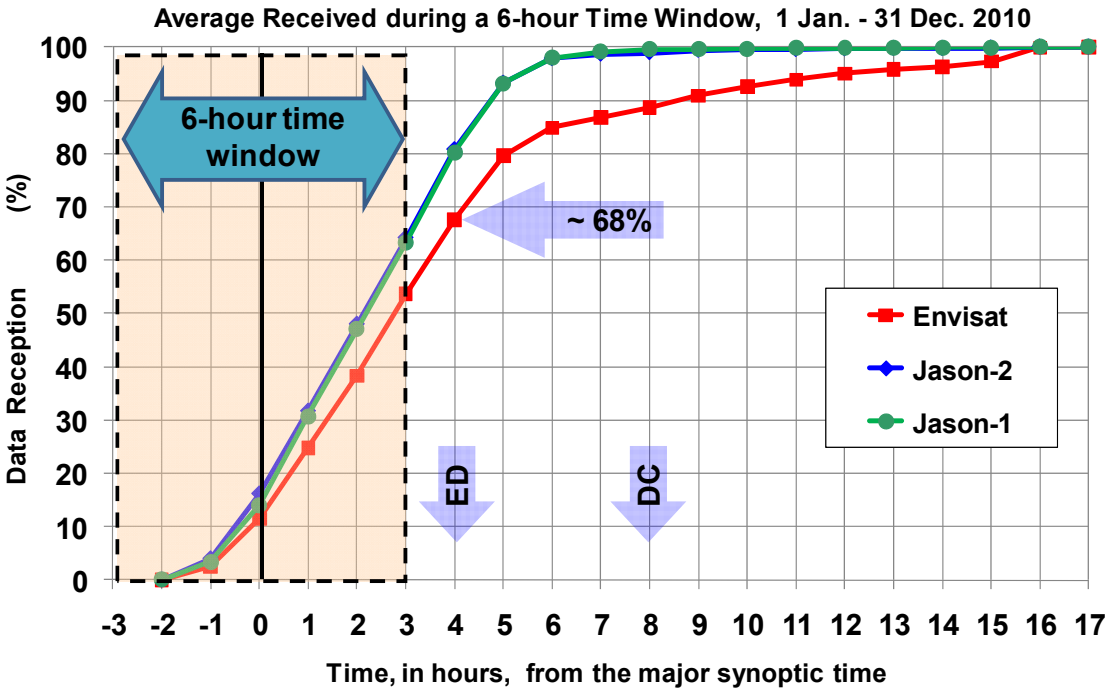

Figure I.2: Amount of operational data reception of RA-2 data in 2010 as a function of waiting time. The cut-off for the "Early Delivery" (ED) suite and the critical cut-off for the "Delayed Cut-off" (DC) suite are indicated. The same results from Jason-1/2 are also presented.

In order to quantify the timeliness of the arrival of the RA-2 products, the products within each 6-hour time window (centred at 00, 06, 12 and 18 UTC) were discriminated based on their arrival time measured from the centre of the window. The accumulative amount of data received at each hour is averaged over a long period of time (e.g. a full year). Fig. (I.2) shows the average accumulated amount (normalised by the total amount of data received at the end of 48 hours) of data received for all 6-hour time windows during 2010 as a function of the time since the middle of the time windows. The official ECMWF forecasts are issued from the "Early Delivery (ED)" cut-off, which is 1 hour after the close of the 6-hour window. This makes 4 hours from the centre of the analysis window. RA-2 products available for assimilation at this cut-off time is about 68% of the total received after waiting long enough. This is a slight improvement compared to the 65% of 2009. Although this is quite good amount of data, better performance can be achieved as can be seen in Fig. (I.2) for Jason-1 and Jason-2 products (about 80%). For the minimum cut-off of the DCDA suite (5 hours after the end of the window), about 90% of the data are available for analysis (slightly worse that last year). This, again, shows that there is quite a good room for improvement as Jason-1/2 data products were almost fully received. It seems that delivering the data through the GTS, which is the medium used for delivering Jason-1/2 data, does not help much to improve this.

I.4 RA-2 Radar Backscatter and Surface Wind Speed

In general, the FD RA-2 Ku band backscatter coefficient (σ°) behaves as expected. The monthly mean values of σ° since May 2003 are plotted in panel (a) of Fig. (I.3). One can notice that the monthly mean Ku-band σ° values vary within a narrow band between 10.9 and slightly above 11.2 dB. The monthly mean of S-band σ° values are shown on the same plot. The S-band has been declared permanently lost since early January 2008. The time series of the S-band is rather stable except for two events. There was a jump of about 0.6 dB between November and December 2003. The jump coincides with the implementation of the IPF Version 4.56 processing chain on the 26 November 2003. The second event was the drop in the Side B S-Band transmission power as can be clearly seen in Fig. (I.2) for May and June 2006. For comparison, Jason-1 and Jason-2 radar altimeter monthly mean σ° values from both Ku- and C-Bands are also plotted in Fig. (I.3). Apart from the fact that Jason mean backscatter values are higher than those of ENVISAT, they are all run more or less parallel to each other. However, it seems that Jason-1 mean values suffer gradual decrease.

At the end of 2009, there was an apparent drop in the backscatter values of all altimeters. This can be clearly seen in panel (b) of Fig. (I.3) which shows the 1-year running averages of the mean σ° values to filter out all seasonal and shorter scale fluctuations. Therefore, a drop in RA-2 Ku-band mean values of about 0.15 dB can be clearly seen. However, this value is about twice those suffered by the Ku-band altimeters (about 0.08 dB) onboard Jason-1/2. The drop in the Jason-1/2 C-bands is about 0.05 dB. The RA-2 higher drop needs to be looked at. One reason for that may be the fact that ENVISAT reaches much higher latitudes where the atmospheric conditions may be different from low-mid latitudes covered by Jason-1/2. An investigation will be starting soon in order to verify this.

Collocated pairs of RA-2 super-observation and the analysed (AN) ECMWF model wind speeds are plotted as a density scatter plot in Fig. (I.4) for the whole globe over a period of one year from 2 February 2009 to 1 February 2010 in panel (a) and from 2 February 2010 to 1 February 2011. On the

other hand, Fig. (I.5) shows a similar plot comparing the altimeter winds against in-situ (buoy) data for a period slightly less than a year from 2 February 2010 to 31 December 2010. In general, RA-2 wind speed data are in good agreement with the model and buoy data. There used to be a capping to the RA-2 wind speeds at 21.3 m/s as can be seen in panel (a) of Fig. (I.4). This was corrected (see panel b of Fig. I.4) as part of the IPF 6.02L04 which was implemented on 1 February 2010.

The global wind speed bias (defined as the RA-2 minus the model or the buoy) is about 0.28 m/s. On the other hand, the RA-2 wind speeds are lower than the buoys by about 0.15 m/s. One needs to keep in mind that most of the in-situ (buoy or platform) instruments are located around North America and Europe. Therefore, the comparison against in-situ observations mainly reflects the quality of the wind speed product in the NH (and to less extent in the Tropics). The global RA-2 wind speed scatter index (SI, defined as the standard deviation of difference divided by the mean of the model or the buoy) is about 14% when compared against the model and about 18% compared to the buoys.

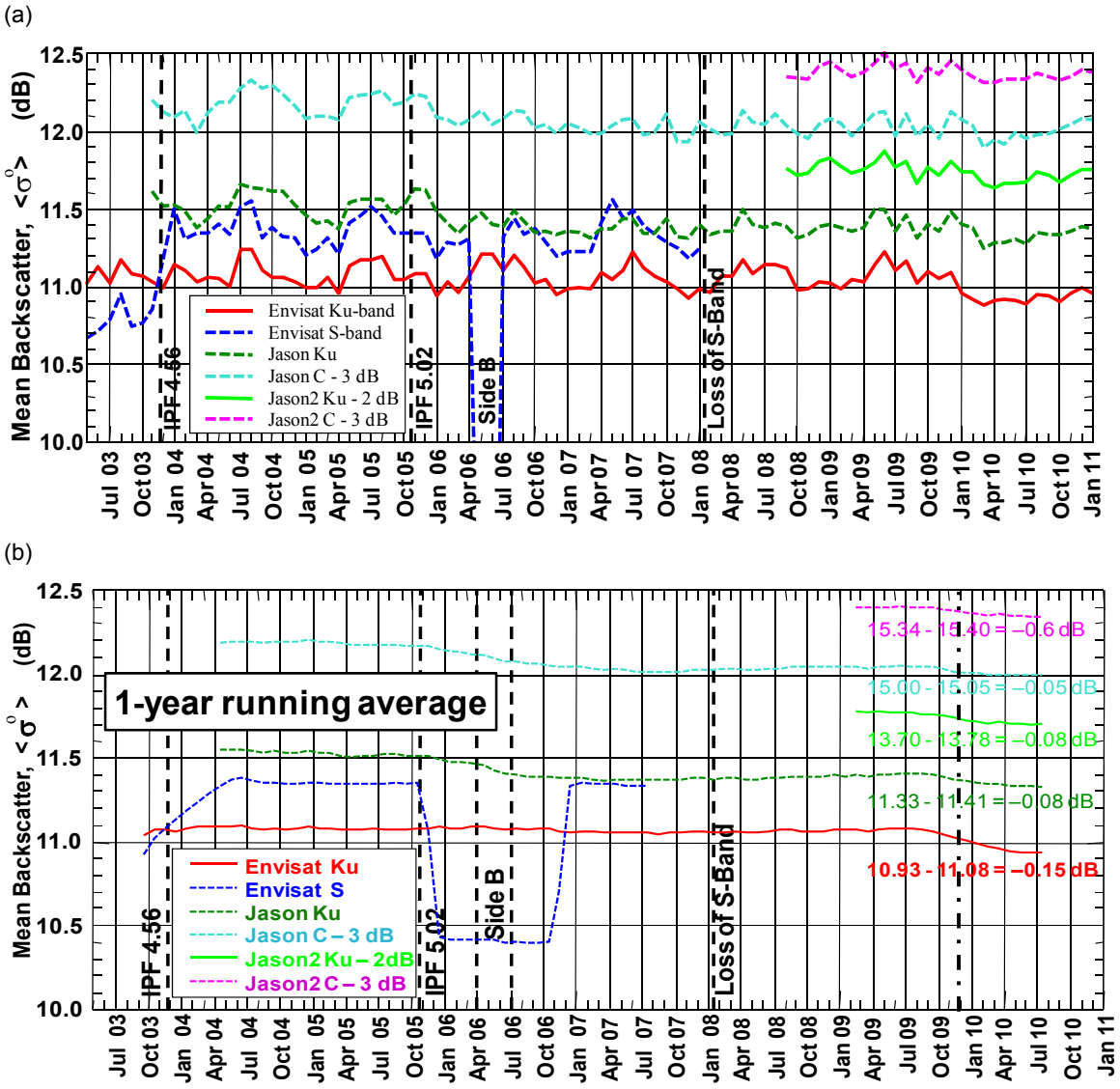

Figure I.3: Monthly global mean backscatter coefficient of Ku- and S-band altimeters after quality control. Jason-1 and Jason-2 Ku- and C-band mean backscatter values are also shown for comparison. (a) Individual monthly means, (b) 12-month running average of the monthly means.

(a)

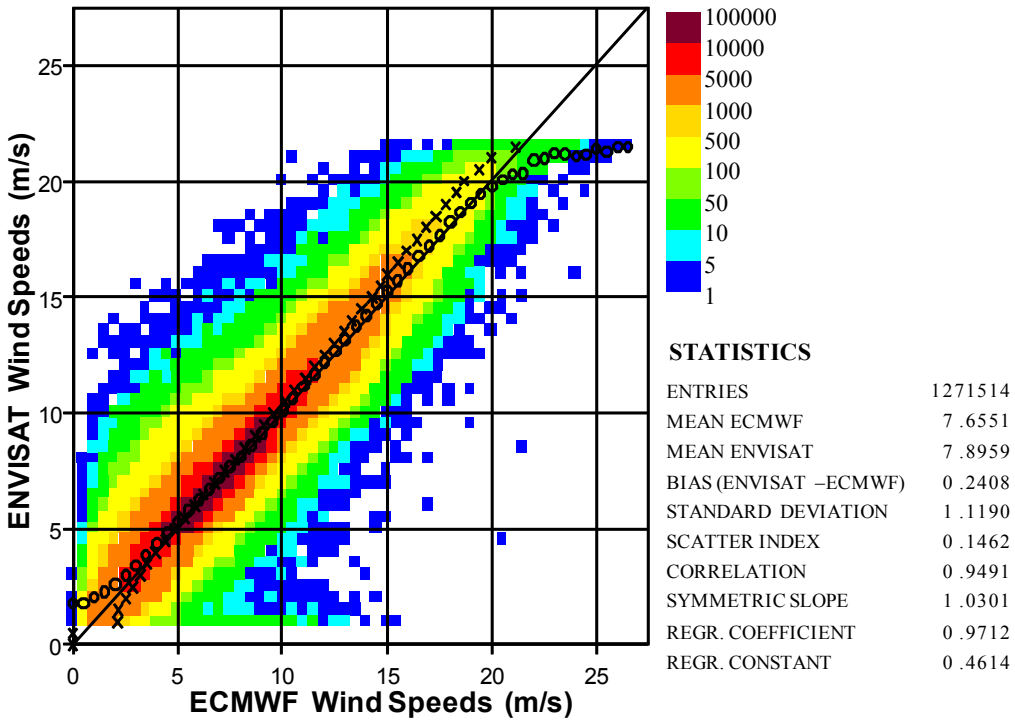

(b)

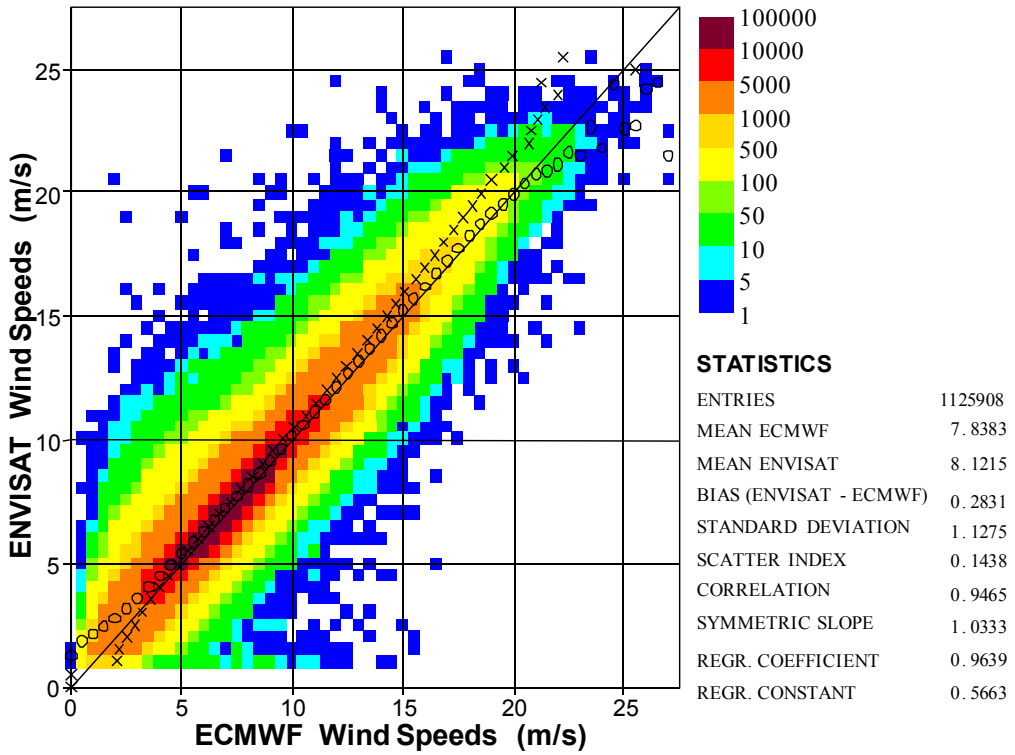

Figure I.4: Global comparison between RA-2 and AN ECMWF model wind speed values during the periods: (a) from 2 February 2009 to 1 February 2010; and (b) from 2 February 2010 to 1 February 2011.

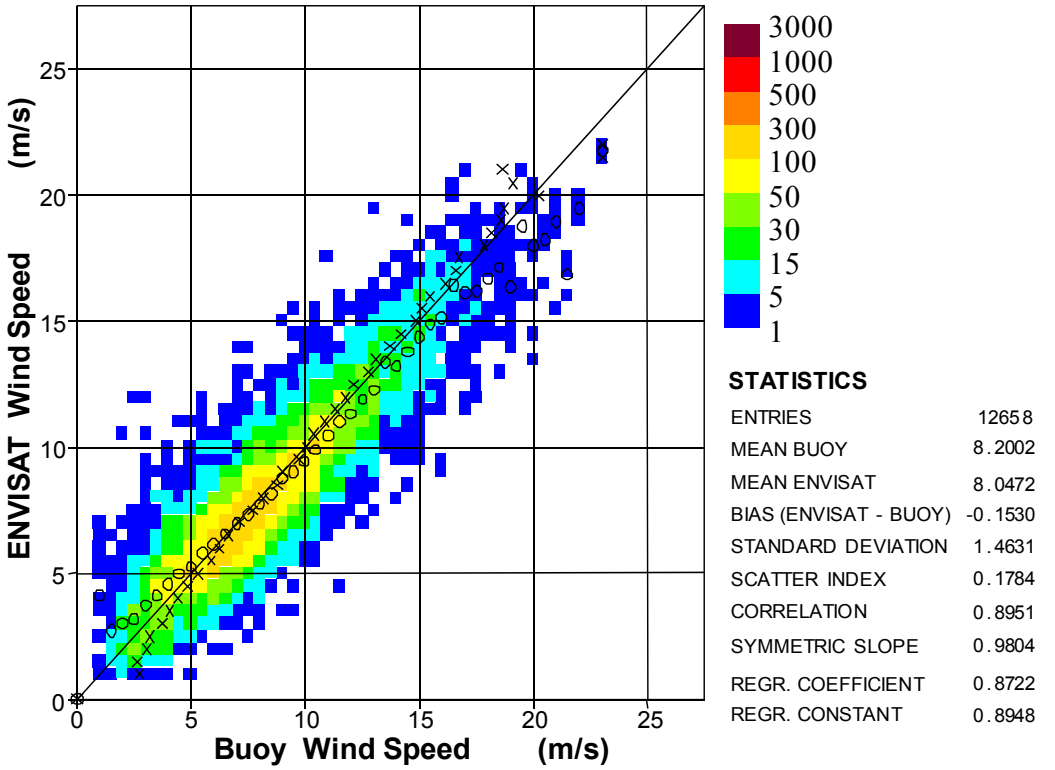

Figure I.5: Global comparison between RA-2 and in-situ wind speed values during the period from 2 February to 31 December 2010 (mainly in the NH).

The time series of weekly bias and standard deviation of the difference (SDD) between RA-2 and model AN wind speeds since late 2003 are shown in panel (a) of Fig. (I.6) and during the last 3 years in panel (b) of Fig. (I.6). The major altimeter related events and the ECMWF model changes are shown as well. One can clearly see the seasonal variation of the bias. After the implementation of IPF Version 5.02 (October 2005), the seasonal variation is much suppressed especially in the NH and the Tropics (not shown). For example, the range of variation in the NH reduced from about 1.3 m/s (-0.9 to 0.4 m/s) to about 0.9 m/s (-0.2 to 0.7 m/s). The global range of variation reduced by half from about 0.4 m/s to about 0.2 m/s (Fig. I.6). The implementation of IPF 6.02L04 on 1 February 2010 resulted in slightly higher bias than before due to the removal of the cap (~ 21.4 m/s) which was imposed before. On the other hand there was an increase in bias and SDD just after the orbit change. This lasted for a couple of days only and the statistics returned back to normal. There was no obvious reason for this. However, M. Roca (personal communication, 2010) postulated that this may be due to the colder than normal conditions of the platform as most of the instruments on-board ENVISAT were switched off during the orbit changing manoeuvres. Of course it is not possible to prove or disprove this postulation easily.

Wind speed from RA-2 is not assimilated in the ECMWF models. The main reason for that is the existence of the overwhelming amount of scatterometer winds making the altimeter wind observations of very minimal impact, if any. However, the altimeter wind speed observations is playing a very important role as an independent source of data which can be used to assess the ECMWF model developments as can be seen, for example, in Fig. (I.6).

(a)

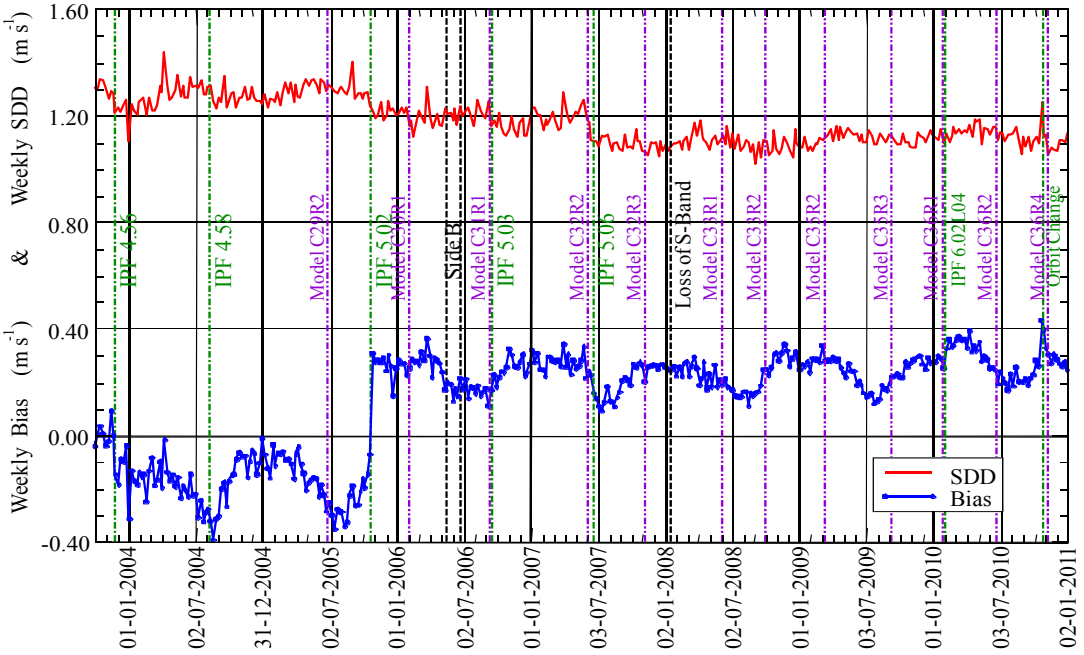

(b)

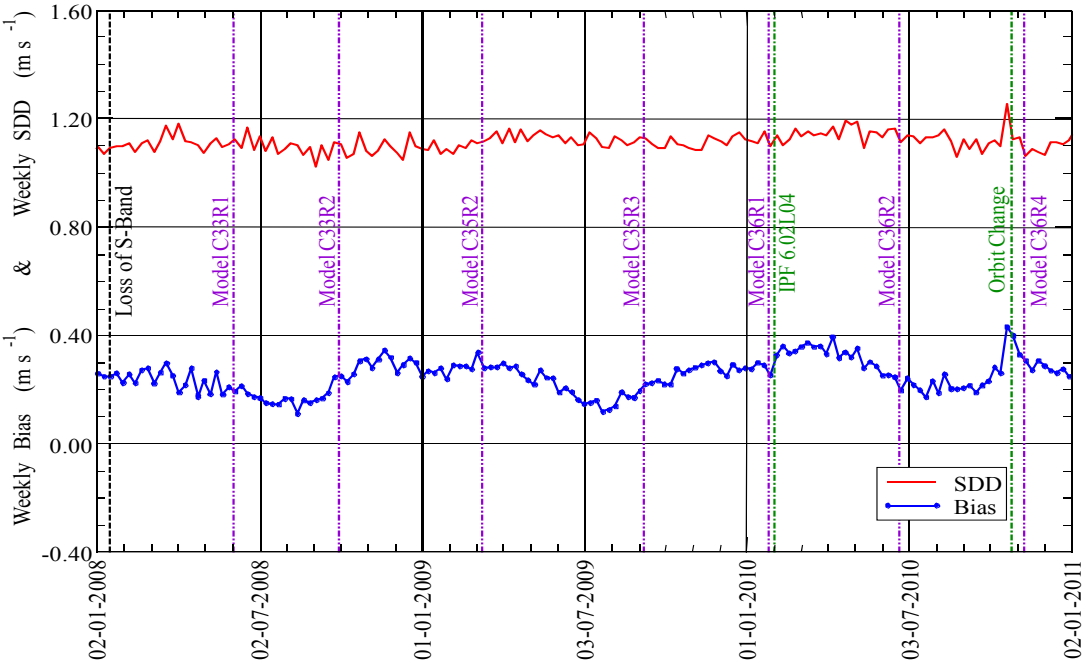

Figure I.6: Time series of weekly wind speed bias (m/s) and standard deviation of difference (SDD) between RA-2 and ECMWF model AN since late 2003 (a) and during the last 3 years (b).

I.5 RA-2 KU-Band Significant Wave Height

Ku-band SWH product is characterised by stable performance and good quality since the start of the mission. Collocated SWH pairs of RA-2 super-observation and the first-guess (FG) WAM model are plotted as a density scatter plot in Fig. (I.7) for the whole globe over a period of one year from 2 February 2009 to 1 February 2010 in panel (a) to represent a comparison before the implementation of altimeter processing chain IPF 6.02L04 on 1 February 2010 and from 2 February 2010 to 1 February 2011 in panel (b) representing a comparison after the implementation of IPF 6.02L04. The RA-2 used to overestimate SWH values globally by about 4% (~10-12 cm). The IPF 6.02L04 brought the bias down to very close to zero (~0.3% or ~2 cm). Similar results can be obtained from the comparison against in-situ buoy data as shown in Fig. (I.8). For technical reasons, the scatter plot shown in Fig. (I.8) covers the period from 2 February to 31 December 2010. It should be stressed here that buoy observations are mainly in the NH.

The time series of weekly bias and SDD between RA-2 and model FG SWH since late 2003 are shown in panel (a) of Fig. (I.9) and during the last 3 years are shown in panel (b). Significant model or RA-2 processing changes are plotted as well so that the correspondence between those events and the change in statistics are clearly seen. Fig. (I.9), or the cross-verification of model and altimeter time series represents a valuable tool to detect and assess changes on both sides. Fig. (I.9) represent the time series for model or altimeter processing improvement (or degradation) by following the trend of the SDD over time. For example; RA-2 side B operation during May and June 2006 caused one of the most significant impacts on the statistics. The abrupt reduction in SWH bias and SDD between RA-2 and ECMWF model FG during the period when RA-2 was configured to the redundant side B (May-June 2006) cannot be missed. Ku-band SWH from side B was nominally unbiased compared to the model. Another prominent change is the implementation of IPF 6.02L04. The bias clearly reduced by about 12 cm due to this change. It also leads to a slight increase in SDD. The latter will be discussed below. The impact of the revised bias corrections to the altimeter SWH values applied in November 2009 and March 2010 can be clearly seen in Fig. (I.9).

One of the important observations made in Fig. (I.7), which can be easily noticed by comparing the SDD (or the scatter index) value in panel (b) to that in panel (b), is the increased value of the SDD (or scatter index) from about 24 cm (~9.8%) before IPF 6.02L04 to about 27 cm (~10.5%) afterwards. This is also confirmed by the SDD time series of Fig. (I.9). There was a significant model change about one week before the implementation of IPF 6.02L04. The spatial resolution of the ECMWF atmospheric model was upgraded to TL1279 (about 16 km) in addition to wave model increased resolution and other changes (model C36R1) were implemented on 26 January 2010. The limited verifications carried out for the pre-operational model runs did not reveal any degradation of the model results. Some investigations were carried out to understand this degradation.

(a)

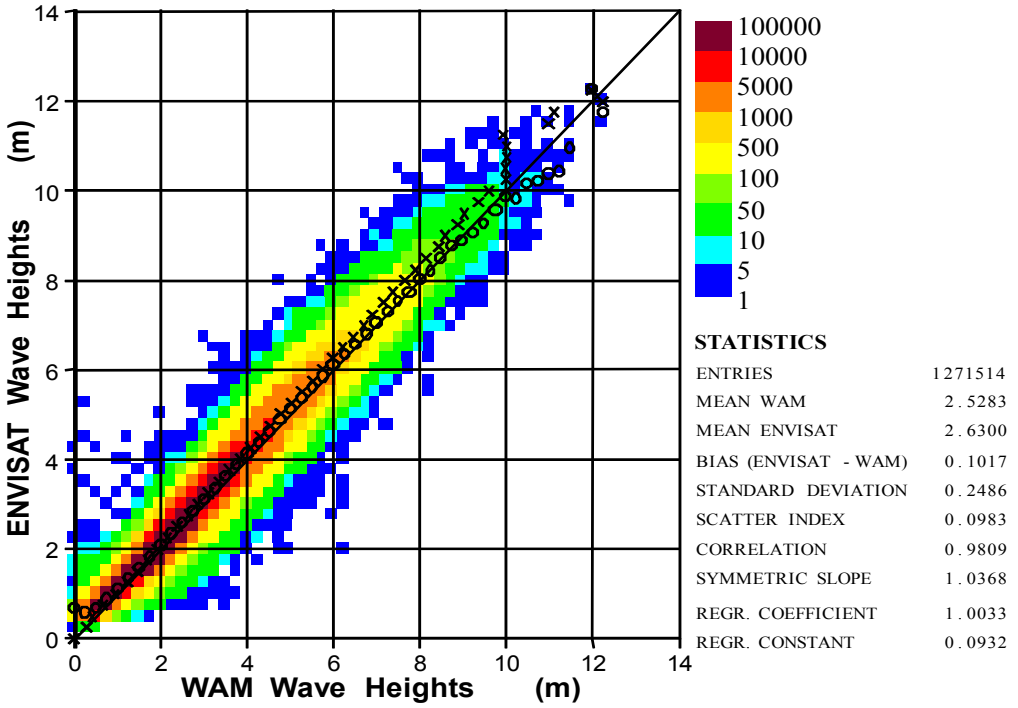

(b)

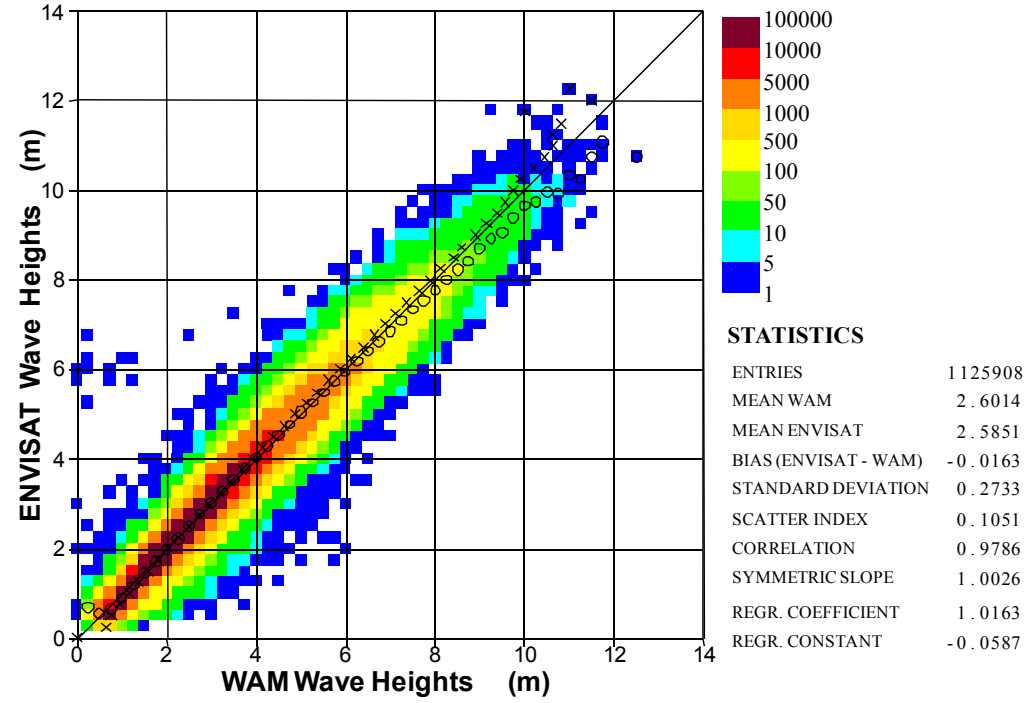

Figure I.7: Global comparison between RA-2 Ku-Band and WAM wave model SWH FG values during the periods: (a) from 2 February 2009 to 1 February 2010; and (b) from 2 February 2010 to 1 February 2011.

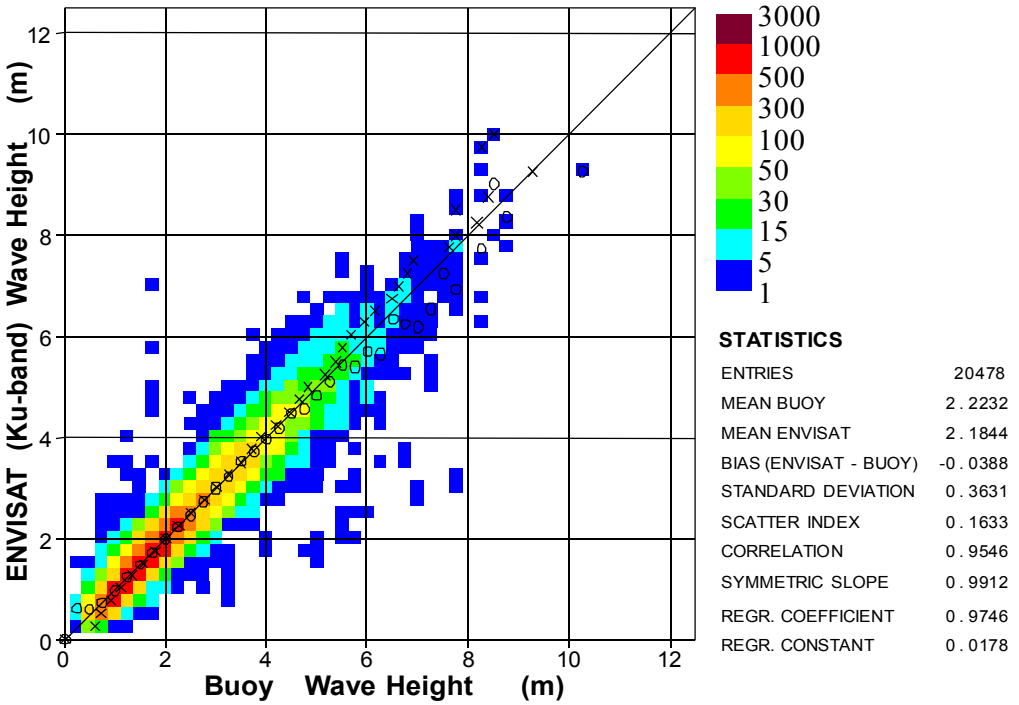

Figure I.8: Global comparison between RA-2 Ku-Band and in-situ SWH values during the period from 2 February to 31 December 2010 (mainly in the NH).

Panel (a) of Fig. (I.10) shows the distribution of the SWH bias and SDD between RA-2 and ECMWF model FG as functions of SWH values for the whole globe over one year before the IPF 6.02L04 (the period from 2 February 2009 to 1 February 2010 and will be referred to as "old") and another year afterwards (the period from 2 February 2010 to 1 February 2011 and will be referred to as "new"). The reduction of bias due to IPF 6.02L04 is clearly seen. The old bias is quite linear for SWH values in excess of about 1.4 m. However, the new bias is highly non linear. Although the new RA-2 SWH is virtually unbiased, the change of bias with respect to SWH is not desirable. At lower wave height values, the bias increases with the reduction of SWH for both new and old products. When it comes to the SWH SDD, it is clear that the SDD of the new product with respect to the model FG is higher than the old product. The situation becomes even worse at low SWH (below ~0.8 m).

These hints of degradation can be attributed to one or more of the following reasons:

- some degradation due to IPF 6.02L04,
- some degradation due to model C36R1, or
- some (unknown) geophysical reasons.

(a)

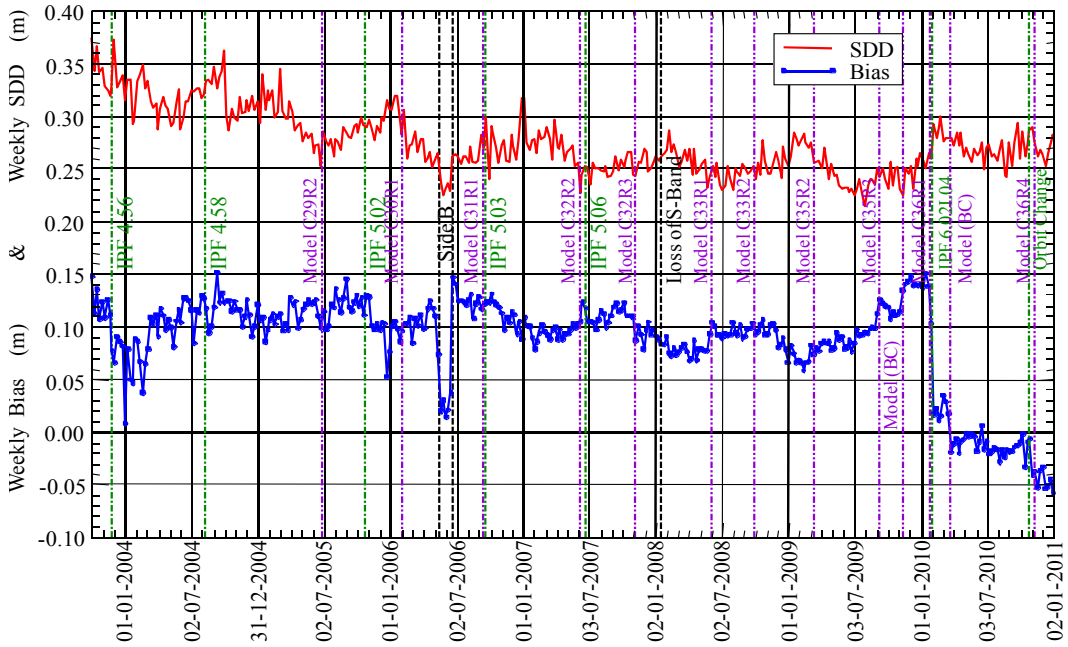

(b)

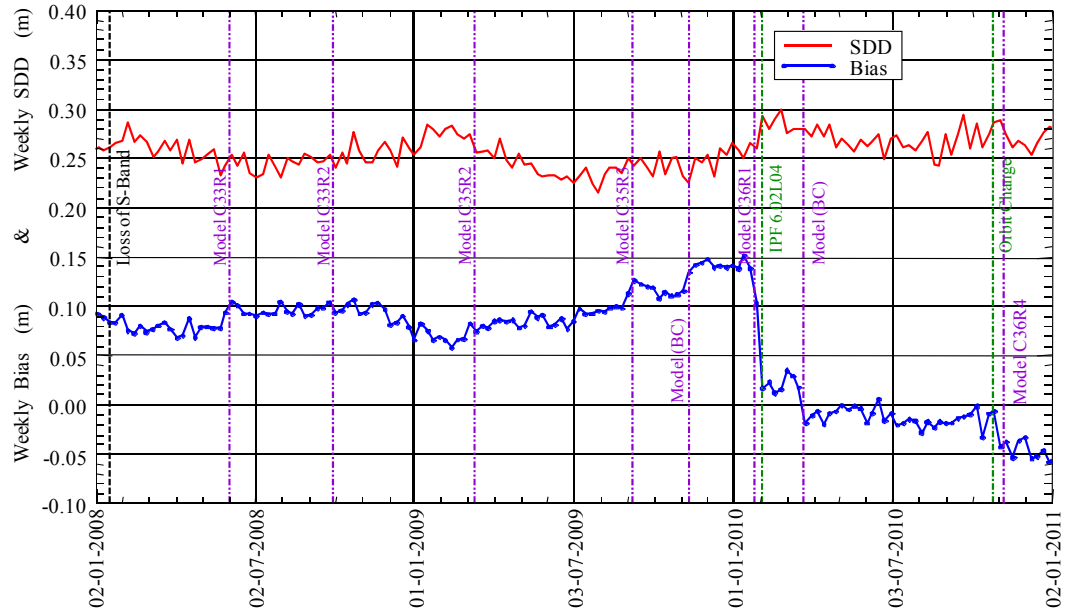

Figure I.9: Time series of weekly SWH bias and standard deviation of difference (SDD) between RA-2 Ku-Band and WAM model FG since late 2003 (a) and during the last 3 years (b).

In order to clarify this, the same analysis was done for Jason-2 SWH. The SDD between altimeter and model FG for both ENVISAT RA-2 (same SDD curves shown in panel a of Fig. I.10) and Jason-2 are shown in panel (b) of Fig. (I.10). To aid the comparison, the difference between the new and the old SDD for both altimeters are also plotted (after multiplying them by 5 to make them easier to read and compare). One should not try to get any conclusion from the high SWH part of the plots due to the limited number of occurrences of those cases and. It is clear that Jason-2 SWH SDD values show similar degradation. However, the magnitude of this degradation is smaller. Although, one can conclude that the IPF 6.02L04 may not be totally responsible for the degradation, it still shares the responsibility. For lower SWH values, Jason-2 – model SDD values during the new period are better than the old period. As there was not any announced change in Jason-2 processing, it is possible to conclude that the model change C36R1 resulted in improved SWH values for low wave conditions (roughly below 1.4 m). This improvement at lower SWH for Jason-2 – model clearly contrasts the extremely large degradation in the case of RA-2 – model SDD. It is worthwhile mentioning that most of the SWH values occur globally in the range between ~0.6 m and ~4.5 m with more than half of them below ~2.5 m. This explains the absence of similar degradation in the scatter plots comparing Jason-2 and model.

To eliminate the impact of geophysical conditions due to different coverage of Jason-2 compared to ENVISAT, the same exercise was repeated with the observations constrained within the common coverage region at low- to mid-latitudes (i.e. between 60°N and 60°S). The results (not shown) are not different from those shown in panel (b) of Fig. (I.10). Therefore, the same conclusions are still valid.

I.6 RA-2 S-Band Significant Wave Height

“Envisat RA-2 (A-Side) S-band transmission power suddenly dropped at 23:23:40 UTC on 17 January 2008”. All S-band products are no longer valid since then. This was declared to be a permanent failure by ESA.

Before the failure, the quality of S-band wave height product used to be of acceptable quality after some quality control procedure to filter out the observations contaminated by the “S-band Anomaly” (which disappeared shortly before the permanent failure of the S-band altimeter).

(a)

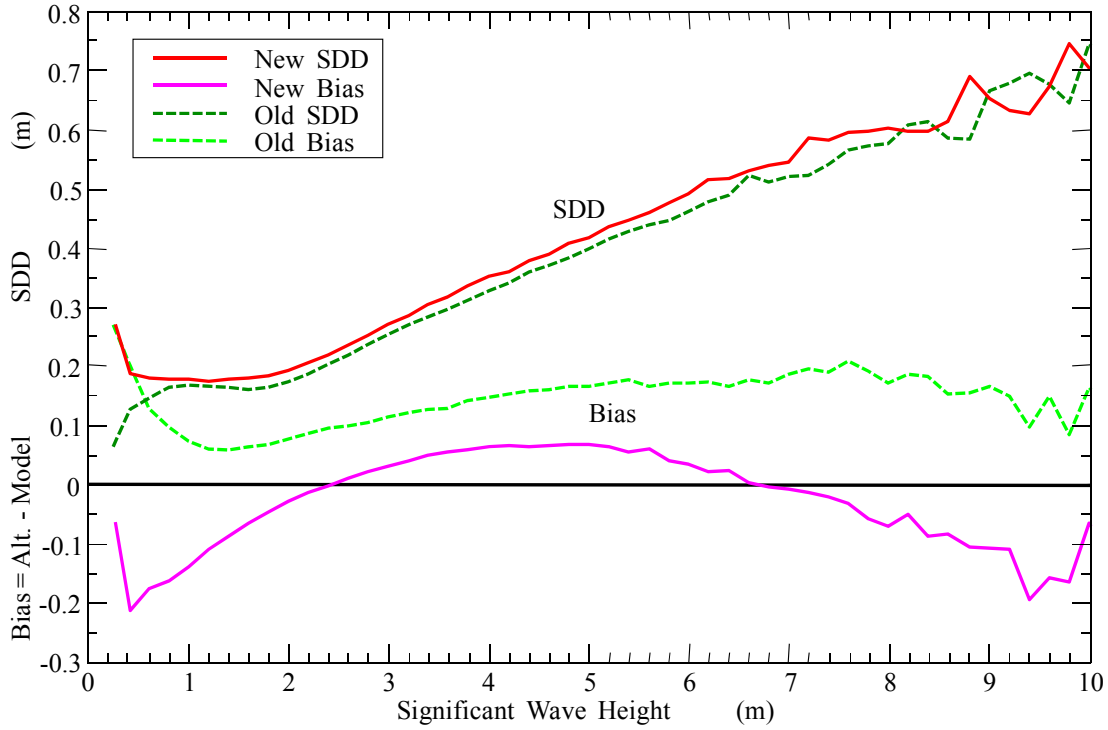

(b)

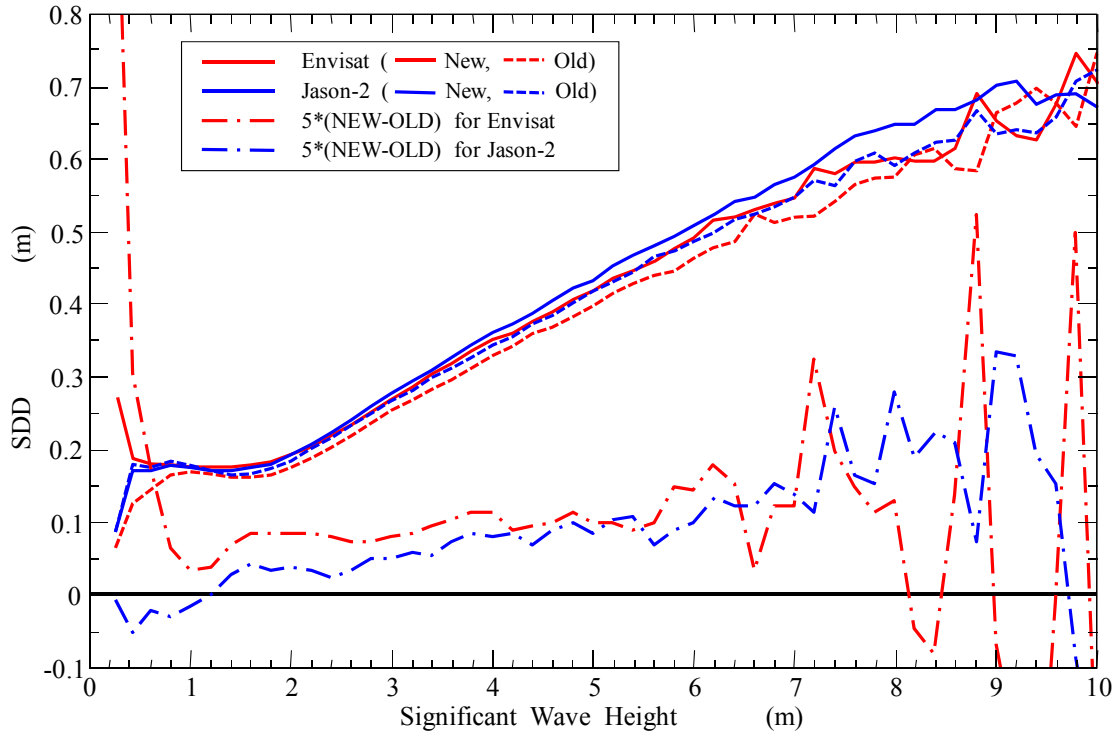

Figure I.10: (a) RA-2 Ku-band SWH bias (RA2 - model) and standard deviation of the difference (SDD) between RA-2 and ECMWF wave model FG as functions of SWH for the periods from 2 February 2009 to 1 February 2010 (Old) and from 2 February 2010 to 2011 (New). (b) The comparison between ENVISAT RA-2 and Jason-2 altimeter SDD for the two periods.

I.7 MWR Products

Two MWR products are monitored and validated: the total column water vapour (TCWV) and the wet tropospheric correction (WTC). Both parameters are functions of the 23.8-GHz (TB23) and 36.5-GHz (TB36) brightness temperatures and wind speed. ECMWF atmospheric model computes TCWV as one of its standard output products. Model WTC can be calculated from pressure, temperature and humidity fields. For the validation of the MWR products analysis (AN) model fields are used.

Collocated TCWV pairs of MWR super-observation and the ECMWF model AN are plotted as density scatter plots in Fig. (I.11) for the whole globe for the periods from 2 February 2009 to 1 February 2010 in panel (a) and from 2 February 2010 to 1 February 2011 in panel (b). The former period represents a full year before the implementation of RA-2 processing chain IPF 6.02L04 on 1 February 2010. The latter period represents a full year with data processed with IPF 6.02L04. It should be stressed that strict quality control based on Altimeter products was implemented to remove a large number of outliers resulted from sea-ice contamination. Apart from a handful of outliers, the MWR TCWV observations agree very well with the model for both periods. Some of outliers happen very close to the coast, which suggests possible land contamination. The agreement is very good with a scatter index (SDD normalised by the mean value of the model) of about 8% and a correlation of 99%.

The main difference between the two scatter plots is the hump below the main cloud between model TCWV values of 15 and 20 kg/m^2 for the earlier period (panel a of Fig. I.11). This hump, which used to occur at every region or sub-region, was a puzzle that could not be explained. Some investigation was carried out, but it seems that the outliers within this hump do not follow any specific pattern and can happen anywhere. The IPF 6.02L04 was able to eliminate that hump (panel b of Fig. I.11). This is one of the positive impacts of the processing chain IPF6.02L04.

The time series of weekly bias and SDD between MWR and ECMWF model TCWV since late 2003 are shown in panel (a) of Fig. (I.12) while the time series for the last three years are shown in panel (b). Fig. (I.12) suggests that there is a seasonal cycle in the bias during the last 4 years or so. However, it was not possible to neither prove nor disprove the genuine existence of this seasonal cycle. The other remark is the drier nature of the MWR observations compared to the model values.

The impact of various IPF instrument processing chains, like IPF Ver. 4.56 (November 2003) and IPF Ver. 6.02L04 (February 2010) and model changes like model Cycle 32R2 (November 2007), Cycle 35R2 (March 2009) and Cycle 36R4 (November 2010) can be clearly seen in Fig. (I.12). The MWR TCWV product is used to assess the ECMWF atmospheric model changes as an independent source of data. For example, the significant improvements, both the random and the systematic errors, of the model Cycle 36R4 were very obvious when compared against MWR products. The improvement of the MWR products due to the implementation of IPF6.02L04 can also be detected from the time series plot (Fig. I.12). The “hump” mentioned earlier was certainly one of the reasons for this improvement.

(a)

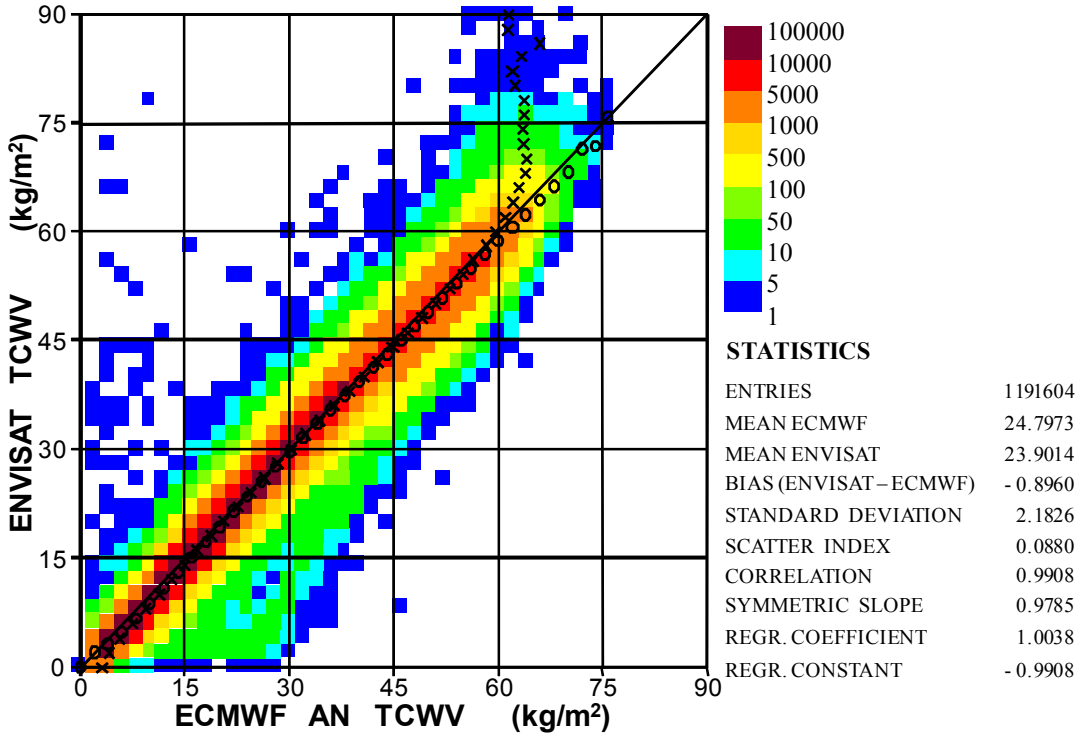

(b)

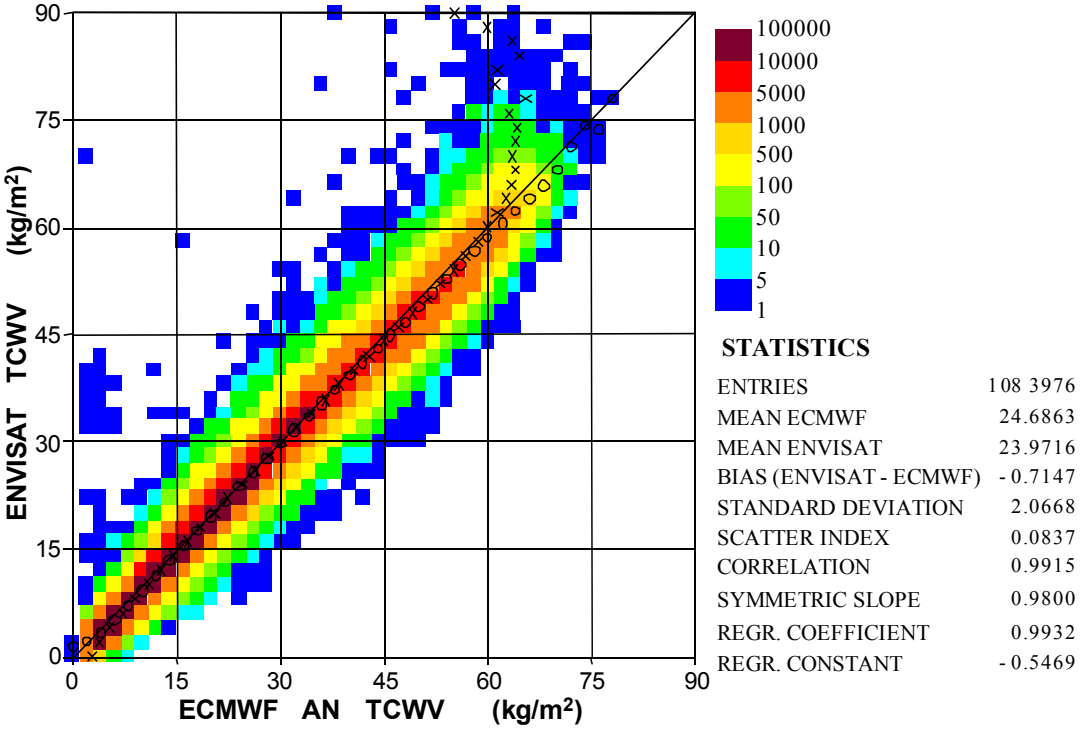

Figure I.11: Global comparison between MWR and ECMWF model AN TCWV values during the periods: (a) from 2 February 2009 to 1 February 2010; and (b) from 2 February 2010 to 1 February 2011.

(a)

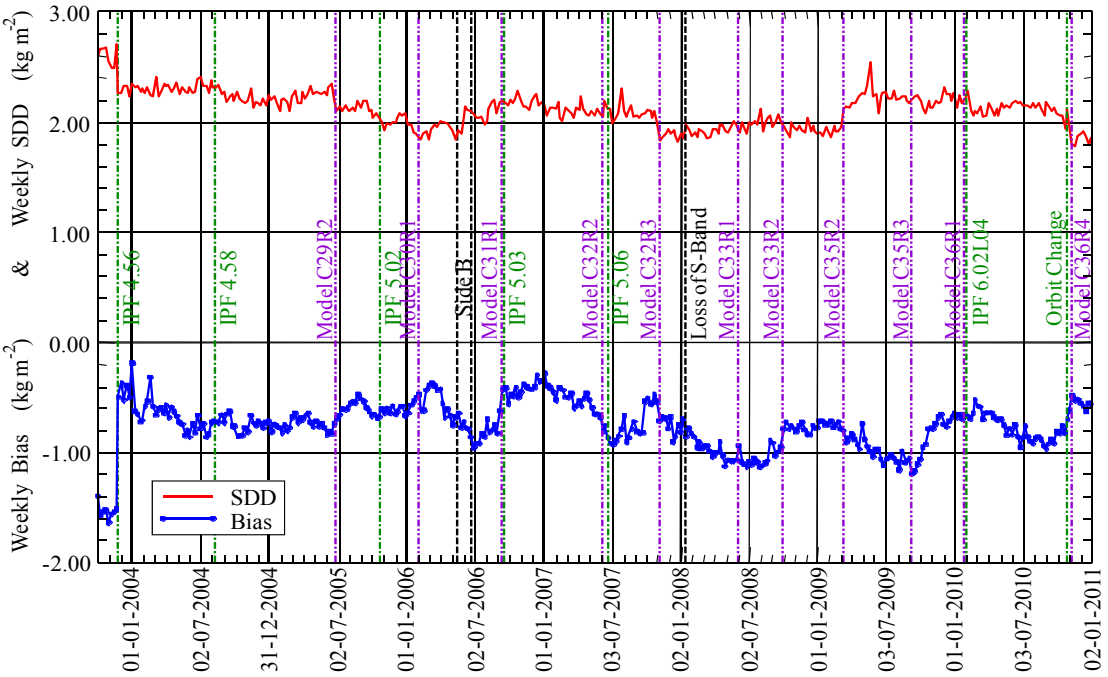

(b)

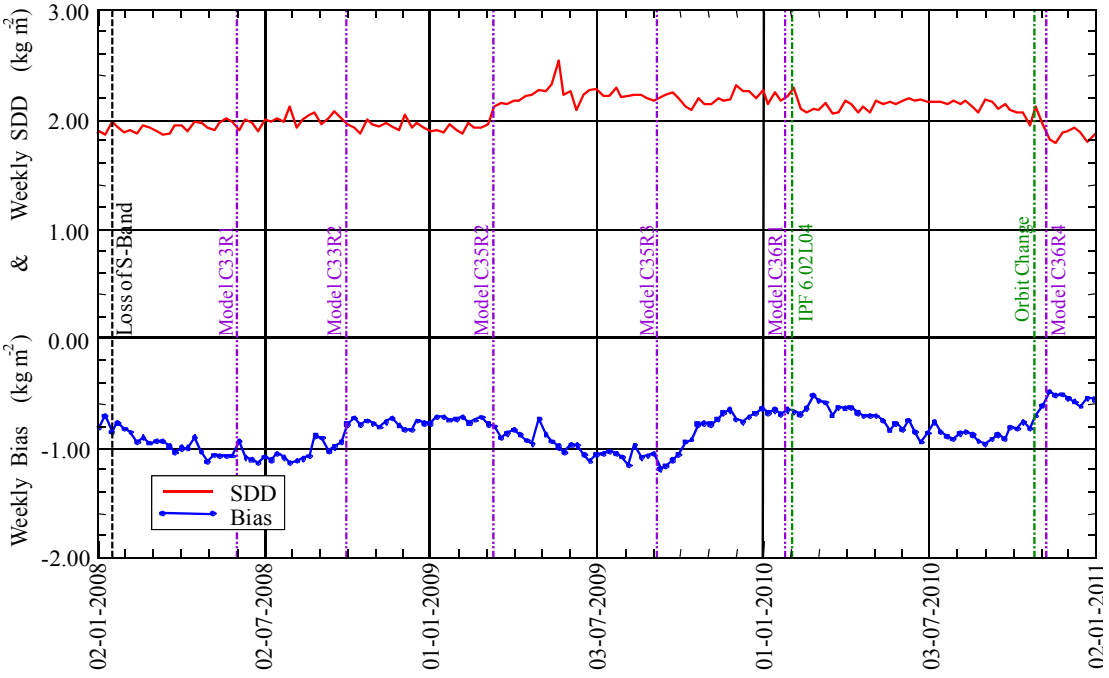

Figure I.12: Time series of weekly TCWV bias and standard deviation of difference between MWR and ECMWF model AN since late 2003 (a) and during the last 3 years (b).

Collocated WTC pairs of MWR super-observation and the ECMWF model AN are plotted as density scatter plots in Fig. (I.13) for the whole globe for the periods from 2 February 2009 to 1 February 2010 in panel (a) and from 2 February 2010 to 1 February 2011 in panel (b). The latter period represents a full year with data processed with the RA-2 processing chain IPF 6.02L04 (since 1 February 2010) while the former represents the earlier situation. Similar to the TCWV product, the majority of the MWR WTC observations agree very well with the model counterpart. The agreement is very good with scatter index of about 9% and a correlation of about 99%. However, there are quite a number of outliers as well. The outliers are mainly associated with model low values (less than ~10 cm). As for the case of TCWV, the major parts of the outliers occur near the ice edges. Therefore, stricter QC criteria involving model sea ice information were used in an attempt to eliminate most of those outliers. It is clear that the WTC scatter plot in Fig. (I.13) does not show any hump similar to that appears in the TCWV plot of Fig. (I.11). However, one of the adverse impacts of the IPF 6.02L04 can be seen by comparing panel (b) with panel (a) of Fig. (I.13). The existence of a secondary cloud of collocations running parallel to the main cloud with MWR values higher than the model can not be missed. This cloud did not exist before the implementation of IPF6.02L04 (panel a of Fig. I.13). Investigations are being carried out to understand the possible reasons for this.

The time series of weekly bias (MWR-model) and SDD between MWR and ECMWF model analysis WTC over the last few years is shown in panel (a) of Fig. (I.14). The same plot over the last 3 years is shown in panel (b) of Fig. (I.14). It is clear that MWR globally underestimates the WTC on average by about 13 mm compared to the model everywhere. The bias with respect to the model follows a seasonal cycle similar to that of TCWV. A slight degradation as a result of the implementation of IPF6.02L03 can be spotted as an increase of the SDD. This is mainly due to the existence of the secondary cloud of collocations appeared in the scatter plot shown in panel (b) of Fig. (I.13). Apart from that, there is quite good resemblance between the WTC time series (Fig. I.14) and the TCWV ones (Fig. I.12). Therefore, the same conclusions can be drawn for WTC regarding the impact of the IPF (except for IPF6.02L04) and the model changes and the seasonal cycle.

I.8 Wind and Wave Random Error Estimation

Comparisons of altimeter (or, in fact, any measuring system) products against model results and against in-situ buoy observations are the usual way to verify those products. This is done here and is shown in a form of scatter plot as it is the case for Fig.'s (I.4), (I.5), (I.7) and (I.8) or in a form of time series as was the case for Fig.'s (I.6) and (I.9). Abdalla et al. (2010) described the validation and the use of wind and wave products from Jason-2 radar altimeter fast delivery OGDR-BUFR products in a similar way. Those types of comparisons can give some qualitative indications about the quality of altimeter product. However, it is not possible to provide a precise statement about the errors of each product.

(a)

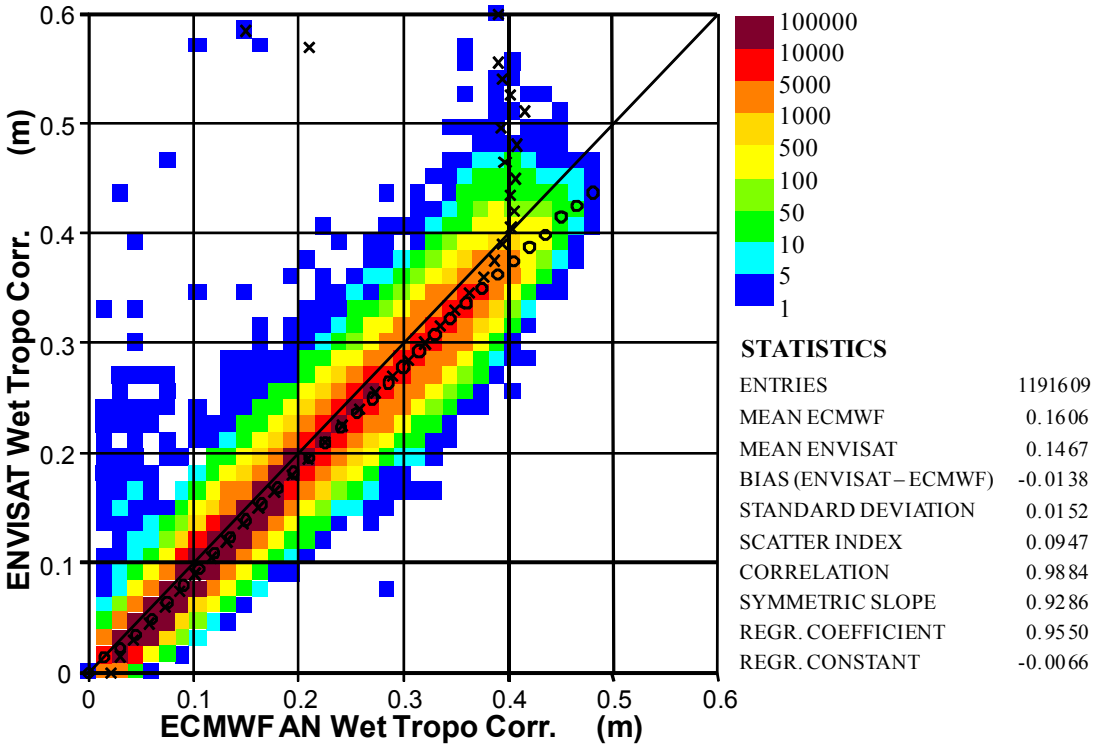

(b)

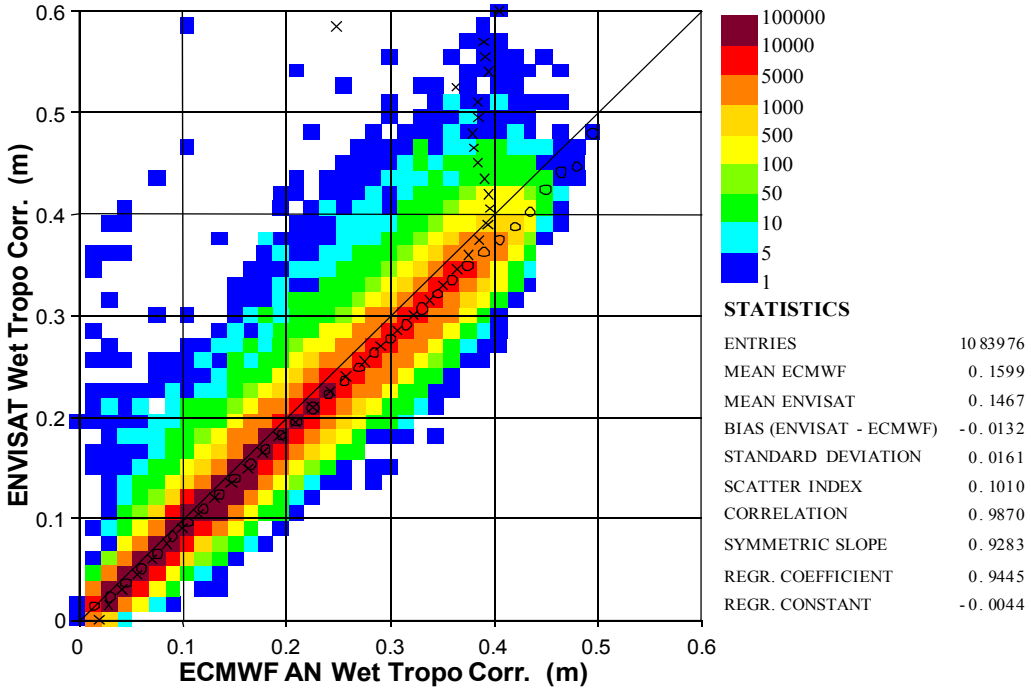

Figure I.13: Global comparison between MWR and ECMWF model AN WTC values during the periods: (a) from 2 February 2009 to 1 February 2010; and (b) from 2 February 2010 to 1 February 2011.

(a)

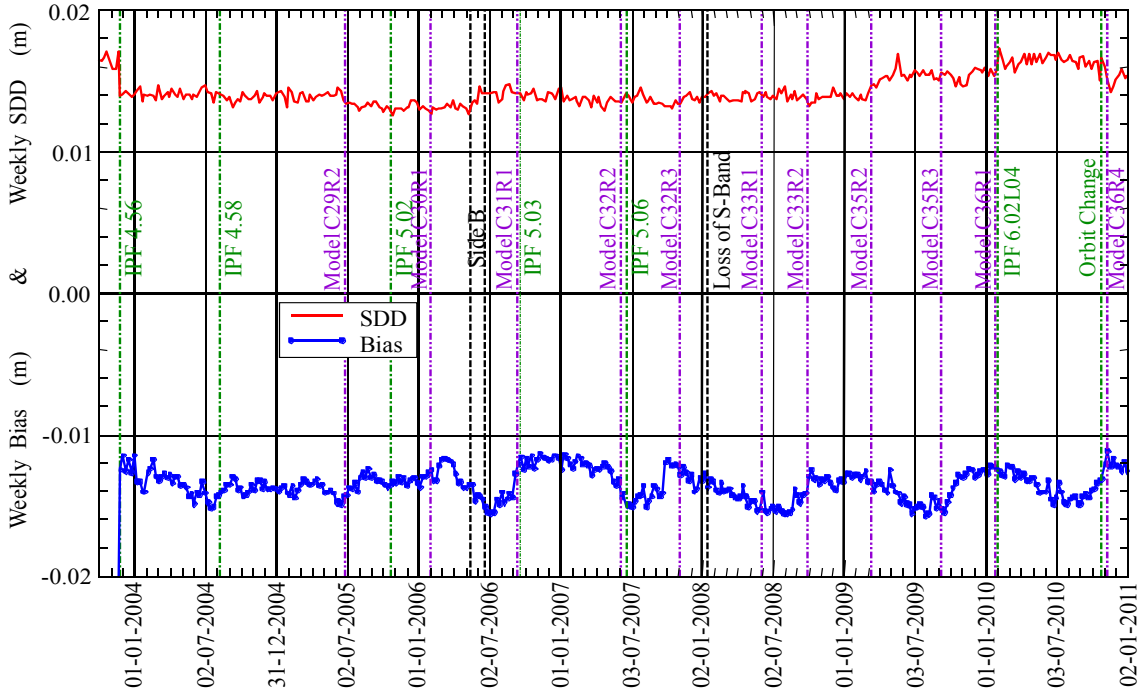

(b)

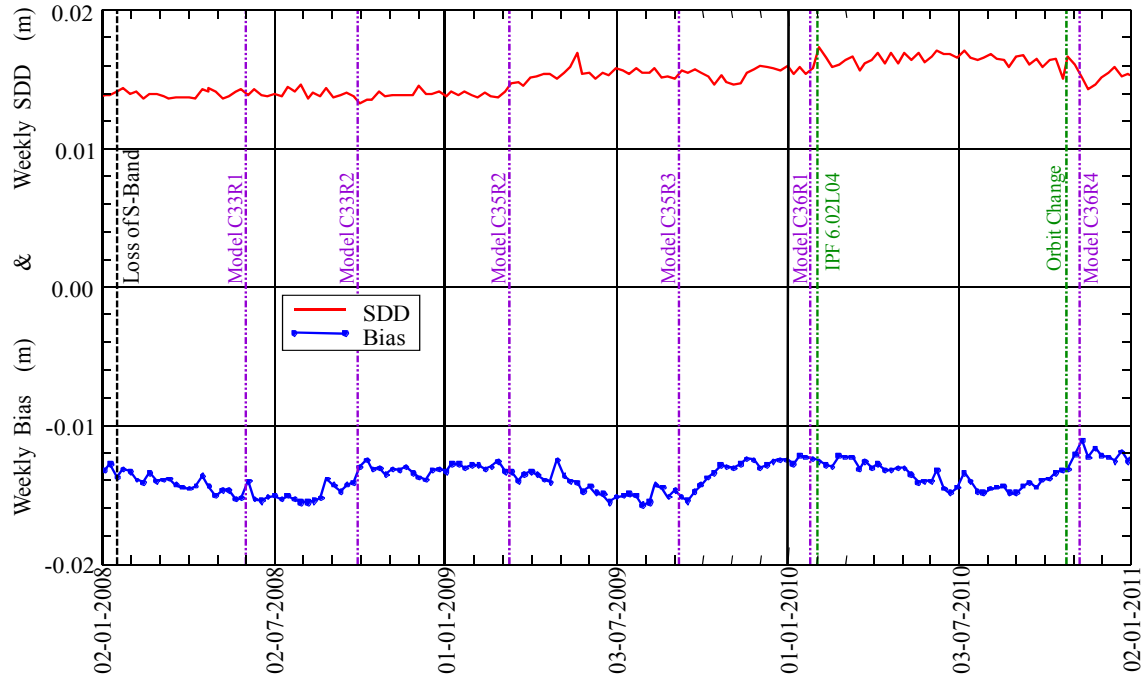

Figure I.14: Time series of weekly WTC bias and standard deviation of difference between MWR and ECMWF model AN since late 2003 (a) and during the last 3 years (b).

The triple collocation technique has been used by several researchers to fill this gap. Stofflen (1998) applied this technique to estimate the errors of wind measurements from ERS-1 scatterometer, buoys and model analysis. Caires and Sterl (2003) used the same technique to estimate the errors in the 40-year ECMWF Re-Analysis (ERA-40) wind speed and significant wave height. Tokmakian and Challenor (1999) implemented the same technique to estimate the mean sea level anomalies from the model, ERS-2 and TOPEX/Poseidon altimeters. Freilich and Vanhoff (1999) and Quilfen et al. (2001) used a similar approach with an assumption that the true wind speed is Weibull distributed. Janssen et al. (2007) estimated significant wave height errors in ERS-2, buoy and ECMWF model analysis, first guess and hindcast. They extended the method to include two extra sources of information, i.e. quintuple collocation, to estimate the covariances due to the existence of correlations between the errors in ERS-2 and ENVISAT observations. This was the way out to estimate the errors in ENVISAT RA-2 wave heights in a collocation data set that involves ERS-2 data and model first-guess data. Triple collocation technique was also used by Abdalla and Janssen (2007) in a different context to estimate the error of the total column water vapour from the micro-wave radiometers onboard ENVISAT and Jason-1 as well MERIS onboard ENVISAT and the ECMWF model analysis. On the other hand, Janssen et al. (2007) also proposed a totally different approach that does not require three estimates for the truth. Instead, they made use of the change of the standard deviation of the difference between the ERS-2 altimeter wave height super-observations and the ECMWF model by varying the number of observations used for the super-observation.

The term “error” is commonly used, in fact, to describe the uncertainty in the measurement or the model output. Strictly speaking the error, or better the instantaneous error, is the difference between the estimate and the “unknown” truth. The standard deviation of the instantaneous errors is what is usually termed as “error”. However, the term “error” as commonly accepted will be used here.

Given three independent estimates, with uncorrelated errors, of the truth, T, it is possible to show that error in each estimate can be found using the “known” variances and covariances of the three data sets in addition to the “unknown” covariances of the errors. Therefore, further assumptions are needed to estimate the error covariances. The assumption that the errors are not correlated is very useful as under such an assumption the error covariances vanish. If the assumption is not correct, the error estimates would not be correct. It is also important to note that although the errors in two data sets may not be correlated directly, it may possible to have a pseudo correlation due to the nonlinear nature of both errors. This is what Janssen et al. (2007) found when they tried to estimate the errors of ERS-2 and ENVISAT altimeters from a collocation that involves both altimeters and the buoys and another collocation that involved ENVISAT, which was not assimilated in ECMWF model at the time, and the model first guess. Contradictory results were obtained. Then with the help of two extra data sets, it turned out that there was a strong correlation between the errors in both altimeters.

I.8.1 Data Used

Apart from the covered period, the data sets used for this study are mainly similar to those used by Abdalla et al. (2010). Therefore, only a short description is given here with emphasis on the different aspects.

The first data set used in this study consists of the Ku-band significant wave height (SWH) and surface wind speed within the BUFR (Binary Universal Form for the Representation of meteorological data) version of the Operational Geophysical Data Record (OGDR) of Jason-2 radar altimeter received in near real time (NRT) from EUMETSAT and NOAA. The OGDR product may be of slightly degraded quality compared to the final Geophysical Data Record (GDR) which is not available for operational weather prediction. However, the quality of the SWH and the surface wind speed parameters does not differ between the OGDR and the GDR. It is only the retracker which is of lower quality.

The second data set consists of SWH and wind speed collected by wave buoys or various wave gauges mounted on offshore platforms as disseminated to the weather centres via the Global Tele-Communication System (GTS). It is commonly believed that this type of data represents the ground truth. The total number of in-situ stations is very limited (slightly above 100) and most of them are located in the Northern Hemisphere (NH) around the North American and European coasts including two buoys in the Western Mediterranean. The exceptions are a few buoys in the Tropics (mainly around Hawaii). Therefore, any assessment involving in-situ data would not be of global coverage strictly speaking. The term “buoy” is usually used to refer to this type of data even if it is originated from a different in-situ source. More information about in-situ ocean wave data, including the pre-processing method used for the quality control and averaging, can be found in Bidlot et al. (2002).

The triple collocation technique with the assumption of uncorrelated errors does not work with the model analysis (AN) or the model first-guess (FG). Even short term model forecasts (FC) may not be suitable as well. The SWH from Jason-2, Jason-1 and Envisat RA-2 are all assimilated into the ECMWF ocean wave model. Jason-1 SWH has been blacklisted since late March 2010 following the degradation of the product caused by the instability of the platform. Even if the SWH from one or more of the altimeters are not used, it cannot be considered that the errors in the model AN and FG are independent from that altimeter (Janssen et al., 2007). All altimeters share the same principles of measurements and algorithms. The dependency becomes weaker further along the forecast range. Therefore, altimeter data and the model forecast (FC) can be assumed to have independent errors, especially for forecasts beyond 2-3 days except for any possible systematic errors in the observations. Therefore, it was decided to run a wave model stand-alone experiment without any data assimilation (model hindcast). The model (Janssen, 2004) is configured very similarly to the ECMWF wave model operational configuration that has been in place since late January 2010. The details are given in ECMWF (2010). The experiment used the 6-hour wind vector analysis fields from the high resolution T1279 (16-km horizontal resolution) atmospheric model operational since late January 2010. The wind fields for the period prior to the operational implementation of the high resolution model were obtained from the pre-operational experimental suite (e-suite).

On the other hand, the wind speed data from altimeters are not assimilated in the ECMWF atmospheric model. However, the buoy wind data are assimilated. This leads to a high correlation in error between the model analysis winds and the buoys and the model first-guess winds and the buoys preventing the use of those model fields in triple collocation. An atmospheric model run without the assimilation of buoy winds for a long period of a year, or even few months, is very expensive. Fortunately, the impact of assimilating wind data is short-lived. It is commonly accepted that 24 hours in the forecast is enough for the model to loose the impact of assimilated wind information. Therefore, 1-day forecast fields will be used for wind speed.

The NRT altimeter data from Envisat and Jason-1 are used to form two independent triple collocated data sets. The former data stream is made available by ESA. In particular, Level 2 of RA2 Fast Delivery Marine Abridged Records (FDMAR) product is used. For Jason-1, OSDR product is used here. In fact, the two data sets are not needed here for the estimation of Jason-2 products. Instead, two other triple collocation data sets are constructed each consisting of the altimeter (Jason or Envisat), the buoy and the model. The corresponding errors are estimated independently for each data set ending in three error estimate for the buoys (one from each triple collocation set), three error estimates for the model in addition to single error estimates for each altimeter. If the three error estimates for the buoy are almost equal and similarly for the three model errors, then one can be more confident about the robustness of the approach.

The altimeter data are pre-processed in a way similar to the approach outlined in Abdalla and Hersbach (2004) with slightly modified parameters. The data go through quality control process to remove erroneous and inconsistent observations. The data is then averaged along the track to form super-observations with scales compatible with the model scales of around 75 km. This corresponds to 13 individual (1 Hz) Jason-1 and Jason-2 observations and to 11 individual (1 Hz) Envisat observations.

The data cover the period from 1 August 2009 to 31 July 2010. It should be noted that the model is changed few times a year. Although this may impact the results, it is not the case for this study as the model changes during this period are expected to be of limited impact on wind and waves. However, there was an important change of the Envisat RA-2 processing chain introduced on the 2nd of February 2010. This change has a significant impact as far as the SWH and wind speed are concerned. Furthermore, Jason-1 suffered a period of instability starting from late March 2010. This was reflected in a degradation of Jason-1 products especially the wind speed.

I.8.2 Triple Collocation

Comparisons of pairs of observation products are usually not enough to estimate the error in each product. If enough data products are available, a multiple collocation analysis can be used to give some absolute error estimates of each product. A simplified version of the approach proposed by Janssen et al. (2007) was used here. Three triple collocation exercises were performed. For the first exercise, Jason-2, buoys and model (hindcast for SWH and forecast for wind speed) were collocated. The second and the third data sets are similar to Jason-2 being replaced by Envisat RA-2 and Jason-1, respectively. The collocation is built up by collocating first the altimeter super-observations with the model using proper interpolation. Then the buoy observations are collocated with the model as well.

Finally, the altimeter observations (and the model values at the altimeter locations) are collocated with the buoy observations (and the model values at buoy location) within 2 hours and 200 km (this will be adjusted for later). The model values at the altimeter and the buoy locations are used for the triplet selections as will be described later.

Ideally, it is desirable to collocate the altimeter and buoy observations at no spatial or temporal difference. Unfortunately, there would be very few collocations, if any. Fig. (I.15) shows the number of Jason-2-buoy-model triplets in a year for various limitations on the collocation distance. It is clear that the more restricted the distance is the less the number of collocations are and, therefore, the less statistically representative the results are. It will be shown later that the more relaxed this condition is, the more the representativeness errors become. On the other hand, the temporal restriction was not tested as the buoy super-observations are constructed using 5 observations with 1-hour increments. The 2-hour restriction is within the 4-hour duration of the buoy super-observations.

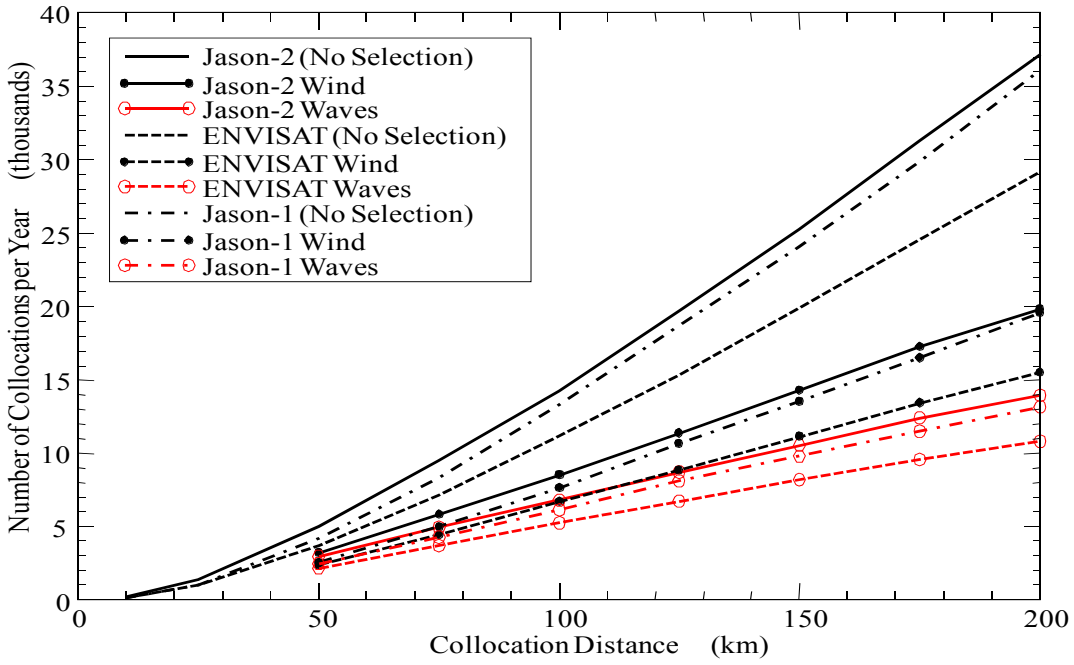

Figure I.15: Number of collocations for various restriction conditions for the period from 1 August 2009 to 31 July 2010.

It is essential that assumptions have to be made regarding the relation between model and observations on the one hand and the truth on the other hand. At the same time this gives an implicit definition of the error. Because of an assumed relation between observation and truth it follows that in case that this relation is incorrect the error has both a systematic and random component. Therefore, the assumption of uncorrelated errors is by no means evident, and should, if possible, be tested.

Suppose we have three estimates of the truth, denoted by X_p, p=1,2,3, obtained from observations or from simulations by means of a forecasting system of the same truth, T. In the following all these

estimates of the truth will be referred to as measurements. Furthermore, it is assumed that the measurements depend on the truth T in a linear fashion for any triplet, i, as follows:

$$X_{pi} = \beta_p T_i + e_{pi} \quad (1)$$

where e_{pi}, p=1,2,3 denote the instantaneous (or individual) residual errors in the measurements X_p and β_p are the linear calibration constants.

The calibration constants are found by an iterative procedure utilizing a neutral regression (Marsden, 1999) and the errors in the variable X_p using the method described by Janssen et al. (2007). For the simplicity of the formulation below, the variables Xp are divided by the calibration constants; i.e. $X_p = X_p / \beta_p$. By taking mean-square of the differences between each pair in the triplets, it is possible to write for the variance of the unknown error of each product (Janssen et al. 2007) as:

$$< e_{pi}^2 >= 0.5 \left[<\left(X_p - X_{p1}\right)^2> + <\left(X_p - X_{p2}\right)^2> - <\left(X_{p1} - X_{p2}\right)^2> \right] \quad (2)$$

Here, X_{p1} and X_{p2} are the other two products in the triplet. It is only possible to reach to Eq. 2 by assuming that there is no correlation between the errors of the triplets. For example, Eq. 2 cannot be used to estimate the errors if the triplet includes a model analysis or first guess together with the observations that have been assimilated into that model. Furthermore, two altimeter products can not be used in a triplet to estimate errors through Eq. 2 due to the intrinsic correlation arising from sharing the same algorithm and nature of error (Janssen et al., 2007). Detailed description of the technique can be found in Janssen et al. (2007).

I.8.3 Estimation of SWH Errors

One of the keys to the success of the triple collocation technique as presented above is to ensure the independence of the errors in all data sets used. This was done by selecting the altimeter, the buoy and the model hindcast data. The three data sources are totally independent estimation of the truth and therefore, their errors are expected to be uncorrelated.

The second key of success is the proper selection of triplets. The collocated altimeter and buoy measurements should be very close to each other to represent the same truth and, at the same time this restriction should be relaxed to have enough triplets to yield statistically representative error estimates. Fig. (I.15) shows that the number of collocation triplets of Jason-2, buoy and model within a collocation distance between the altimeter and the buoy over a period of a year is about 37 thousand. With some quality control checks, this number reduces to about 14 thousand. The quality control checks are composed of few basic tests to ensure that all the measurements in the triplet are valid (e.g. SWH values between 0.5 and 20 m). Another selection criterion is to ensure that both the altimeter and the buoy see the same truth. This is done by rejecting any triplet when the model estimates at the altimeter location and at the buoy location differ by more that 5% as was recommended by Janssen et al. (2007). The assumption here, which is a fair one, is that the model is able to reproduce the true atmospheric variability. Therefore, too different model SWH value is a strong indication of the non-homogeneity of the wave fields and the altimeter and the buoy measurements do not represent the same truth. Furthermore, any triplet with the model mean wave direction at the altimeter and at the

buoy locations are different by more than 45 degrees is rejected. This is again another measure for the homogeneity of the field. Reducing the acceptable collocation distance to 100 km, for example, reduces the number of collocations to slightly above 7,000. At 50-km distance, the number of collocations over a year is only few hundreds.

Using Eq. 2 to estimate the SWH error for the three altimeter-buoy-model data set with the dependence of the error on the collocation distance is shown in Fig. (I.16). It was found that the change of error with respect to the collocation distance is linear. Altimeter (at different levels but have more or less same slope) and buoy SWH errors are found to increase by increasing the collocation distance at a rate of about 0.024 m and 0.004 m, respectively, per 100 km. The model error was found to reduce at a rate of about 0.023 m/100 km. More or less the same slopes were found for the other triple collocation data sets; namely: Envisat-buoy-model and Jason-1-buoy-model.

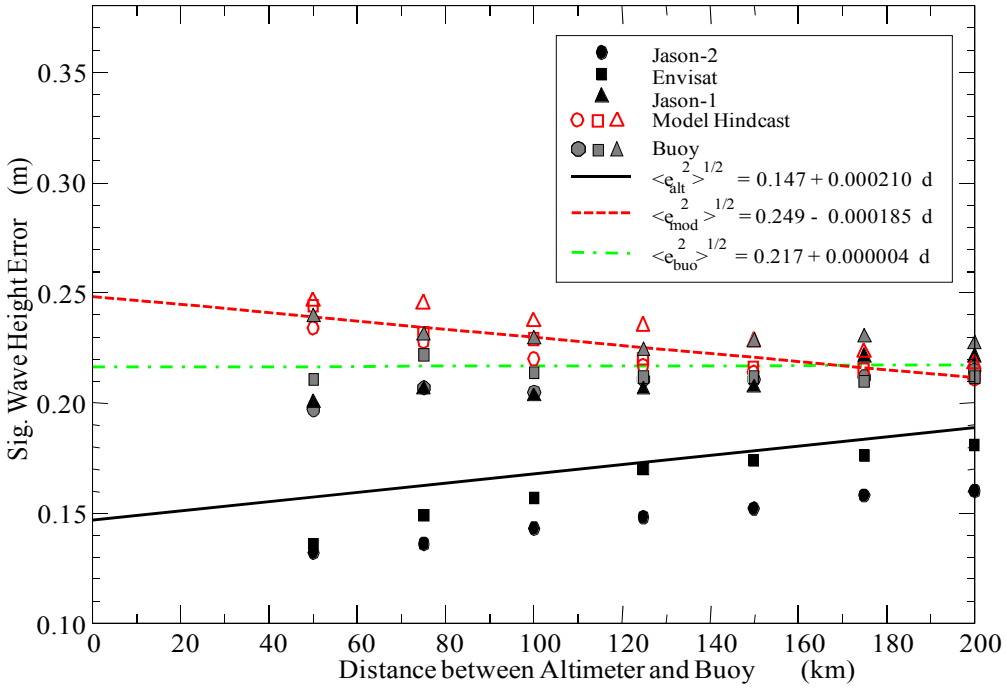

Figure I.16: Change of wind speed errors as functions of the maximum allowed collocation distance. The linear regression fits are given. The errors $<e_{alt}^2>^{1/2}$, $<e_{mod}^2>^{1/2}$, $<e_{buo}^2>^{1/2}$ of the altimeters, the model and the buoys are in m while the collocation distance d is in km.

When the collocation data set is binned based on the wave height values or the month in order to estimate the errors at each bin, the number of collocations may not be enough to draw firm conclusions. Therefore, the result above can be utilized to increase the number of collocations by adopting the 200-km restriction of the collocation distance. The error estimates are then adjusted by using the results in Fig. (I.16). An argument can be raised if one needs to adjust for a zero collocation distance or for a collocation distance depending on the scale of the model and super-observations which is about 75 km in the current data sets. Using the 75-km distance instead of the 0-km distance, would add about 0.018 m and 0.003 m to the altimeter and the buoy errors, respectively, and will reduce the model error by about 0.017 m. It was decided that a collocation distance equals to the scale of the data would be a proper selection here.

Table I.1 The absolute and relative (SI) significant wave height errors of Jason-2, Envisat RA-2, Jason-1, model hindcast and buoy as estimated using the triple collocation technique using three data sets each involving one of the altimeters in addition to the model hindcast and buoys for the period from 1 August 2009 and 31 July 1010 (mainly in the NH).

	Jason-2 Data Set		*Envisat RA-2 Data Set*		*Jason-1 Data Set*	
Number of collocations	13,920		11,005		13,281	
	Abs. (m)	**SI (%)**	**Abs. (m)**	**SI (%)**	**Abs. (m)**	**SI (%)**
Altimeter Error	0.130	5.4	0.152	6.2	0.192	7.8
Model Hindcast Error	0.234	9.7	0.235	9.7	0.241	9.8
Buoy Error	0.206	8.6	0.203	8.4	0.218	8.9

The estimated SWH errors, both the absolute values and the relative values with respect to the mean (also called scatter index, SI), in the three altimeters: Jason-2, Envisat and Jason-1, the model hindcast and the buoys are listed in Table I.1. The altimeter SWH relative errors (with respect to the SWH mean value) are about 5.4%, 6.2% and 7.8% for Jason-2, Envisat RA-2 and Jason-1, respectively. The model hindcast SWH error is slightly less that 10%, irrespective of the data set used for this estimation, while the buoy SWH error is slightly less than 9%. These values have been adjusted for a maximum collocation distance of 75 km as discussed earlier. It is clear that Jason-2 has the lowest error followed closely by Envisat RA-2. It is important to remind that the Envisat processing has changed in early February 2010 while Jason-1 had few periods of instability. Finally, although the model set-up was very close to the operational ECMWF wave model, it is not exactly the same. The main differences are: The hindcast experiment was forced by 6-hour wind fields compared to changing wind field at each time step in the operational set-up. Furthermore, the impact of gustiness and variable air density was not considered in the experiment. Finally, the operational model assimilates altimeter wave heights and this is not the case for the hindcast experiment used for the error estimation.

To get a better idea about the SWH errors at various regimes of SWH values, the collocated data sets were binned and the triple collocation technique was applied for each bin of wave heights. Fig. (I.17) shows the SWH error at various SWH values. Note that the number of collocations at the bins with high SWH values is very few and may not be representative at those bins. It is clear that the error of Jason-2 SWH is more or less the same at all SWH values while Envisat error is relatively large at low SWH values. The buoy error is lower at higher waves. Finally the model error is high at lower waves and gets better for wave heights above 4 m.

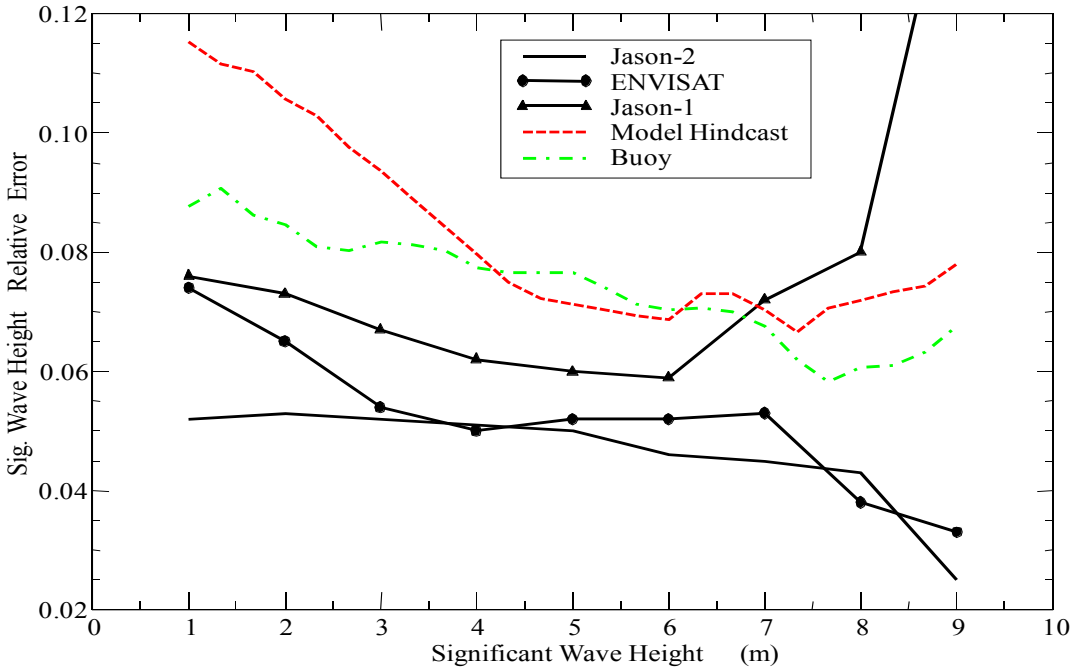

Figure I.17: The SWH relative error as a function of the wave height value.

To get an idea about the seasonal variability of the errors or the error variations due to the changes in the model or measurement quality, the triple collocation procedure was applied to the monthly data. The SWH error as a function of the month of the year is shown as 3-monthly running averages in Fig. (I.18). Jason-2 monthly errors show very small variability over the whole year. Envisat RA-2 shows higher errors around October 2009 and during the summer months of 2010. The impact of the problems of Jason-1 can be clearly seen in a form of increased errors during the last 6 months of the considered period. During the early months (summer 2009), the buoy error was higher than the other months. This may be due to the presence of the hurricanes in the North Atlantic during that period. The model error is almost unchanged over the whole period.

I.8.4 Estimation of Wind Speed Errors

The wind speed from the buoys is assimilated into the ECMWF atmospheric model. Therefore, Eq. 2 cannot be used for any collocation data set involving the buoys and the model AN or FG. Therefore, model forecast which is expected to be independent from the buoy measurements during the forecast range after about 24 hours. The 5%-criteria used for wave height cannot be justified for the wind speed. Compared to the SWH, the wind fields show much higher natural variability. Therefore, constraining the difference between model values at altimeter and at buoy location to 5% would be an artificial constraint. Therefore, this criteria was changed into another that restricts the difference between the SWH (not wind speed) values to 50% ensuring a fair amount of homogeneity and allowing for local winds to have their impact with any constraints. On the other hand, the restriction on the model wind direction difference was tightened up. Any triplet with the model wind direction at the altimeter and at the buoy locations with a difference of more than 20 degrees is rejected. Therefore, within a collocation distance of 200 km and during a whole year, the number of the quality-controlled valid collocation triplets of Jason-2, buoy and model after this criteria is reduced to about

20,000 (out of the original number of 37,000) as can be seen in Fig. (I.15). Reducing the acceptable collocation distance to 100 km reduces the number of collocations to about 9,000. At 50-km distance, the number of collocations over a year is only few 100's.

Similar to what was done for the SWH, the wind speed errors for the triple collocation data set were estimated using Eq. 2 for different collocation distances between the altimeter and the buoy. Fig. (I.19) shows those results. Similar to the SWH case, the relation between the error and the corresponding collocation distance is linear. However, the rates of the change of the error with respect to the distance are rather large compared to those from the SWH. The altimeter and the buoy wind speed errors increase by increasing the collocation distance at a rate of about 0.13 $m.s^{-1}$ and 0.17 $m.s^{-1}$, respectively, per 100 km. On the other hand, the model error decreases at a rate of about 0.24 $m.s^{-1}$ per 100 km. Almost the same slopes can be found from the other triple collocation data sets; namely: Envisat-buoy-model and Jason-1-buoy-model. This result is used to relax the collocation distance to 200 km for more triplets in the collocation data set. The estimated errors are then adjusted based on Fig. (I.19).

The estimated errors for all data sources are tabulated in Table I.2. The wind speed errors were estimated as 1.00 $m.s^{-1}$ (~11.9%) for Jason-2, 0.93 $m.s^{-1}$ (~11.1%) for Envisat RA-2, 1.01 $m.s^{-1}$ (~12.0%) for Jason-1, 1.15 $m.s^{-1}$ (~13.7%) for the buoys and 0.97 $m.s^{-1}$ (~11.5%) for the 1-day model forecast. These figures were adjusted for a maximum collocation distance between the altimeter and the buoy of 75 km. This was selected to reflect the model scale and the scale used to form the altimeter and buoy super-observations. It should be stressed here that the model error here is the ECMWF 1-day forecast error which is quite higher that the analysis error.

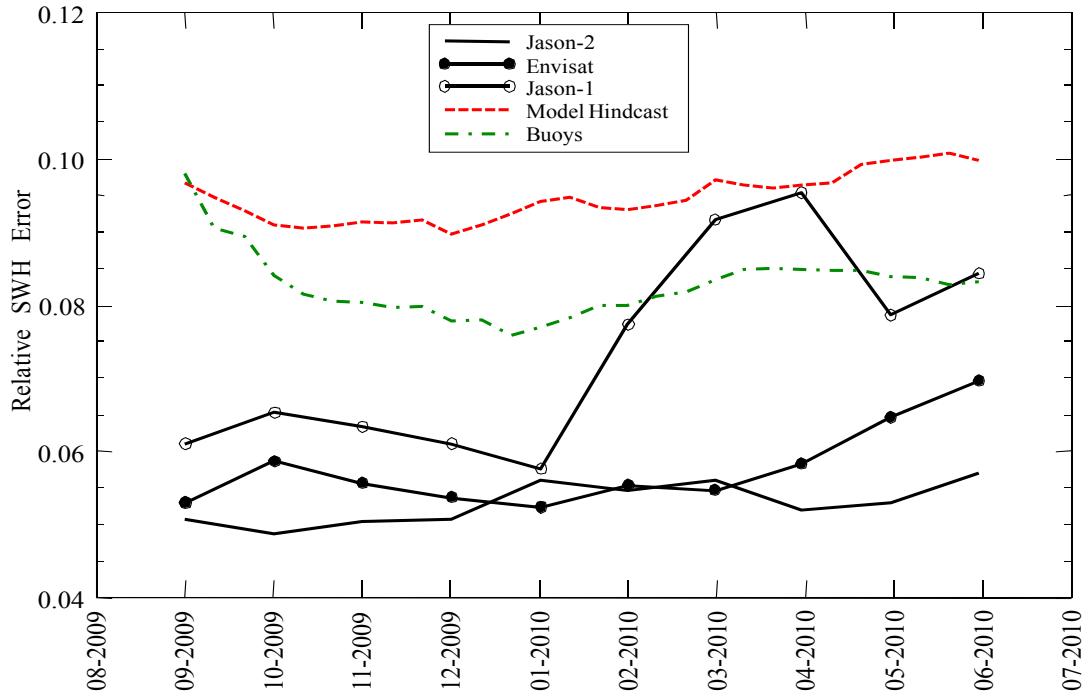

Figure I.18: The time series of the monthly SWH errors (3-month running means).

Table I.2: Similar to Table I.1 for wind speed and the model hindcast is replaced by the ECMWF model 1-day forecast.

	Jason-2 Data Set		*Envisat RA-2 Data Set*		*Jason-1 Data Set*	
Number of collocations	19,856		15,552		19,613	
	Absolute ($m.s^{-1}$)	**SI (%)**	**Absolute ($m.s^{-1}$)**	**SI (%)**	**Absolute ($m.s^{-1}$)**	**SI (%)**
Altimeter Error	1.00	11.9	0.93	11.1	1.01	12.0
Model 1-Day FC Error	0.97	11.5	0.94	11.2	0.97	11.6
Buoy Error	1.15	13.6	1.14	13.7	1.17	13.8

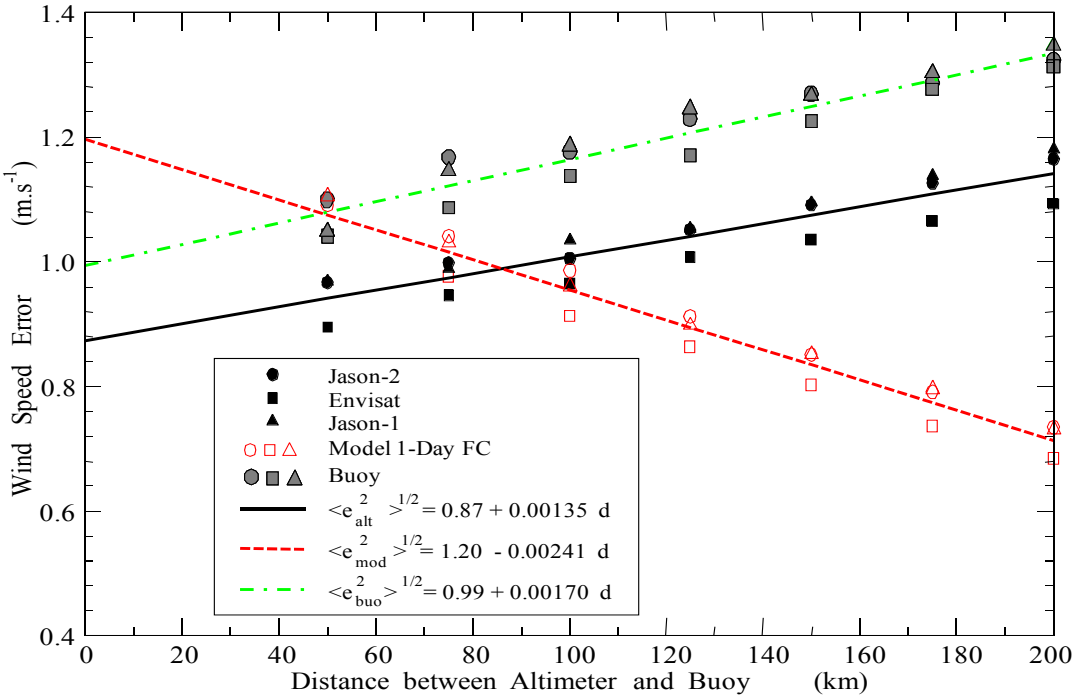

Figure I.19: Change of wind speed errors as functions of the maximum allowed collocation distance. The linear regression fits are given. The errors $<e_{alt}^2>^{1/2}$, $<e_{mod}^2>^{1/2}$, $<e_{buo}^2>^{1/2}$ of the altimeters, the model and the buoys are in $m.s^{-1}$ while the collocation distance d is in km.

To find out what is the wind speed error at various wind speed values, the data sets were binned and the triple collocation technique was utilized to estimate the wind speed error for each subset. Fig. (I.20) shows the wind speed relative error as a function of the wind speed itself. Although Fig. (I.20) suggests that the errors are relatively high at lower wind speed values and decreases for higher values, it should be mentioned that the absolute wind speed errors, in fact, increase by increasing the wind speed value (not shown). However, the increase in the error is not fast enough and therefore the

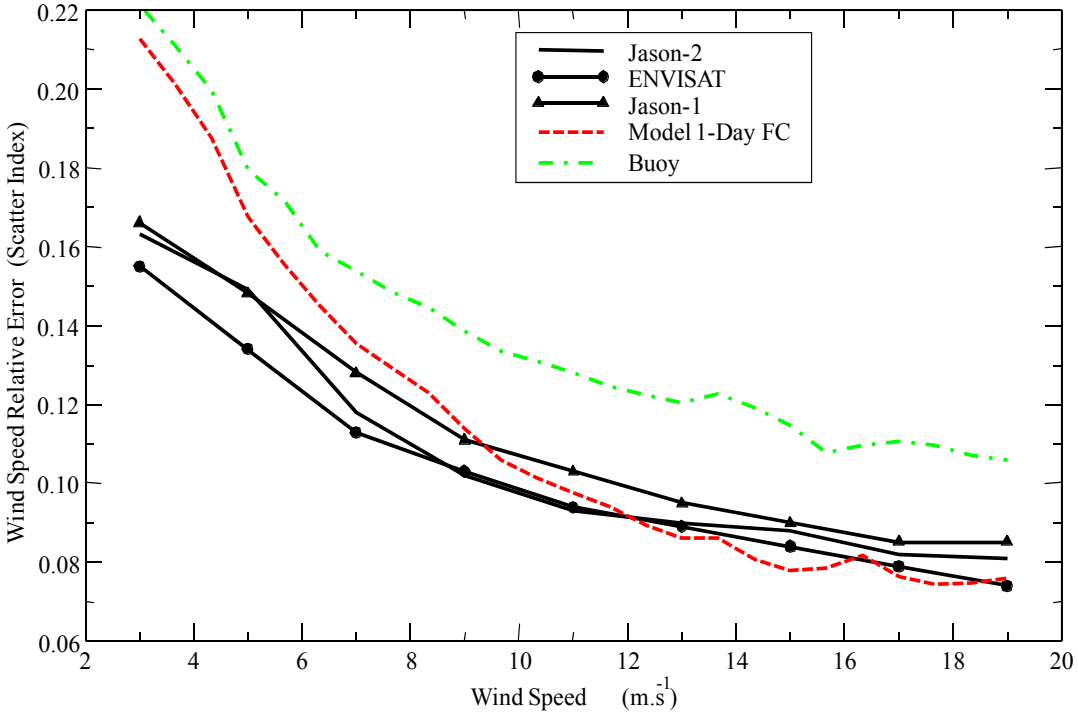

Figure I.20: The wind speed relative error as a function of the wind speed value.

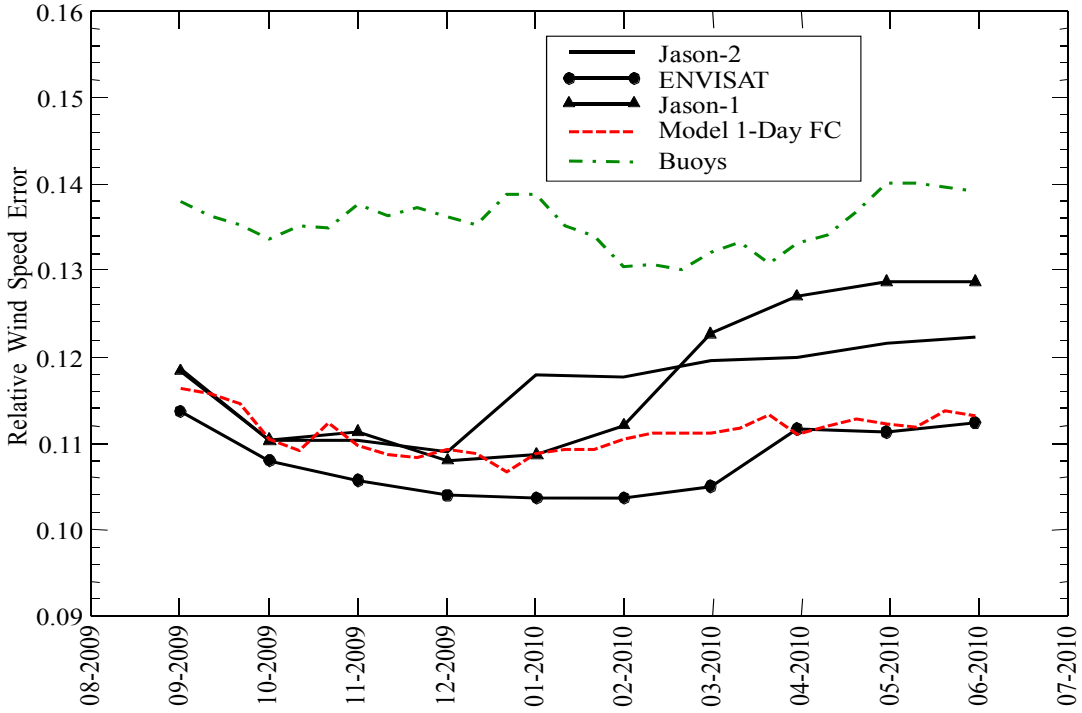

Figure I.21: The time series of the monthly wind speed errors (3-month running means).

relative error appears to be decreasing with wind speed increase. Fig. (I.20) indicates that Jason-2 wind speed is not good at the low wind speed regime. Furthermore, it is clear the error of all instruments, especially the model and the buoys, are very high at low wind speeds with errors of about 16% of the mean for the altimeters and about 25% of the mean for the buoys and the model 1-day forecast. The high buoy error, especially at lower wind speed values, may be a reflection of the fact that the buoy wind speeds communicated through the GTS are reported to the closest 1 $m.s^{-1}$. An interesting observation in Fig. (I.20) is the relative low wind speed error in the model 1-day forecasts for wind speeds higher that 12 $m.s^{-1}$.

The temporal variation of the wind speed errors is shown in Fig. (I.21). Jaons-2 wind speed product seems to have suffered some degradation in February 2010 and may be May 2010. Such possible degradations are responsible for the increase of Jason-2 errors seen in Fig. (I.21) in January 2010 as the plot represents the 3-monthly running average. The impact of Jason-1 degraded products can be clearly seen starting from March 2010.

I.8.5 Summary

Jason-2 near real time OGDR-BUFR wind and wave products have been analysed to estimate their random errors. The triple collocation technique was utilised for this purpose. Jason-2 Ku-band significant wave height (SWH) product turned out to be of very high quality. The SWH error was estimated to be 0.13 m or about 5.4% of the mean. Its relative error is rather equal at most of the SWH range. Envisat RA-2 SWH, which has some degradation at wave height values lower than 3 m, has a slightly higher error of about 0.15 m. Jason-1, which suffered some stability problems between the end of March and end of summer 2010, showed relatively higher errors especially after March 2010.

On the other hand, Jason-2 wind speed error at a level of 1.00 $m.s^{-1}$ (~11.9%) may not be the lowest compared to the other instruments. Envisat RA-2 wind speed error, which was estimated to be 0.93 $m.s^{-1}$ (~11.1%), is the lowest one. It seems that the error in the wind speed at low wind speed values is relatively high for all instruments especially the buoys and the model. The model 1-day forecast winds seem to be of relatively small error for wind speeds in excess of 12 $m.s^{-1}$.

I.9 Conclusions

Continuous monitoring and validation of the ENVISAT RA-2 wind and wave products together with the MWR water vapour products are carried out at ECMWF. Data from ECMWF atmospheric and wave models, from other satellites; namely: ERS-2 and Jason-1 and Jason-2, and from in-situ buoy and platform observations are used for this purpose.

The Ku-band backscatter coefficient has a rather stable monthly mean value. However, the monthly mean values were decreased by about 0.15 dB towards the end of 2009. Similar, but at about half the value, reductions were witnessed for Jason-1/2 altimeters. The S-band backscatter had few jumps due to processing changes before it was lost in January 2008. RA-2 wind speed data are in good agreement with the model and buoy data except for very high wind speeds (~21.4 m/s and above). This was corrected in the RA-2 processing chain IPF Version 6.02L04 (1 February 2010). Ku-band SWH

product is of high quality. The absolute error in Ku-band SWH is about 6%. This is a low value compared to the other wave height observations available to us. The Ku-Band SWH used to be too high by about 4.0% compared to the ECMWF model and the wave buoys before IPF 6.02L04 and virtually unbiased afterwards. There was also an increased standard deviation of the difference between the Ku-band SWH and the model after the implementation of IPF6.02L04. Ku-band SWH product has been assimilated in the ECMWF wave model since 22 October 2003.

The quality of the S-Band wave height product used to be acceptable after some quality control procedure was used to filter out the *RA-2 S-Band Anomaly*. Unfortunately, the S-Band was permanently lost in January 2008.

The MWR products (TCWV and WTC) are stable during the last few years. Apart from a few outliers, the MWR products compare very well with the model. Most of the outliers can be attributed to ice and land contamination and can be filtered out using model information regarding the sea ice. In general, the MWR products are slightly drier than the model except for the Tropical TCWV. A group of outliers, with lower MWR values, that used to appear in the TCWV scatter plots, have disappeared after the implementation of the IPF6.02L04. Instead, a cloud of outliers (with higher MWR values) over most of the range of model values started to appear in the WTC scatter plots. This is still under investigation.

The change of ENVISAT orbit in October 2010 did not have any impact on RA-2 and MWR products except for a slight impact on the wind speed product for only few days just after the end of the manoeuvres.

II. ADVANCED SYNTHETIC APERTURE RADAR (ASAR) WAVE MODE PRODUCTS

II.1 Introduction

ASAR consists of a coherent, active phased array SAR which is a distributed matrix of 320 transmitter/receiver elements operating at C-Band. The long axis of the SAR antenna is aligned in the direction of the satellite path (the azimuth direction). It images a strip of ground to the right side of the platform (range direction). The SAR produces two-dimensional representation of the scene reflectivity at high resolution. ASAR can operate in different modes with Wave Mode is the one of interest here. In the wave mode, ASAR senses the changes in the backscatter from the ocean surface due to the action of long ocean waves. As a result it produces small images (of ~ 5 km x 5km or larger) with 100 km spacing. This intermittent operation provides a low data rate so that the data can be stored on board the satellite and communicated whenever possible. The small images are then processed to produce the SAR cross-spectra (ASAR Wave Mode Level 1b, ASA_WVS_1P) product. Further processing produces the inverted ocean wave (ASAR Wave Mode Level 2, ASA_WVW_2P) product. In fact this latter step can be done offline using several other inversion methods. One method, which is used at ECMWF for the verification of Level 1b product, is the MPIM scheme developed by Hasselmann et al. (1996). ASAR Wave Mode products represent a unique opportunity to provide ocean wave spectra with global coverage. However, there are several limitations. The most important is the inability of the instrument to resolve high frequency (short) ocean wave components. The shortest resolvable wavelength is called the azimuthal cut-off.

II.2 ASAR Data Processing

FD ASAR Wave Mode Level 1b (ASA_WVS_1P) and Level 2 (ASA_WVW_2P) products are validated. Level 1b product is the main product upon which basic quality control is done. Data processing is similar to the procedure used for ERS-2 SAR processing (see Abdalla and Hersbach, 2004). Here is a summary of this procedure:

The stream of ASAR product is split over 6-hour time windows centred at the main synoptic times to coincide with the model output times. The data contents of each time window is pre-processed to generate a list with output positions for the WAM model in order to produce a collocation file of wave spectra to be used for the SAR-inversion system. This includes basic pre-processing quality control checks to reject any spectrum with obvious anomalies and/or inconsistencies. The product parameters are checked and if any is found to be not logical, a quality control flag is set and the spectrum is rejected.

The nearest WAM wave spectra are extracted and used as the first guess (FG) to invert the ASAR product. The MPIM scheme (Hasselmann et al., 1996) which is an iterative method based on the forward closed integral transformation, is used for the inversion. During and after the iterative inverting procedure further quality checks are done. The iterations stop when there is a convergence (within a given tolerance) or until the iteration procedure starts to be unstable. The value of the final cost function (the lower the cost function the better the inverted spectrum is) and the stability of the procedure are used to define the quality of the final inverted spectrum.

Any Level 2 product is accepted only if the corresponding Level 1b product passes the quality control. Further quality checks are performed over accepted Level 2 products to ensure their consistency. Each quality controlled product is then collocated with the closest wave model spectrum. It should be noted that most of the comparisons (scatter plots and time series derived from those plots) between Level 2 product and the wave model are carried out within the spectral range resolvable by ASAR. Therefore, the part of the spectrum with wavelengths higher than the azimuthal cut-off length (as provided by the ASAR Level 2 product) is considered. This is different from the comparisons between ASAR Level 1b product and the wave model where the whole spectrum is considered. Therefore, one needs to be careful in drawing conclusions when inter-comparing both products.

Validation of wave spectra with large number (100's) of degrees of freedom is not a straightforward task. Therefore, the validation is usually done in terms of a limited number of integrated parameters. Significant wave height (SWH), mean wave period (MWP), wave spectral peakedness factor of Goda (WPF), wave directional spread (WDS) and mean wave direction (MWD) are among the most commonly used. These parameters can be defined as:

1. Significant wave height (SWH), H_s, is defined as:

$$H_s = 4.0\sqrt{m_0}$$

where m_0 is the "zeroth" moment of the wave spectrum. In general, the "n-th." moment of the spectrum, m_n, is defined as:

$$m_n = \int \mathrm{d}\theta \int \mathrm{d}f \; f^n \, F(f,\theta)$$

with F is the wave spectrum in frequency, f, - direction, θ, space. The first integration is done over all directions while the second is usually carried out from frequency 0 to ∞. However, for the verification of Level 2 product, the frequency integration is limited up to the frequency corresponding to the azimuthal cut-off wavelength.

2. The mean wave period (MWP) based on the "-1 th." moment (m_{-1}), T_{-1}, is defined as:

$$T_{-1} = m_{-1} / m_0$$

where m_0 and m_{-1} are the "zeroth" and the "-1 th." Moments, respectively, of the wave spectrum with the "n-th." Moment, in general, is defined above.

3. The wave directional spread (MDS), σ, is defined as:

$$\sigma = \sqrt{2[1 - r_1(f)]}$$

$$r_1 = m_0^{-1} \int \mathrm{d}f \int \mathrm{d}\theta \, F(f,\theta) \cos[\theta - \varphi(f)]$$

$$\varphi(f) = \mathrm{atan}\left\{ \left[\int \mathrm{d}\theta \, F(f,\theta) \sin(\theta) \right] \Big/ \left[\int \mathrm{d}\theta \, F(f,\theta) \cos(\theta) \right] \right\}$$

4. The mean wave propagation direction (MWD), φ, is defined as:

$$\varphi = \text{atan}\left\{ \left[\int df \int d\theta F(f,\theta)\sin(\theta) \right] \Big/ \left[\int df \int d\theta F(f,\theta)\cos(\theta) \right] \right\}$$

5. The wave spectral peakedness factor of Goda, (WPF), Q_p, is defined as:

$$Q_p = 2 m_0^{-2} \int d\theta \int df \; f F^2(f,\theta)$$

Voorrips et al. (2001) suggested the use of the narrowband equivalent wave height, $H_{T1,T2}$, between wave periods T_1 and T_2 defined as:

$$H_{T_1,T_2} = 4\left\{ \int_{1/T_2}^{1/T_1} df \int d\theta F(f,\theta) \right\}^{1/2}$$

Typically, the wave period interval [T_1, T_2] is selected as 2 seconds (2-s wave-period interval equivalent wave height). This enables a more detailed validation in terms of a rather limited number of parameters.

II.3 ASAR Level 1B Product

SWH is the most commonly used parameter for typical validation of ocean wave products. Fig. (II.1) shows a density scatter plot for globally collocated SWH pairs of inverted ASAR Wave Mode Level 1B and the analysis WAM wave model for the period of one year from 1 January to 31 December 2010. As can be seen in Fig. (II.1), the agreement between the ASAR and the model is quite good with ASAR slightly underestimating the wave heights. In general, the underestimation of ASAR for the SWH varies between 3 cm (in the Tropics) to 12 cm (in the SH) while the scatter index varies between 11% (in the Tropics) and 13.5% (in the SH).

Fig. (II.2) shows a density scatter plot for globally collocated mean wave period (MWP) pairs of inverted ASAR WM Level 1B and the analysis WAM wave model for the period from 1 January to 31 December 2010. The agreement between the inverted ASAR and the model MWP is very good with virtually no bias and very small scatter index. Considering the various geographical areas (not shown), the bias is about 0.1 s and the SI is about 6% everywhere.

Similarly, the globally collocated wave directional spread (WDS) pairs of inverted ASAR WM Level 1B and the analysis WAM wave model for the same period are plotted as a density scatter plot in Fig. (II.3). The agreement is quite good. There is virtually no bias (bias less than ~ 1% of the mean) and quite small scatter index value (~9%). Considering the various geographical areas (not shown), the bias is in general less than 1% of the mean while the SI varies between 7.6% (in the Tropics) and 10.5% in the SH.

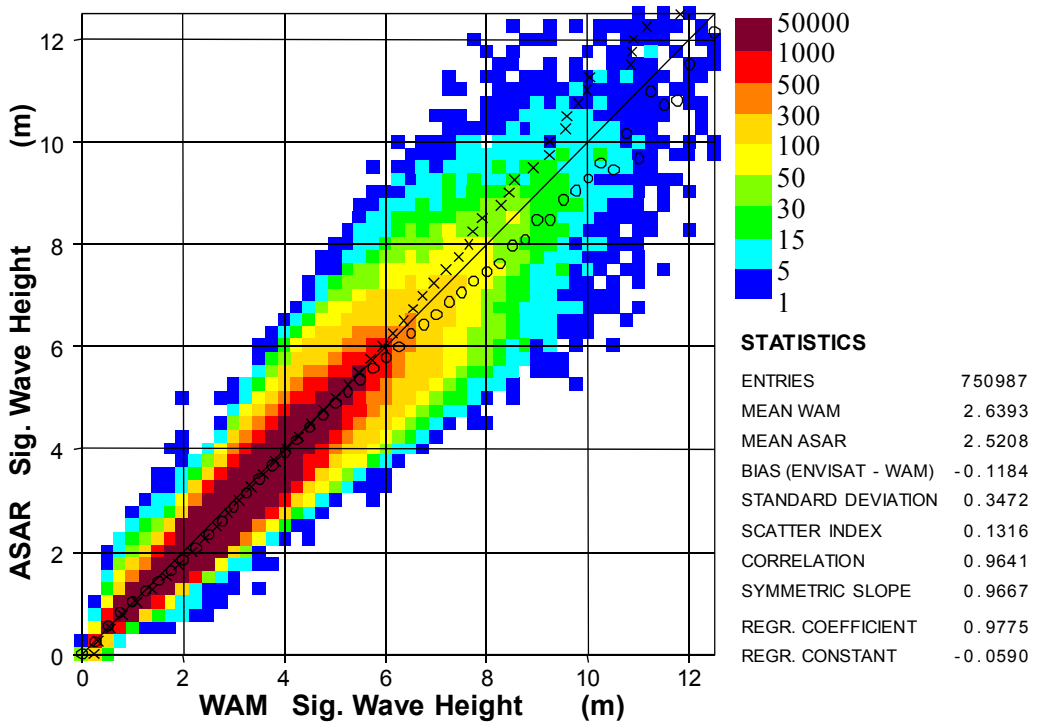

Figure II.1: Global comparison between inverted ASAR level 1b and ECMWF model SWH during the period from 1 January to 31 December 2010.

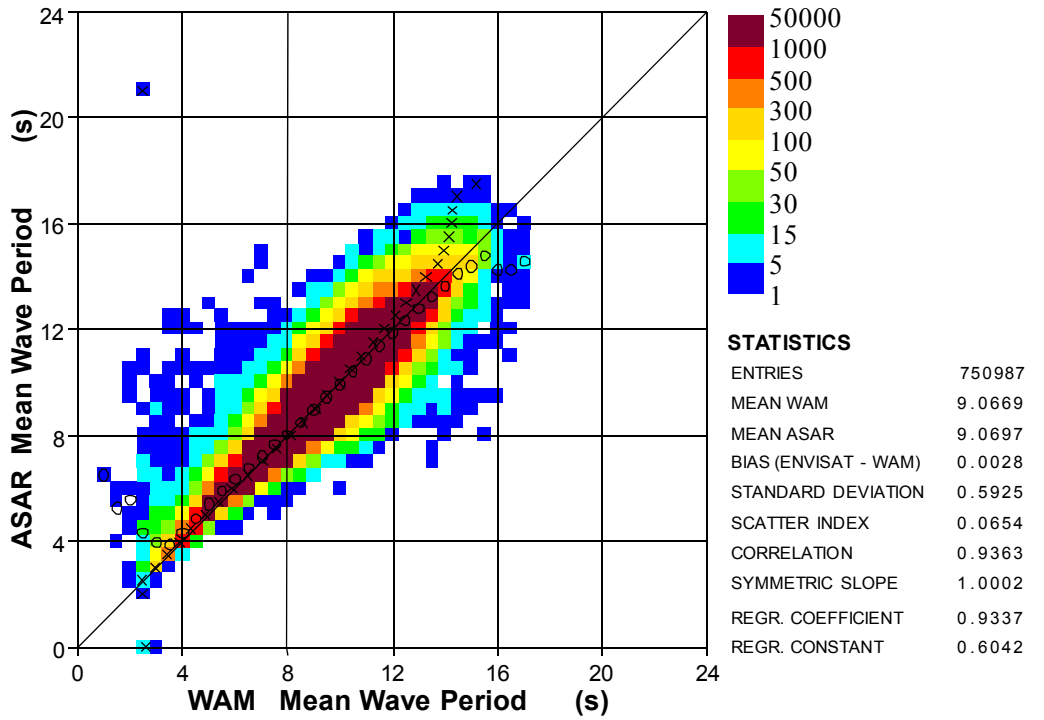

Figure II.2: Global comparison between inverted ASAR level 1b and ECMWF model MWP during the period from 1 January to 31 December 2010.

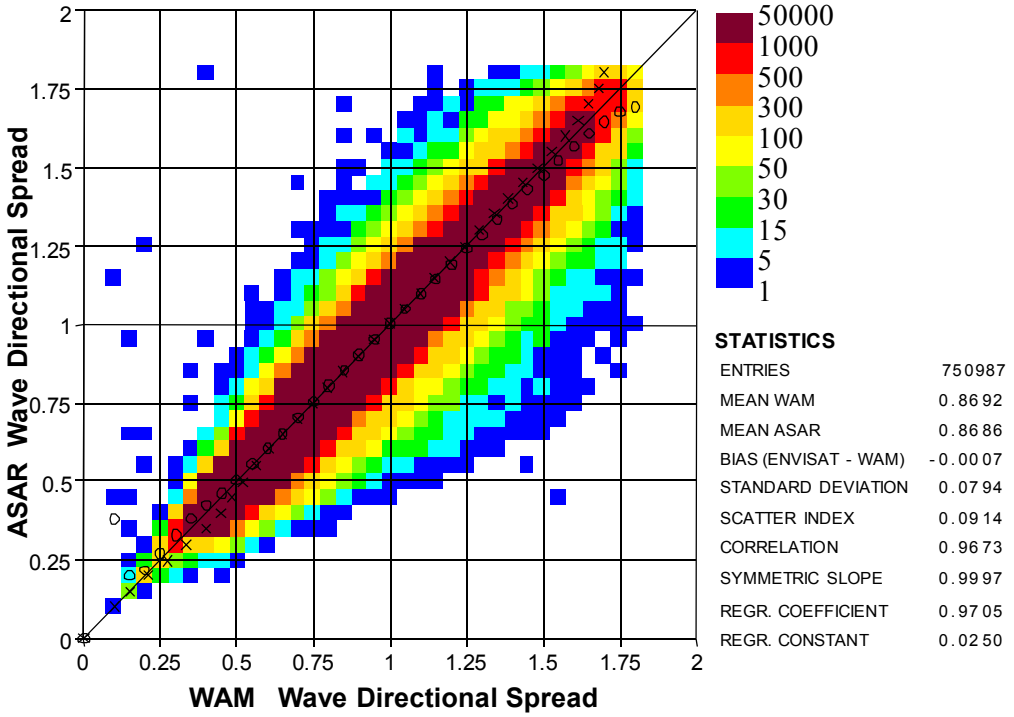

Figure II.3: Global comparison between inverted ASAR level 1b and ECMWF model WDS during the period from 1 January to 31 December 2010.

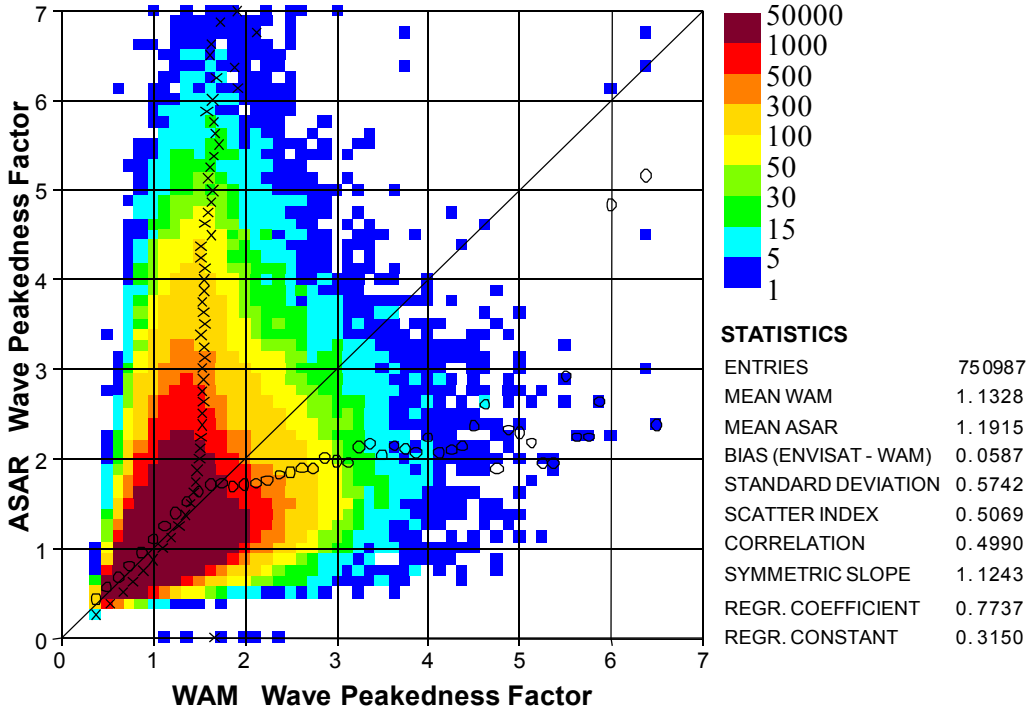

Figure II.4: Global comparison between inverted ASAR level 1b and ECMWF model WPF during the period from 1 January to 31 December 2010.

Globally collocated wave spectral peakedness factor (WPF) pairs of inverted ASAR WM Level 1B and the analysis WAM wave model for the whole year from 1 January to 31 December 2010 are plotted similarly in Fig. (II.4). There is a good agreement for most of the data, which have WPF values less than ~ 1.5. However, for larger peakedness factor values the agreement does not hold anymore with a clear split to form two families. The scatter index is rather high (~50%) while the correlation is rather low (~49%). Considering the various geographical areas (not shown), the bias is less than about 10% of the mean while the SI is about 43% in the Tropics and above 50% in the extra-tropics.

II.4 ASAR WM Level 2 Product

It is stressed that the integrated parameters used here for the various comparisons are computed for the part of the spectrum which is resolvable by the ASAR instrument. This means that wave components with wavelengths longer than the azimuthal cut-off wavelength reported in the ASAR Wave Mode Level 2 (ASA_WVW_2P) product are used. The term swell is used for those parameters to reflect this fact (although strictly speaking is not correct).

Fig. (II.5) shows a density scatter plot for globally collocated swell SWH pairs of ASAR Wave Mode Level 2 and the analysis WAM wave model for a full year covering the period from 1 January to 31 December 2010. The agreement between the ASAR and the model is quite good for the bulk of the data. However, there are quite a number of outliers. The outliers are generally with higher ASAR values in the NH and the Tropics and with lower ASAR values in the SH (see Fig. II.12).

Similarly, Fig. (II.6) shows the density scatter plot for globally collocated swell mean wave period (MWP) pairs of ASAR Wave Mode Level 2 and the analysis WAM wave model for the full year of 2010. The agreement between the ASAR and the model MWP is very good for the bulk of the data. MWP is one of the parameters that definitely benefitted from the implementation of the processing chain of PF-ASAR 4.05 at the end of October 2007. The SDD of the mean wave period is about 0.5 s which is quite good.

The globally collocated swell wave peakedness factor (WPF) pairs of ASAR Wave Mode Level 2 and the analysis WAM wave model for the same period are shown in Fig. (II.7) while the swell wave directional spread (WDS) pairs are shown in Fig. (II.8). The agreement between the ASAR WM L2 and the ECMWF wave model WPF and WDS are rather poor. The implementation of the processing chain of PF-ASAR 4.05 at the end of October 2007 slightly improved those parameters but not to the extent of promoting them to a level which can be described as “in good agreement” with the model. For example, the correlation between the L2 and model WPF is about 10% and for the WDS is about 36%. Fig.’s (II.7) and (II.8) suggest that the ASAR L2 spectra are very narrow both in frequency and direction compared to the model. This “narrowness” can be due to the physical restrictions on the SAR imaging process.

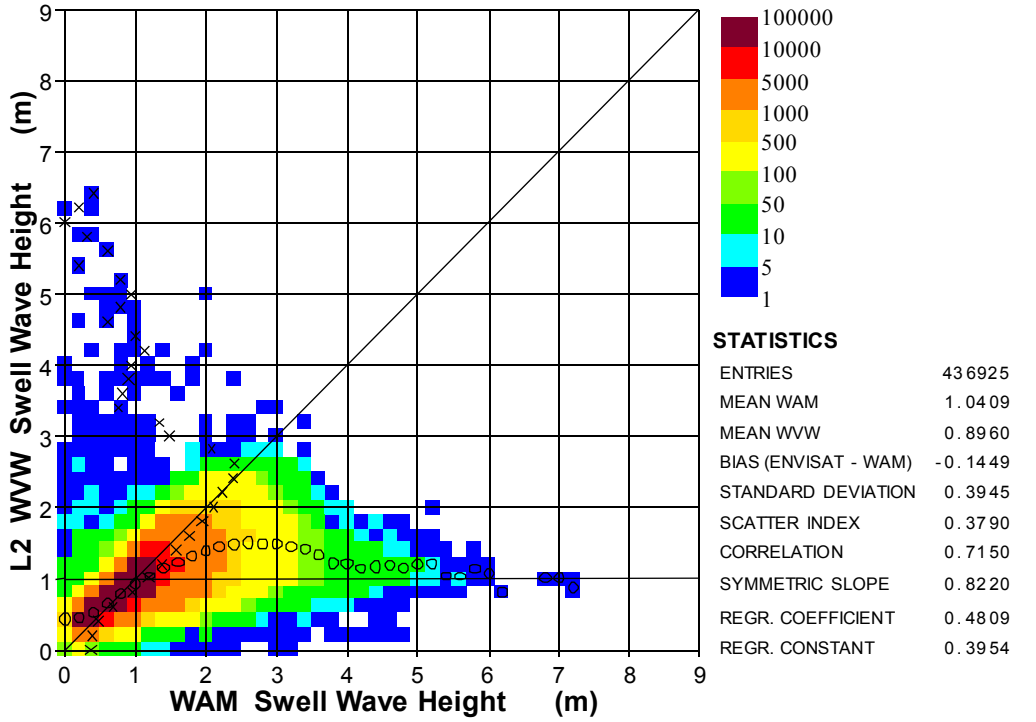

Figure II.5: Global comparison between ASAR level 2 and ECMWF model swell SWH (only within reported azimuthal cut-off) during the period from 1 January to 31 December 2010.

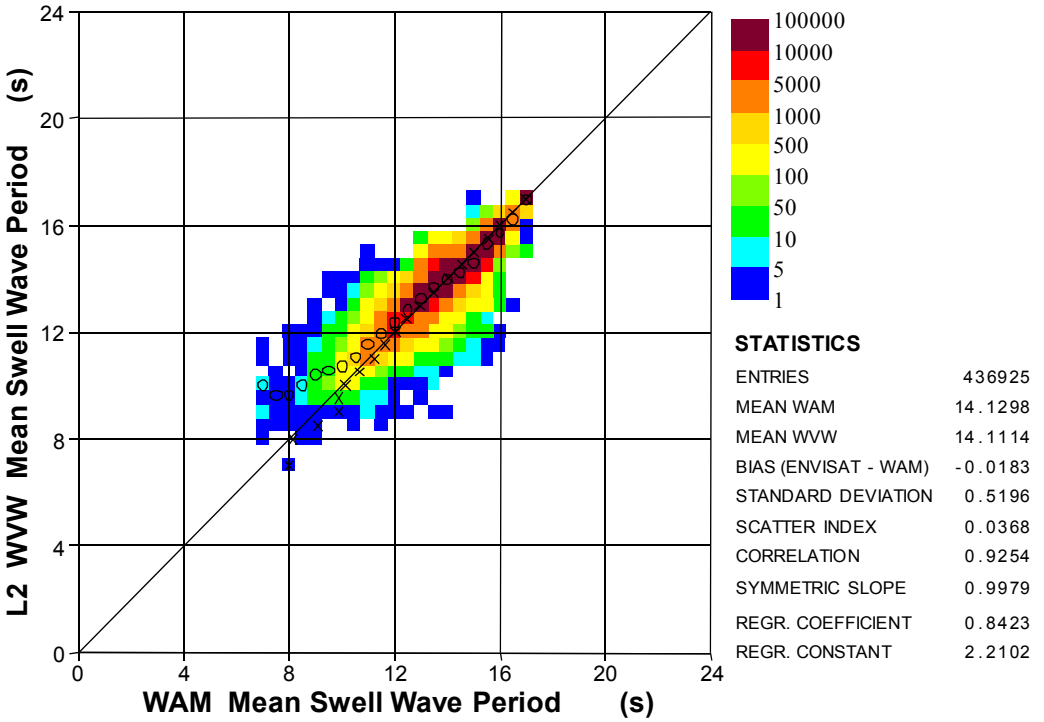

Figure II.6: Global comparison between ASAR level 2 and ECMWF model swell MWP (only within reported azimuthal cut-off) during the period from 1 January to 31 December 2010.

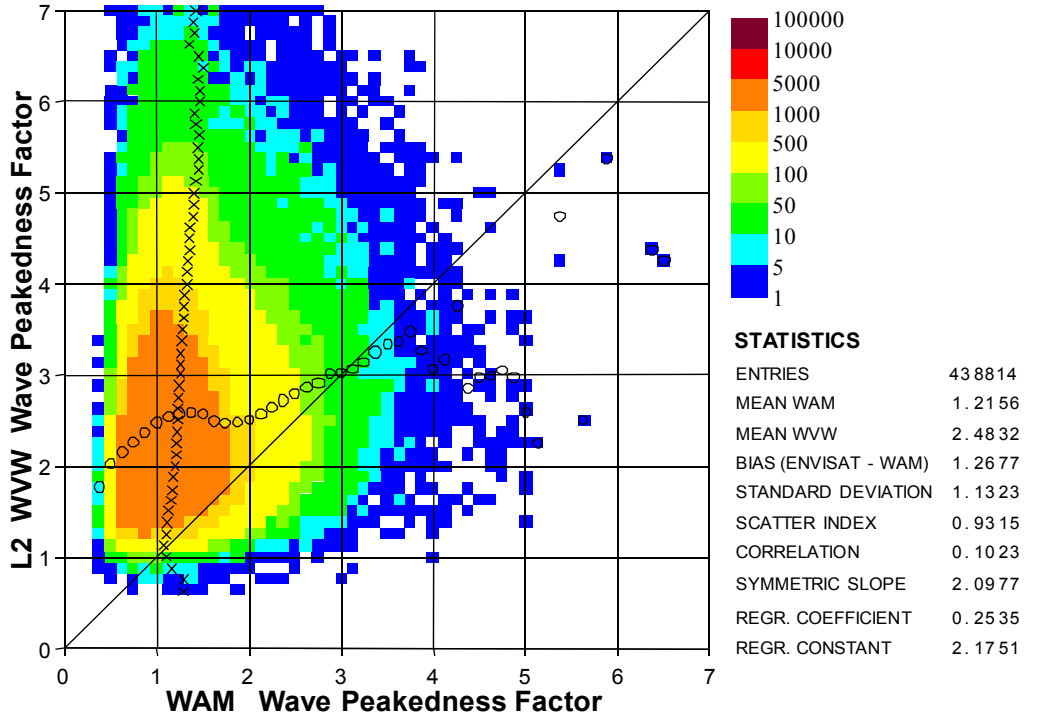

Figure II.7: Global comparison between ASAR level 2 and ECMWF model swell WPF during the period from 1 January to 31 December 2010.

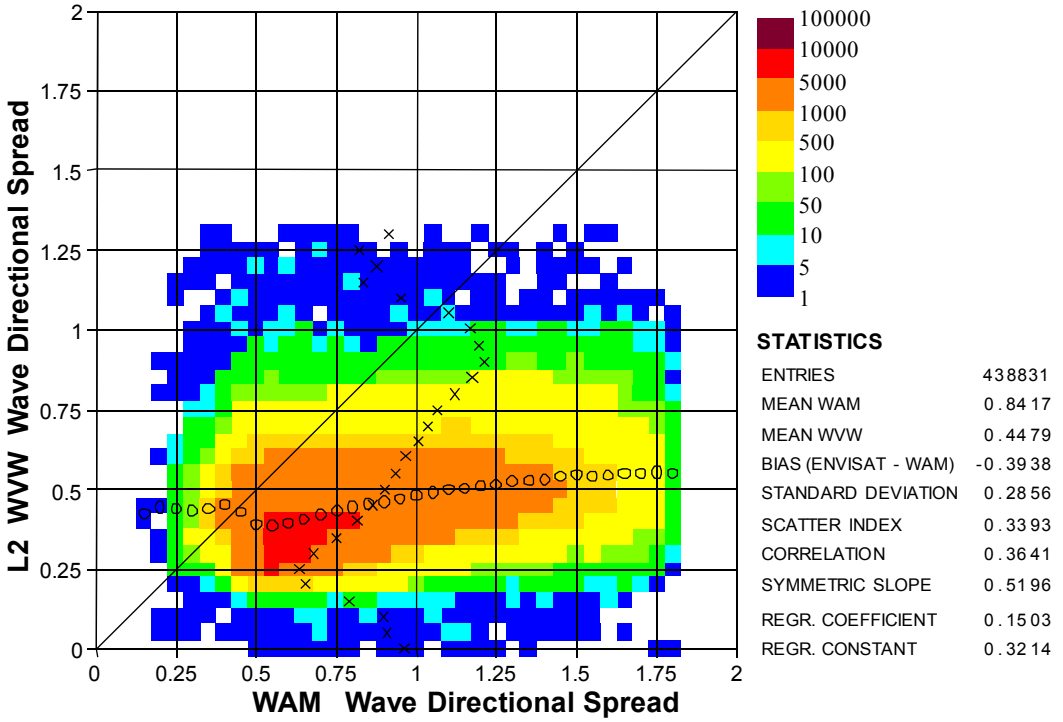

Figure II.8: Global comparison between ASAR level 2 and ECMWF model swell WDS during the period from 1 January to 31 December 2010.

II.5 Assimilation of ENVISAT ASAR Wave Mode Level 2 Product

The change in ASAR processing chain of PF-ASAR 4.05 at the end of October 2007 motivated the experimentation with the assimilation of WM L2 product in the wave model of ECMWF.

To test the impact of assimilating WM L2 product on the wave model predictions, several experiments were carried out. The ECWAM wave model (WAM model as improved at ECMWF, see Janssen, 2004) was run in stand-alone mode forced by operational wind fields for the months of August and September 2008 (after a 10-day warm-up period). The model configuration in the experiments reflected the operational set-up at the time as close as possible. The globe was discretized into a grid with a resolution of about 40 km in both directions. The spectral space was discretized into 30 frequency bins and 24 direction bins. The runs were configured to run using analysis winds for 12 hours ending at 00 and 12 UTC each day. Data assimilation is carried out for the 6-hour windows centred at major synoptic times (i.e. at 00, 06, 12 and 18 UTC). This set-up reflects the configuration of the operational analysis. Further 5-day runs follows the analyses at 00 and 12 UTC using operational forecast winds. A reference model run without any data assimilation was carried out. Another reference model run was carried out with the assimilation of ASAR WM L1b data product, which is assimilated in the operational model. Several experiments were carried out assimilating WM L2 data product. One experiment made use of the product after passing basic quality control checks to ensure the validity of the data. Several runs were carried out using various quality control filters, including the officially recommended ones (cf. Johnsen, 2005). Note that altimeter data is not assimilated in any of the above experiments.

To assess the performance of each experiment, significant wave height data from Radar Altimeters onboard ENVISAT (RA-2) and Jason-1, ECMWF operational analysis and available ocean wave buoy and platform observations are used in the verification process.

The implemented assimilation procedure itself is based on the assimilation of wave systems as derived from a partitioning scheme. The full spectrum is divided into several systems using the principle of the inverted catchment area (e.g. Hasselmann et al., 1997). The different wave systems are characterised by their total energy, mean frequency and mean propagation direction. These integrated parameters are assimilated using a simple Optimum Interpolation (OI) scheme following a cross assignment procedure to correlate the observed systems with the modelled first-guess (FG) ones. The analysis (AN) integrated parameters obtained from the OI scheme are used to construct the AN spectra by resizing and reshaping the FG spectra.

Using the ASAR WM L2 ocean spectra directly without much quality control led to the deterioration of the model results. Fig. (II.9) shows that the SDD of SWH compared to the operational model analysis is worst when WM L2 product is assimilated. It is even worse than the run without any data assimilation. To improve the situation several quality control criteria were used. One need to make a compromise between rejecting, as much as possible, L2 spectra that either look suspicious or deviate from the model counterpart on one hand and retaining, as much as possible, the useful information on the other hand. Too strict quality control allows very few observations to be assimilated and, therefore, results in very minor or no impact.

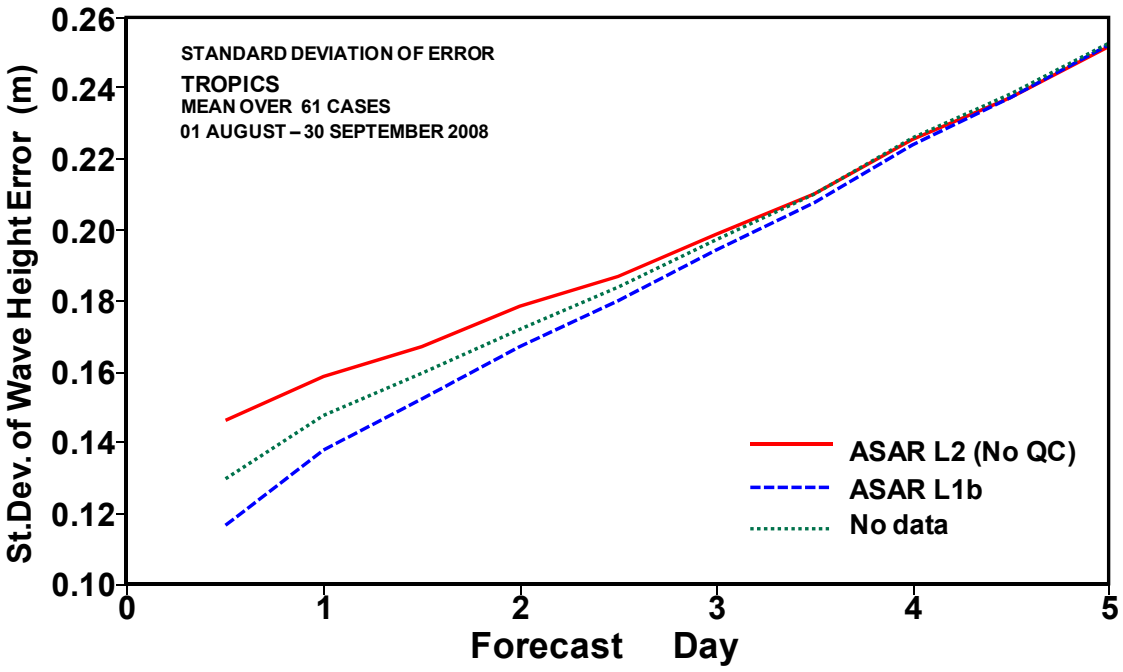

Figure II.9: Impact of the assimilation of WM L2 Product with almost no QC on the standard deviation of the SWH error in the Tropics as verified against ECMWF operational analysis.

The best quality control configuration was achieved by, first rejecting any L2 product that reports:

- land observation;
- no confidence in the inversion;
- signal to noise ratio below 3 or above 200; and
- wind speed below 3 m/s or above 16 m/s.

Furthermore, the assimilation procedure only considered the information in the product within an ellipse (will be termed hereafter as the "cut-off ellipse") in the wave number vector space with a major axis extending over the whole wave number range in the range direction and a minor axis covering wave numbers below the azimuthal cut-off in the azimuthal direction. Beyond this cut-off ellipse, the information is assumed to be useless. Other quality control criteria are based on the comparison with the model counterpart during data assimilation. This is done based on individual systems or partitions. After partitioning the ocean wave spectra from ASAR and the model, corresponding systems or partitions from both products are matched. If an ASAR partition is not matched successfully with a model partition, the ASAR partition is rejected. If there is an indication that part of either the ASAR partition or its matched model partition is outside the cut-off ellipse, the ASAR partition is rejected. Finally if the ASAR and the model partitions are too far apart, in terms of wave-number and/or angle, the observed partition is rejected.

Fig. (II.10) shows the impact of the assimilation of ASAR WM L2 product after filtering suspicious products and partitions. It is clear that in the Tropics, L2 product has minor positive impact compared

to no data assimilation case as verified against ECMWF operational analysis. Stricter quality control leads to almost no impact as most of the products are rejected. However, the similar verification in extra tropics, especially the SH for this case, reveals that L2 assimilation causes a slight degradation of model forecasts as can be seen in Fig. (II.11). A possible explanation is that WM L2 assimilation suites the swell condition which is the case most of the time in the Tropics and during the Northern Hemispheric summer in the NH. Since the change in ASAR processing chain to PF-ASAR 4.05 at the end of October 2007, there was no change in the quality of the ASAR products. Although that change managed to improve the WM L2 product significantly, there still apparently some issues reflected in several outliers in the comparison between the swell (part of the ocean wave spectrum with wavelengths longer than the azimuthal cut-off wavelength) significant wave height from ASAR L2 and the wave model. Examples of such issues are shown in Fig. (II.12) for the Tropics between latitudes 20°N and 20°S (left hand panel) and for the Southern Hemispheric extra Tropics (right hand panel) for the whole of 2009. The outliers are mainly with ASAR swell wave heights higher than the model counterpart.

Similar verification was done against the wave buoy measurements. The wave buoys, which are limited in number, are scattered mainly in the Northern Hemisphere (NH) around North America and Europe. The impact is more pronounced when considering only the Tropical buoys as can be seen in Fig. (II.13). Assimilation of L2 products causes the reduction of the differences between the model analysis and the buoy wave heights. However, this positive impact disappears when all wave buoys are considered for verification. Fig. (II.14) shows the same comparison against buoys for all the buoys. One can notice the slight degradation due to the assimilation of L2 product.

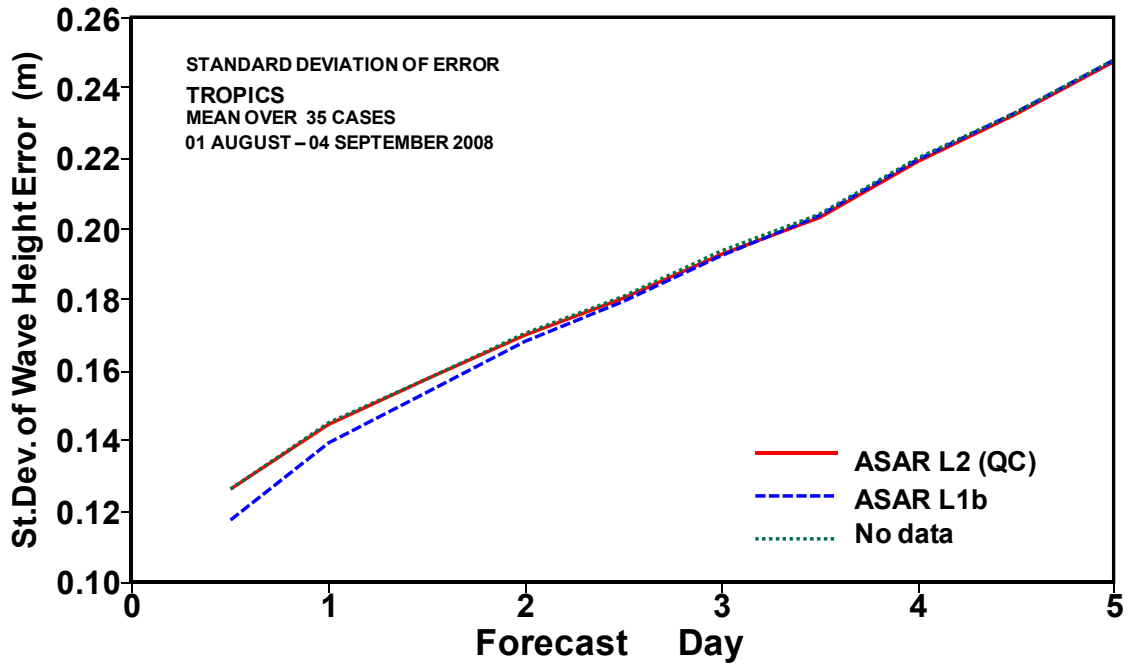

Figure II.10: Same as Fig. (II.9) but with assimilating WM L2 product after passing quite strict QC.

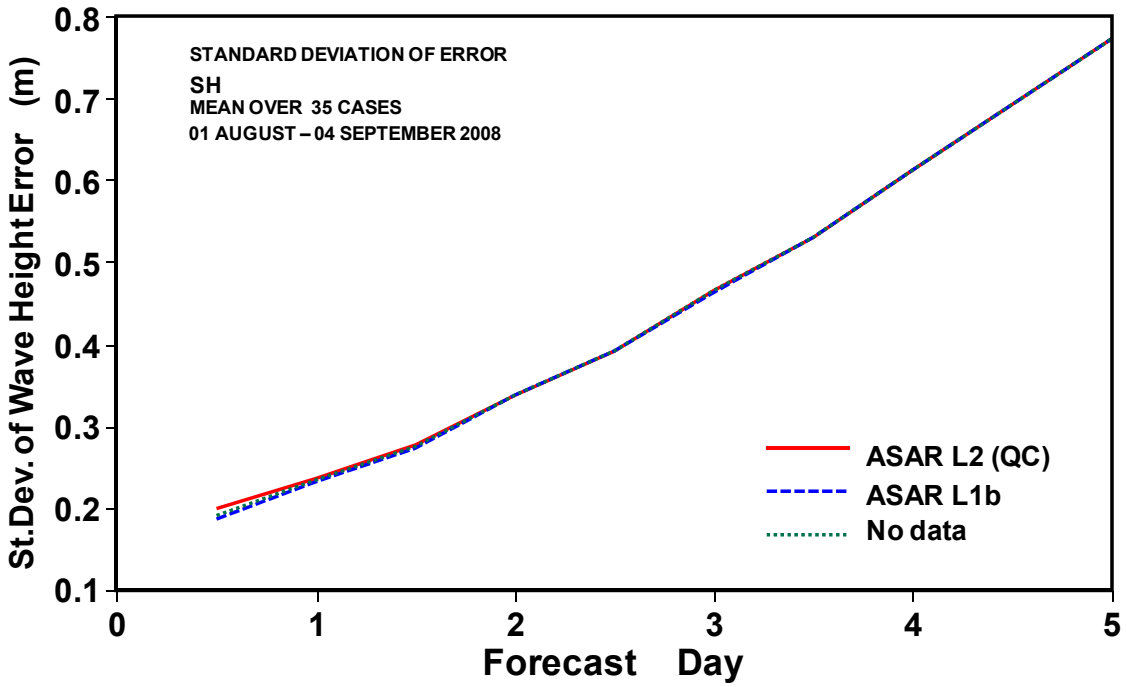

Figure II.11: Same as Fig. (II.10) but for SH.

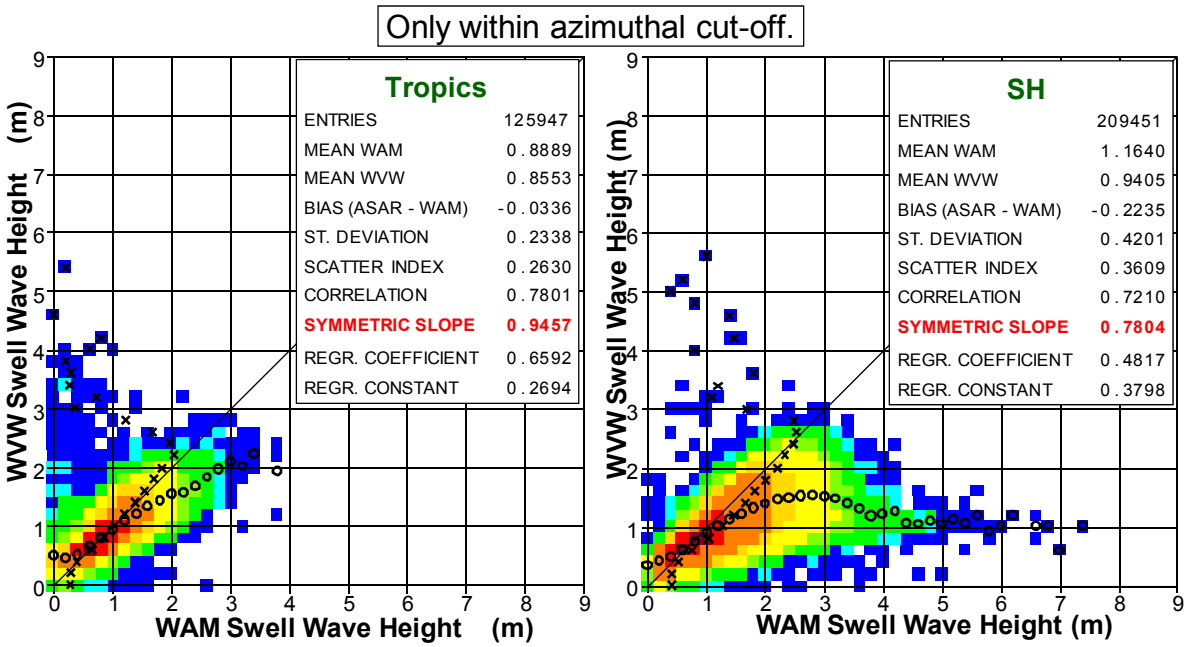

Figure II.12: Comparison between Level 2 and model swell SWH (within azimuthal cut-off wave number) during the whole year of 2009 in the Tropics and the SH.

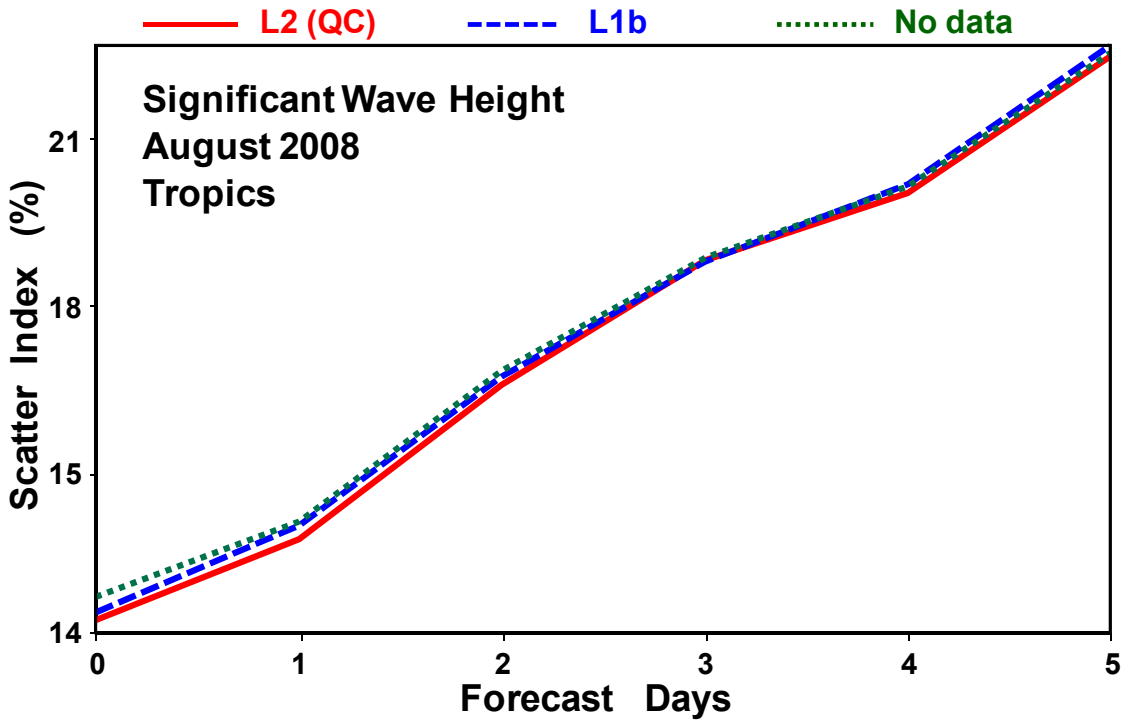

Figure II.13: Impact of assimilating quality controlled WM data on the SWH scatter index (=SDD / mean of buoy data) in the Tropics as verified against ocean wave buoy data.

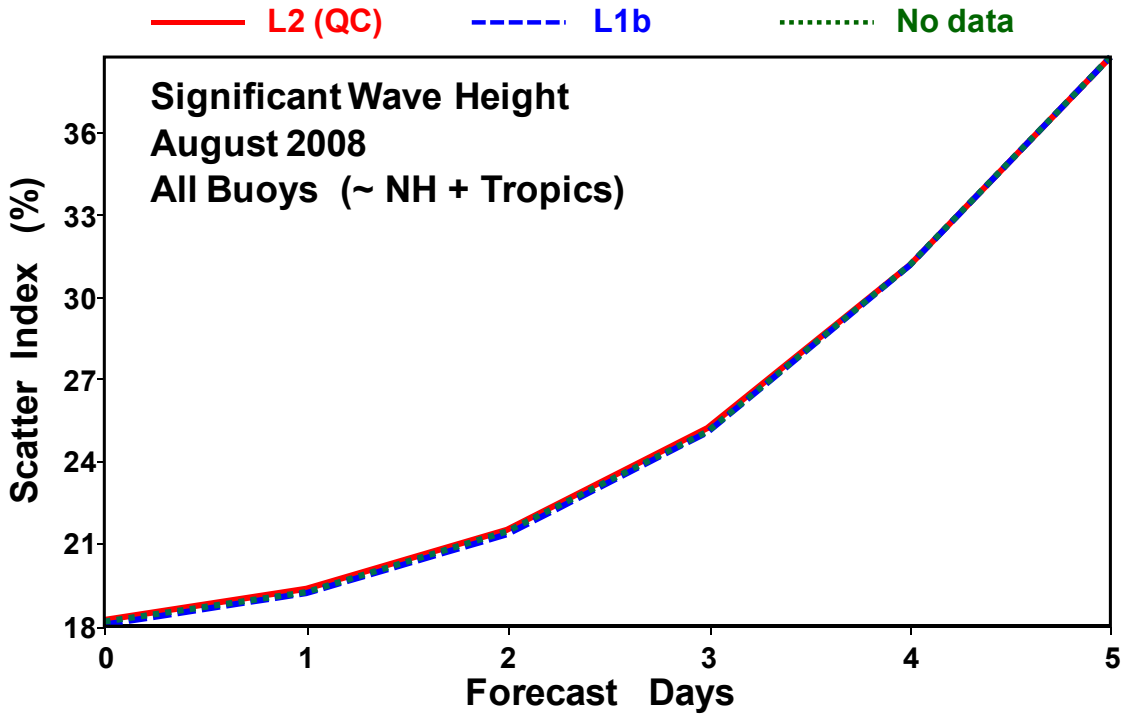

Figure II.14: Same as Fig. (II.13) but for all buoys which are mainly in the Tropics and the NH.

Further verification of the impact of the assimilation of ASAR L2 ocean wave product was carried out against radar altimeter SWH measurements. Wave heights from Envisat Radar Altimeter-2 (RA-2) and Jason-1 were used for this purpose. Fig. (II.15) shows the evolution of the wave model differences (errors) with respect to the altimeter measurements along the forecast range in the Tropics. Again a limited positive impact can be seen when comparing the case with the assimilation of L2 product against the one corresponds to no data assimilation. On the other hand, the positive impact is lower than that of assimilating WM L1b product. As was shown for the wave buoys, the verification in extra Tropics, especially in the Southern Hemisphere (SH), suggests that assimilating ASAR L2 product degrades the model results (not shown).

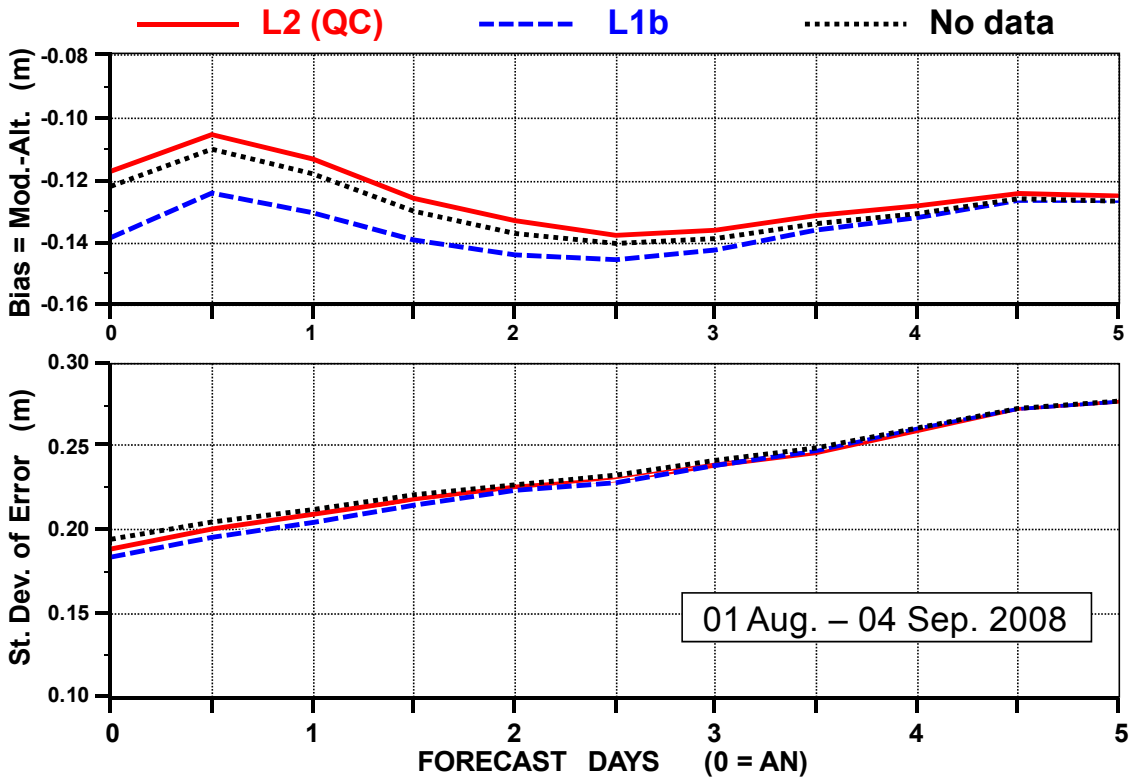

Figure II.15: Impact of the assimilation of WM L2 Product after passing quite strict QC on the SWH bias and SDD in the Tropics as verified against Envisat and Jason-1 altimeter SWH data.

It was clear from various experiments and verifications that although assimilating ASAR WM L2 product has a rather limited positive impact on model results in the Tropics, it failed in extra-Tropical areas especially the Southern Hemisphere, SH, (i.e. south of latitude 20°S). The comparison between swell (within azimuthal cut-off wave number) significant wave height from ASAR WM L2 product and the corresponding values from the operational ECMWF wave model in the Southern Hemispheric extra Tropics is shown in right hand side panel of Fig. (II.12). Comparing the SH plot in the right hand panel of Fig. (II.12) and the one for the Tropics in the left hand side panel of Fig. (II.12) gives a clue for the possible reason behind the model degradation after L2 assimilation. In the SH case there is a number of outliers with ASAR wave height is much lower than the corresponding model values. Similar outliers do not exist in for the case of Tropics. Some of those outliers, or partitions associated with those outliers, pass the quality control procedure and cause the degradation of the model results.

It is clear that there is a need either to eliminate those outliers or to flag them properly in order to stop them intruding the assimilation process and harming the model output.

II.6 Conclusions

Continuous monitoring and validation of the ENVISAT ASAR Wave Mode products are carried out at ECMWF. Data from ECMWF wave model are used for this purpose. Improvements to the ASAR processing chain (PF-ASAR) are carried from time to time. PF-ASAR Ver. 4.05, in October 2007, is one of the important improvements.

ASAR Wave Mode Level 1b spectra are inverted using the MPIM scheme at ECMWF and have been assimilated since February 2006. The inverted ocean wave spectra compare well against the wave model products in terms of a limited number of integrated parameters although the comparison may not be very good as far as the details are concerned.

The comparison between ASAR Wave Mode Level 2 and the wave model is done in terms of the same integrated parameters with the exception that the integration is done for the ASAR resolvable wave components (i.e. with wavelengths longer than the azimuthal cut-off wavelength). Swell significant wave height and mean wave period from Level 2 product agree well with their wave model counterparts. However, the swell spectral peakedness factor and the directional spread parameters show poor agreement.

The change of ENVISAT orbit in October 2010 did not have any impact on ASAR Wave Mode products.

The possible assimilation of ASAR WM Level 2 Product into ECMWF wave model was assessed. Direct use of the Level 2 Product as is (i.e. without strict QC) leads to model degradation. Although applying QC (and other restricting considerations) leads to minor general positive impact, the degradation impact of assimilating Level 2 product in the Southern Hemisphere was not alleviated. It seems that QC is crucial for the success of ASAR data assimilation. In fact assimilating of Level 1b product does involve rather tight QC.

Irrespective of the significant improvement introduced to the ASAR Wave Mode Level 2 ocean wave spectrum product in October 2007 (PF-ASAR 4.05), the product may still be in need of some further improvements. This is clear from the outliers when compared against the wave model counterpart. Assimilation of WM L2 product into ECMWF wave model leads to slight degradation of model results as verified against operational model analysis as well as ocean wave buoy and radar altimeter observations. However, the impact is rather positive in the Tropics. In all cases, the impact is much smaller than that from assimilating WM L1b. Although adjusting the quality control criteria improved the results, it seems that the ASAR WM L2 product needs some improvements.

III. MEDIUM RESOLUTION IMAGING SPECTROMETER (MERIS) WATER VAPOUR PRODUCT

III.1 Introduction

MERIS is a 68.5° field-of-view pushbroom imaging spectrometer that measures the solar radiation reflected by the Earth, at a ground spatial resolution of 300m, in 15 spectral bands, programmable in width and position, in the visible and near infra-red. MERIS allows global coverage of the Earth in 3 days. The MERIS product of interest is the Geolocated Cloud Optical Thickness and Water Vapour Content (a low resolution atmosphere Level 2) product (MER_LRC_2P). Specifically, only TCWV is validated here. This is a very dense product with a 1200 km wide swath at a resolution of 4.16 km (across-track) × 4.64 km (along-track) at nadir.

III.2 MERIS Data Processing for Monitoring

TCWV (or the "atmospheric water vapour content") is one of the products obtained from the MERIS instrument onboard ENVISAT (product MER_LRC_2). This product is validated by comparing it with the corresponding product produced by the ECMWF atmospheric model (IFS). Due to the scale differences between the MERIS product and the IFS model product, it is required to bring both to the same scale. One way to do this is to average the MERIS product over spatial grid boxes comparable with the model resolution. A procedure for the pre-processing including the averaging and the basic quality control can be summarised as follows (Abdalla, 2005):

1. The stream of MERIS MER_LRC_2 product is split over 6-hour time windows centred at the main synoptic times to coincide with the IFS model output times.

2. All MERIS TCWV observations with missing or zero values are filtered out assuming they are not valid.

3. For each time window, the dense MERIS TCWV data set is averaged over grid boxes of 0.5°×0.5° producing the MERIS super-observations.

4. The super-observation is rejected if the number of its individual observations is less than 10.

5. The super-observation is rejected if it is smaller than 0.1 kg/m^2.

6. The super-observation is rejected if its standard deviation exceeds 35% of its mean.

7. The super-observations that pass the quality control are collocated with the model counterparts and various statistics are computed.

This procedure may reject more than 40% of MERIS TCWV products. It is important to stress that part of the rejected data may be of good quality and rejected due to their high variability

III.3 MERIS Water Vapour Product

Fig. (III.1) shows a time series of monthly mean MERIS TCWV data reception and acceptance per 6-hour time window since the mid of 2005. On average, the data received at a rate exceeding 3 million observations per 6-hours. Before the implementation of the MERIS processing chain IPF 5.02 (May 2006), about 50% of the received data pass the quality control. This is already a rather low ratio. The IPF 5.02 lead to more rejections and brought the ratio to about 70%. It is not clear if this low ratio is due to the noise/variability in the observations or due to the current quality control procedure which was derived to optimise the data acceptance against the best fit with respect to the model (c.f. Abdalla, 2005).

Collocated TCWV pairs of MERIS super-observations and the ECMWF model AN are plotted as density scatter plot in Fig. (III.2) for the whole globe over a full year period from 1 January - 31 December 2009 (panel a) and from 1 January - 31 December 2010 (panel b). The major part of the MERIS observations agrees very well with the model counterpart. However, there are quite a number of outliers as well. Some abnormal values (in excess of ~70 kg/m^2) appeared in the scatter plot of 2009 (panel a of Fig. III.2). Smaller number of similar outliers also existed in the 2010 plot. To trace those extreme values, the time series of the bias (MERIS – model) and the standard deviation of difference (SDD) are plotted in Fig. (III.3). It is clear that those extreme outliers occurred during some specific periods. ESA confirmed that there were some experimentations carried out with the instrument during those specific days.

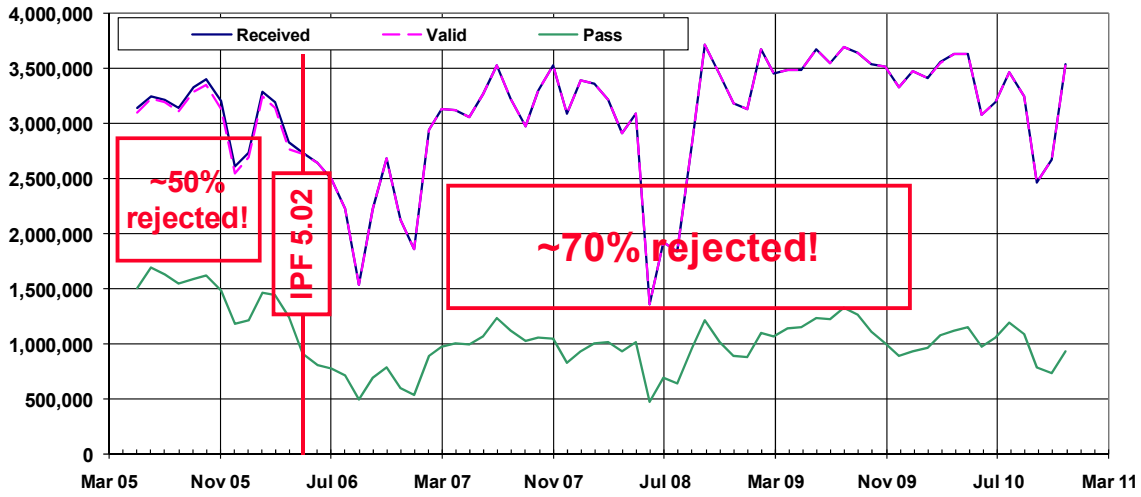

Figure III.1: Time series of monthly mean MERIS TCWV data reception and acceptance per 6-hour windows.

(a)

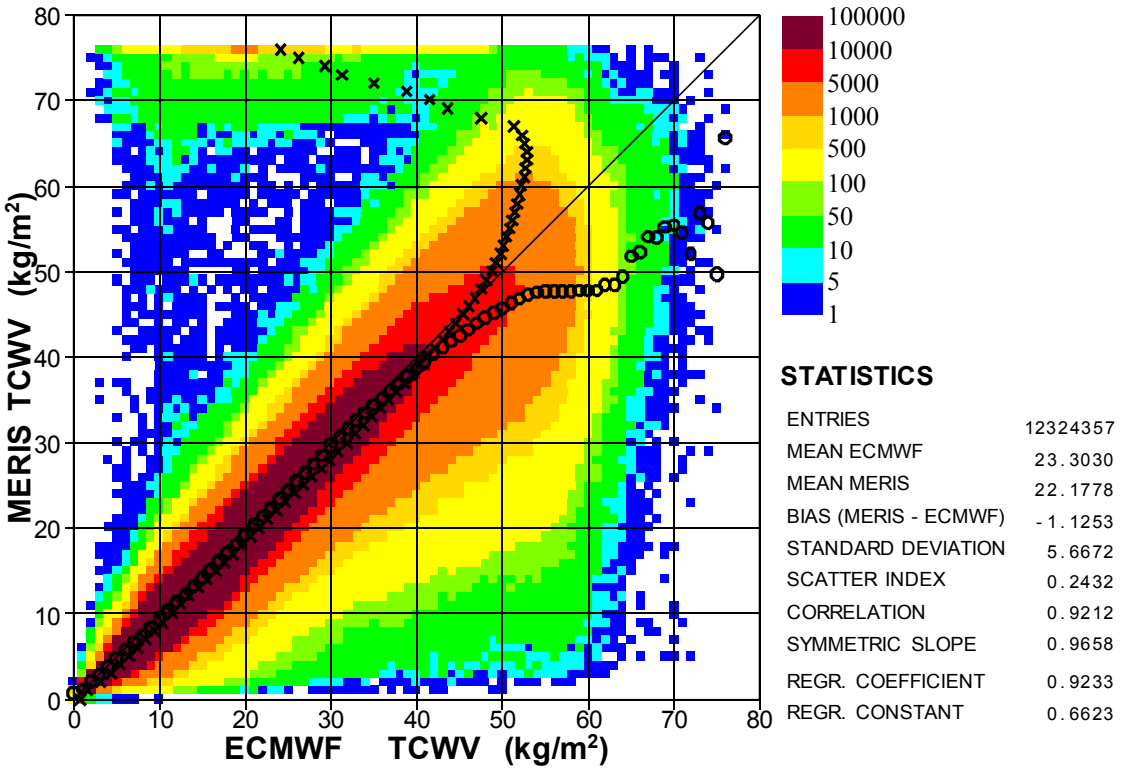

(b)

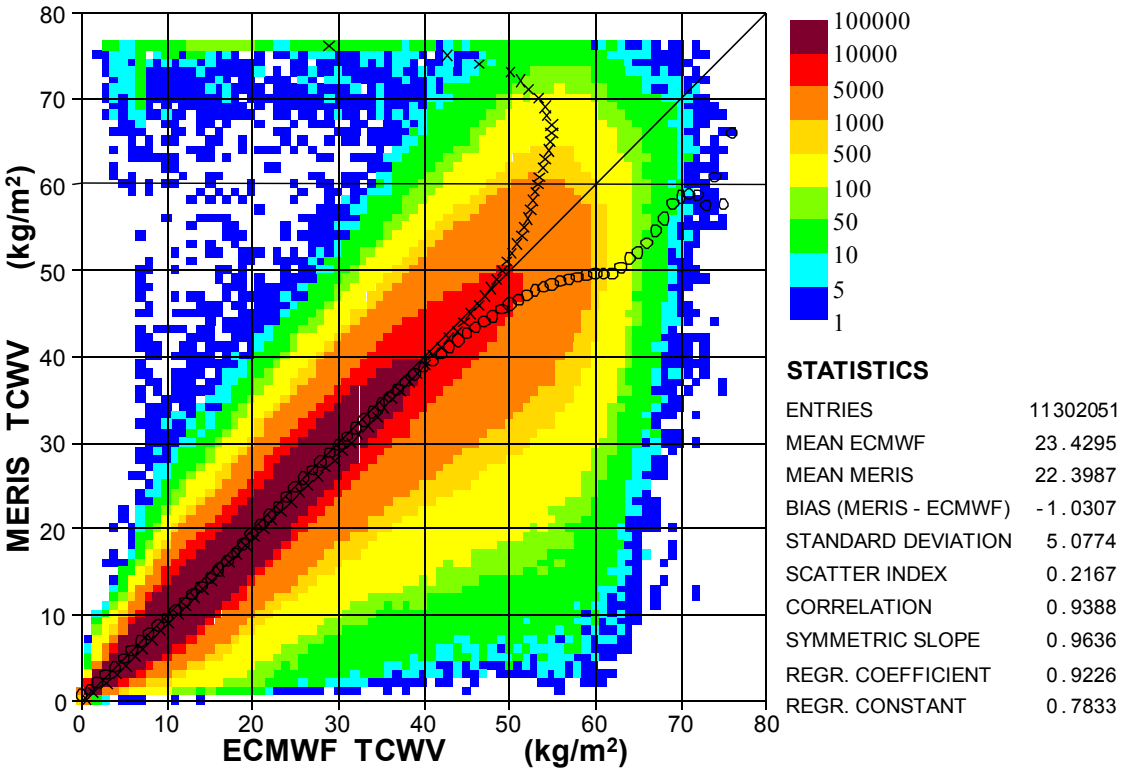

Figure III.2: Global comparison between MERIS and ECMWF model AN TCWV values during periods: (a) from 1 January - 31 December 2009 and (b) from 1 January - 31 December 2010.

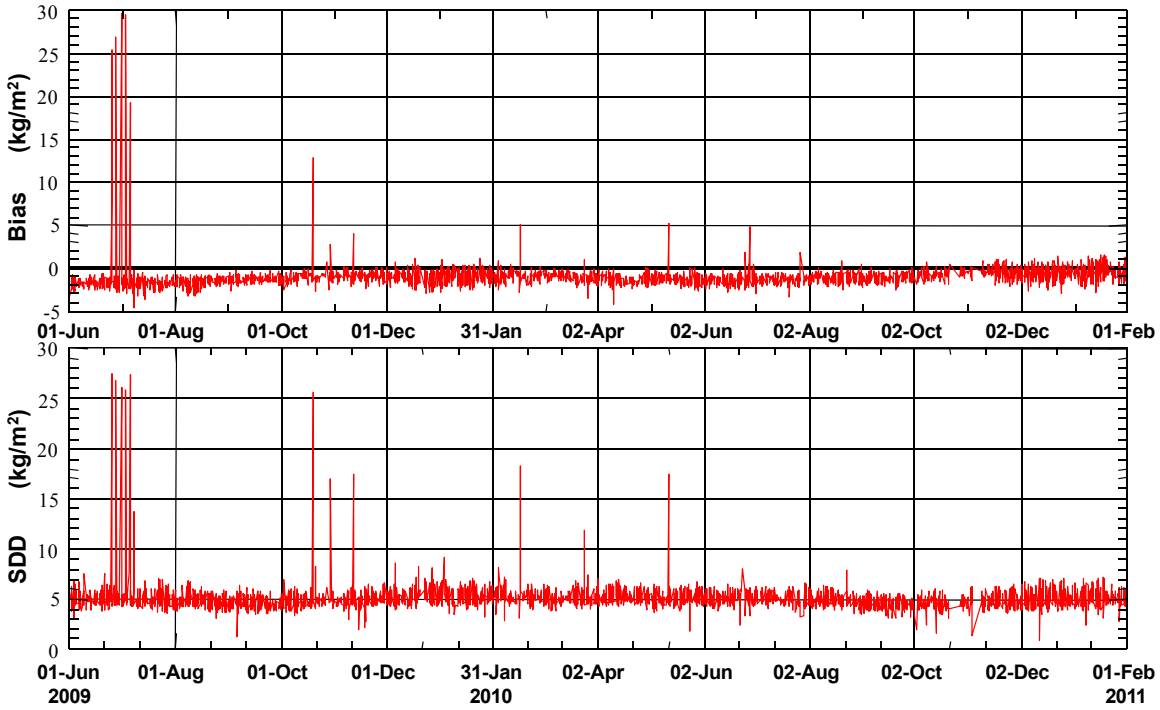

Figure III.3: Time series of global bias and SDD between MERIS and ECMWF model.

Apart from those extreme outliers, MERIS TCWV tends to provide, as can be seen in Fig. (III.2), a significant number of dry observations especially below ~15 kg/m^2 which are not supported by the model. Globally, MERIS underestimates the TCWV by about 1 kg/m^2 with respect to the ECMWF atmospheric model. This is quite an improvement from the 4 kg/m^2 which used to be the typical value before IPF 5.02. For the sake of comparison, it is useful to mention that the typical TCWV bias between the MWR and the model is ~0.5 to 1.0 kg/m^2 depending on the geographical region (see Fig. I.11 for a typical global value). The standard deviation of the difference (SDD) between MERIS and the model is rather high (~5 kg/m^2 or more than 20%). This is quite a large SDD value. Furthermore, MERIS tends to have a secondary population of collocations with the model that runs below the main population by ~10 kg/m^2. Although this cannot be clearly seen in Fig. (III.2), it is very pronounced in scatter plots of shorter time spans, e.g. monthly, and particularly in the Tropics (not shown). A hint of this can be seen in Fig's (III.4) and (III.5).

To study the characteristics of the TCWV product, the data product was separated based on the surface beneath the observation to be either land or sea. For this exercise a month (May 2007) worth of global data was used. Fig. (III.4) shows the scatter plot of all MERIS TCWV data, without any discrimination, against ECMWF model. This is the monthly equivalent of Fig. (III.2). The scatter plot for "sea" observations within the same data set against the ECMWF model is shown in Fig. (III.5). Similarly the scatter plot for the "land" observations is shown in Fig. (III.6). Comparing the three scatter plots, it is evident that MERIS TCWV product over land is of much better quality than that over ocean. As it has already mentioned above, the second population of data that runs below the main population by ~10 kg/m^2 can be noticed in Fig's (III.4) and (III.5).

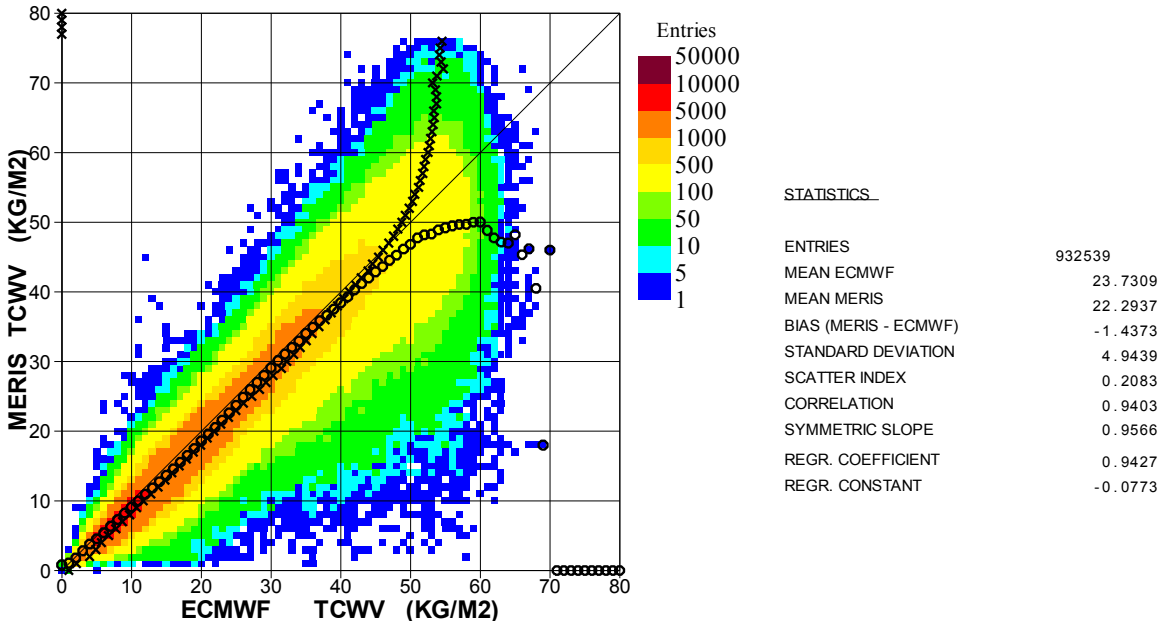

Figure III.4: Global comparison between MERIS and ECMWF model AN TCWV values for all the data both over land and over the ocean (May 2007).

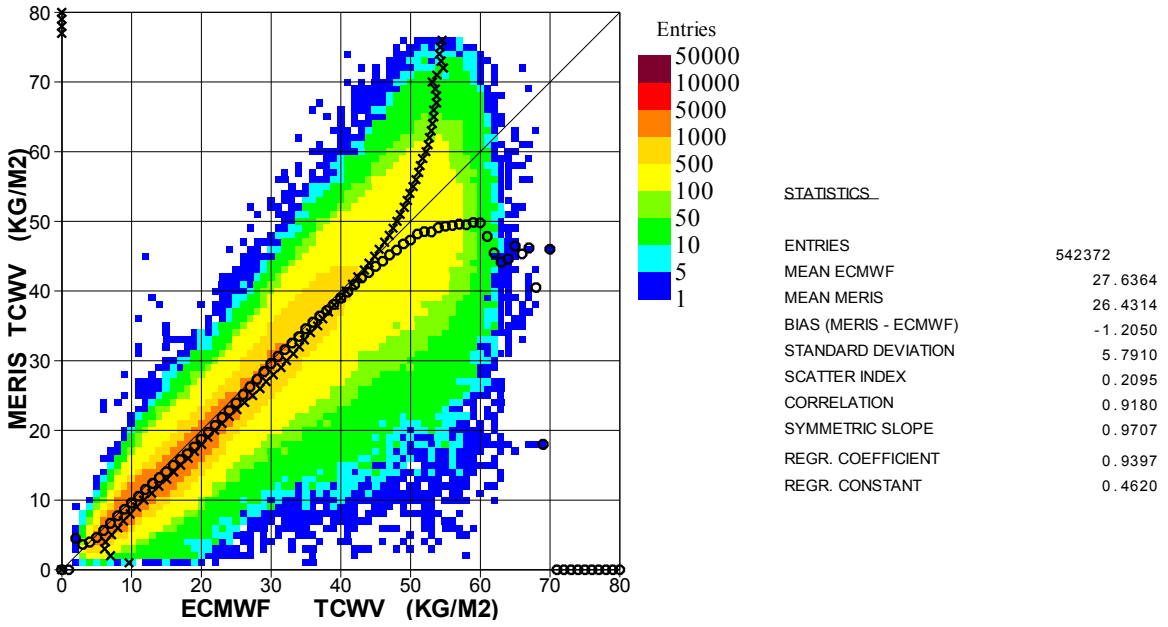

Figure III.5: Global comparison between MERIS and ECMWF model AN TCWV values for the data only over the ocean (May 2007).

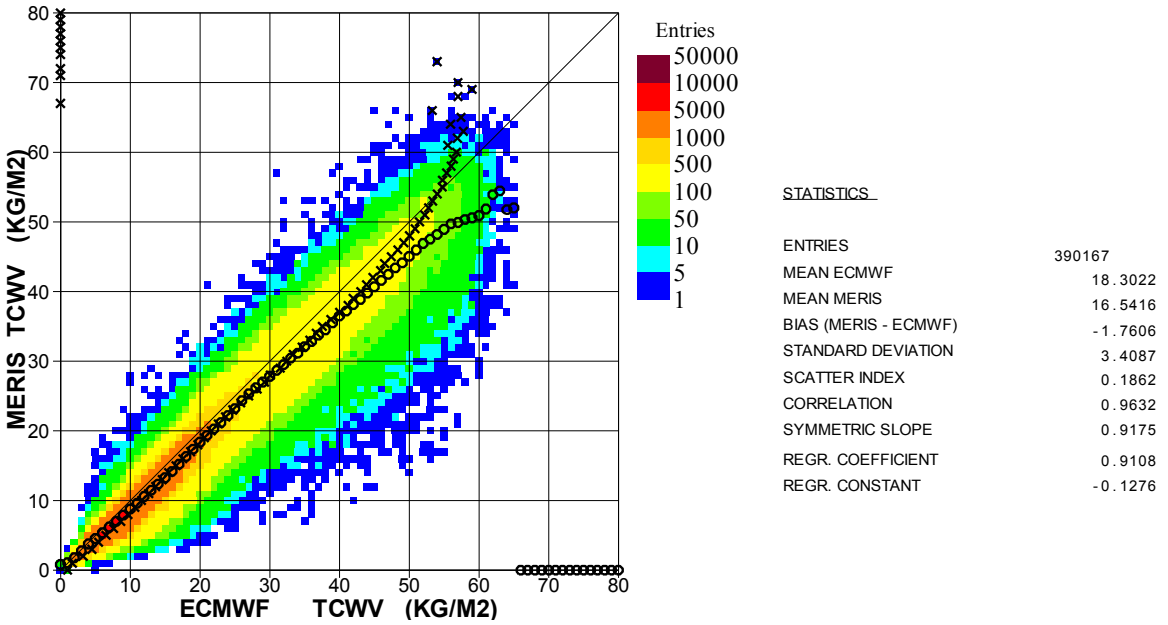

Figure III.6: Global comparison between MERIS and ECMWF model AN TCWV values for all the data only over land (May 2007).

III.4 Assimilation of MERIS TCWV

The fact that there is not much water vapour data over land and the result presented above that MERIS TCWV data are good over land motivated the satellite group at ECMWF to make experiments to test the impact of assimilating MERIS TCWV over land only. They needed to create super-observations comparable with the model resolution and to introduce some screening and quality control (QC) criteria. They also needed to do analysis of the spatial correlation. They found that the results were in general rather neutral compared to the model. However, some positive (and consistent with microwave measurements) impact against radiosondes was noticed. For details, refer to Bauer (2009). Finally, MERIS TCWV product over land has been assimilated with VarBC operationally since 8 September 2009.

III.5 Conclusions

MERIS TCWV product shows that there is quite a good value in the product especially over land. Careful data screening is needed to get rid of the "noise", which may also be a legitimate variability, in the data. This leads to the rejection of about 70% of the data. The product in general is too dry compared to the model. However, it is at a comparable level of dryness as the MWR. Although the product is averaged to form the super-observations which, in principle, should smooth the product and make it of comparable scale like the model, it is still too "noisy" when compared to the model or the MWR.

Being of better performance over land where not many alternative data are available, MERIS TCWV product has been assimilated operationally in the ECMWF atmospheric model since 8 September 2009.

The change of ENVISAT orbit in October 2010 did not have any impact on MERIS water vapour product.

Acknowledgments

This work was carried out with ESA support through ESA contract No. 21519/08/I-OL (Global Validation of ENVISAT Data Products). Special thanks are due to Peter Janssen and Jean-Raymond Bidlot for support and valuable discussion.

References

Abdalla, S. (2005). *Global Validation of ENVISAT Wind, Wave and Water Vapour Products from RA-2, MWR, ASAR and MERIS*. Final Report for ESA contract 17585. Obtainable from: The Library, ECMWF, Shinfield Park, Reading, RG2 9AX, UK. Also available online at: http://www.ecmwf.int/publications/library/do/references/show?id=86908

Abdalla, S. (2007). "Ku-Band Radar Altimeter Surface Wind Speed Algorithm", *Proc. Envisat Symposium* 2007, Montreux, Switzerland, 23-27 April 2007. Available online at: http://envisat.esa.int/envisatsymposium/proceedings/contents.html

Abdalla, S. and Hersbach, H. (2004). *The technical support for global validation of ERS Wind and Wave Products at ECMWF*. Final Report for ESA contract 15988/02/I-LG. Available online at: http://www.ecmwf.int/publications/library/do/references/show?id=86313

Abdalla, S. and Janssen, P.A.E.M. (2007). "Monitoring and Validation of Water Vapour Products from Envisat MWR and MERIS", *Proc. Envisat Symposium* 2007, Montreux, Switzerland, 23-27 April 2007. Available online at: http://envisat.esa.int/envisatsymposium/proceedings/contents.html

Abdalla, S., Bidlot, J. and Janssen, P.A.E.M. (2004). Assimilation of ERS and ENVISAT Wave Data at ECMWF. *Proceedings of the ENVISAT-ERS Symposium*, Salzburg, Austria, 6-10 September 2004.

Abdalla, S., Janssen, P.A.E.M. and Bidlot, J.R. (2010), "Jason-2 OGDR Wind and Wave Products: Monitoring, Validation and Assimilation", *Marine Geodesy*, **33**(S1), 239-255.

Bauer, P. (2009); "4D-Var assimilation of MERIS total column water-vapour retrievals over land", *Quart. J. Royal Meteo. Soc.*; **135**; 1852-1862

Bidlot, J.R., Holmes, D.J., Wittmann, P.A., Lalbeharry, R., and Chen, H.S. (2002), "Intercomparison of the performance of the operational wave forecasting systems with buoy data", *Wea. Forecasting*, **17**, 287-310.

Caires, S. and Sterl, A. (2003), "Validation of Ocean Wind and Wave Data Using Triple Collocation.", *J. Geophys. Res*., **108**, 3098.

ECMWF (2006). *ECMWF System Revisions during 2006*. Internet web page visited on 1 Dec. 2006, http://www.ecmwf.int/products/data/operational_system/evolution/evolution_2006.html

ECMWF (2010), "Atmospheric Model Identification Numbers", a web page accessible from: http://www.ecmwf.int/products/data/technical/model_id/index.html
(Last visited on 30 November 2010).

Freilich, M.H. and Vanhoff, B.A. (1999), "QuikScat Vector Wind Accuracy: Initial Estimates", *Proc. QuikScat Cal/Val Early Science Meeting*, Pasadena, CA, Jet Propulsion Laboratory.

EOO/EOX - Serco/Datamat (2005). *Information to the Users Regarding the Envisat RA2/MWR IPF Version 5.02 and CMA 7.1*. Internet web page visited on 13 Dec. 2005, http://earth.esa.int/pcs/envisat/ra2/articles/RA2_MWR_IPF_5.02.html

ESA (2002). *Envisat Tour*. Internet web page visited on: 13 Dec. 2005, http://envisat.esa.int/instruments/tour-index/

ESA (2004). *ENVISAT Data Products*. Issue 1.2e, Dec. 2004, Internet web page visited on: 13 Dec. 2005, http://envisat.esa.int/dataproducts/

Hasselmann, S., Bruning, C., Hasselmann, K. and Heimbach, P. (1996). An Improved Algorithm for the Retrieval of Ocean Wave Spectra from Synthetic Aperture Radar Image Spectra. *Journal of Geophysical Research*, Vol. **101**, 16615-16629.

Hasselmann, S., Lionello, P., and Hasselmann, K. (1997). An Optimal Interpoltion Scheme for the Assimilation of Spectral Data. *J. Geophysical Research*, Vol. **102**(C7), 15823-15836.

Janssen, P.A.E.M. (2004). *The Interaction of Ocean Waves and Wind*, Cambridge University Press, Cambridge, U.K., 300+viii pp.

Janssen, P.A.E.M., Abdalla, S. and Hersbach, H. (2003). *Error Estimation of Buoy, Satellite and Model Wave Height Data*. ECMWF Technical Memorandum No. 402. ECMWF, Shinfield Park, Reading, RG2 9AX, UK. Available online at: http://www.ecmwf.int/publications/library/do/references/show?id=85650

Janssen, P.A.E.M., Abdalla, S., Hersbach, H. and Bidlot, J.-R. (2007). "Error Estimation of Buoy, Satellite, and Model Wave Height Data", *J. Atmos. Oceanic Technol*., **24**, 1665–1677.

Johnsen, H. (2005). Envisat ASAR Wave Mode Product Description and Reconstruction Procedure. Report for ESA Contract 17376/03/I-OL.

Kahma, K.K. and Donelan, M.A. (1988). A Laboratory Study of the Minimum Wind Speed for Wind Wave Generation. *Journal of Fluid Mechanics*, Vol. **192**, 339-364.

Komen, G.J., Cavaleri, L., Donelan, M., Hasselmann, K., Hasselmann, S., and Janssen, P.A.E.M. (1994). *Dynamics and Modelling of Ocean Waves*, Cambridge University Press, Cambridge, UK, 532 p.

Marsden, R.F., (1999), "A Proposal for a Neutral Regression", *J. Atmos. Oceanic Technol*., **16**, 876-883.

Quilfen, Y., Chapron, B. and Vandemark, D. (2001), "The ERS Scatterometer Wind Measurement Accuracy: Evidence of Seasonal and Regional Biases", *J. Atmos. Oceanic Technol*., **18**, 1684-1697.

Stoffelen, A. (1998), "Towards the True Near-Surface Wind Speed: Error Modeling and Calibration Using Triple Collocation", *J. Geophys. Res*., **103**, 7755-7766.

Tokmakian, R. and Challenor, P.G. (1999), "On the Joint Estimation of Model and Satellite Sea Surface Height Anomaly Errors", *Ocean Modell*., **1**, 39-52.

Voorrips, A.C., Mastenbroek, C. and Hansen, B. (2001). Validation of two algorithms to retrieve ocean wave spectra from ERS synthetic aperture radar. *Journal of Geophysical Research*, Vol. **106**, 16825-16840.

Witter, D.L. and Chelton, D.B. (1991). A Geosat Altimeter Wind Speed Algorithm and a Method for Altimeter Wind Speed Algorithm Development. *Journal of Geophysical Research*, Vol. **96**, 8853-8860.